Steir. Beitr. z. Hydrogeologie / 43 / Seiten 159–228 / Graz 1992

Fractured Rock – Test Site Lindau/Southern Black Forest (Germany)

T. HIMMELSBACH, H. HÖTZL, W. KÄSS, Ch. LEIBUNDGUT, P. MALOSZEWSKI, T. MEYER, H. MOSER, V. RAJNER, D. RANK, W. STICHLER, P. TRIMBORN, E. VEULLIET

Content

1. Area of Investigation (T. HIMMELSBACH, E. VEULLIET)

1.1. General Description of the Test Site

1.1.1. History

Since the late fifties in the valley of the Schwarzenbach in the Southern Black Forest (FRG) a reservoir lake is planned by the SCHLUCHSEEWERKE AG (Freiburg) which should be connected to a network of other reservoir lakes by pumping stations and which was supposed to contribute meeting the peak energy requirements of the German and European interconnected network. This lake LINDAU is expected to cover an area of about 320 ha, having a storage capacity of 70 hm^3. The dam site is planned at the narrowing of the valley close to the location

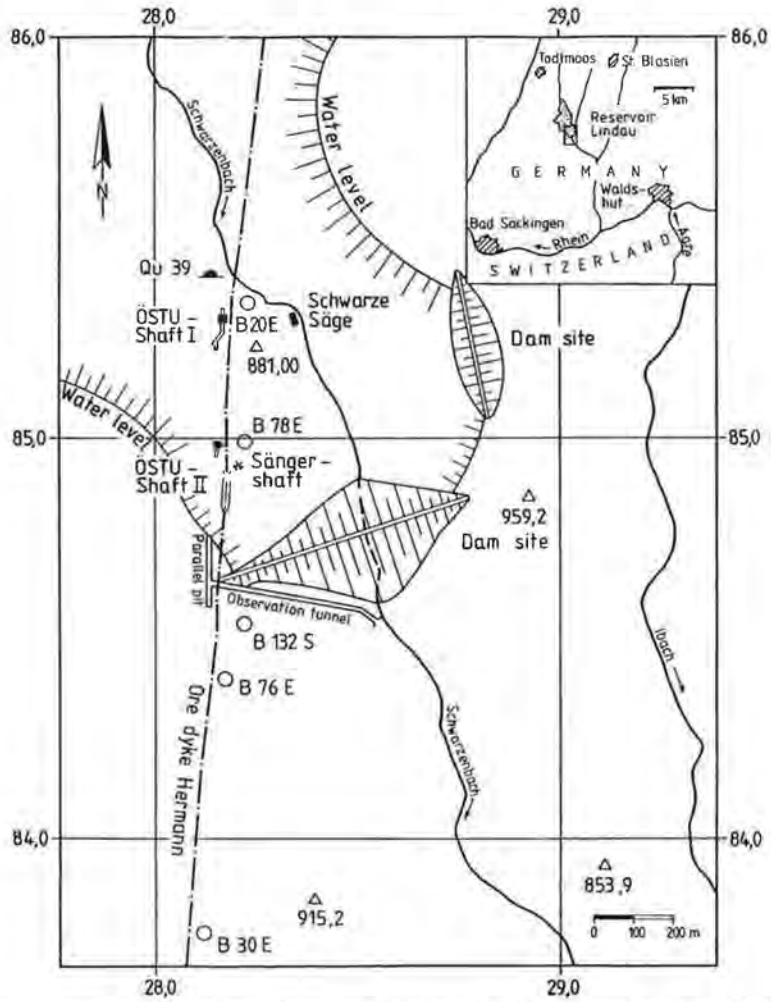

Fig. 1.1: Location map of the planned reservoir lake Lindau. The general striking of the ore dike Hermann is shown as dashed line.

"Schwarze Säge" 5 km in the SE of Todtmoos. At the planned dam site, the SCHLUCHSEEWERKE AG investigated an area of nearly 1 km² size with the aim to prove the watertightness of the reservoir area and particularly of the dam foundation. Of special interest there is the ore dike "Hermann" which crosses the dam site, due to cavernosities and the accompanying 20 m wide fracture zone (Fig. 1.1).

To determine the permeability of this dike zone a comprehensive investigation program with a great number of different hydraulic tests (pumping tests, tracer tests, seepage tests etc.) was carried out during the sixties and seventies. As a result of these investigations the company decided in the late seventies to seal the dike with about 1,000 tons of cement injections. By the successful sealing of the ore dike, which could be proved by drain and tracer experiments (G. ACKERMANN, 1982) the ore dike Hermann was separated into two hydraulic different parts. The southern part of the ore vein shows hydraulic heads of up to 60 m, referring to the level of the so called parallel tunnel, while the northern part of the ore vein shows only heads up to 25 m (T. HIMMELSBACH, 1991). By this results the watertightness of the proposed dam site could be proved.

1.1.2. Instrumentation

In the course of the underground examinations in the area of the planned reservoir lake, more than 200 vertical, horizontal and inclined boreholes were drilled from the surface by the SCHLUCHSEEWERKE AG during several campaigns lasting from 1955–1980 (Series "E" and "S", tab. 1.1). The drillings of the Series "E" were located along 17 profiles, being nearly W–E orientated and perpendicular to the striking of the ore dike (Fig. 1.1). The 135 drillings of the Series "S", placed on the whole area of the planned reservoir lake, form a dense observation network. Some boreholes reach a depth of up to 250 m.

Tab. 1.1: Boreholes in the test area. The Series "E" and "S" are drilled from the surface. The Series "B–C/C–D" and "BL" are drilled from the observation tunnel Lindau.

Series	Date	Quantity	Type	Used today
"E" ERZGANG Total: 5,874 m	1955 to 1978	82	horizontal: 1 inclined: 28 vertical: 53	0 4 6
"S" (SCHWARZENBÄCHLE) Total: 5,544 m	1956 to 1980	135	horizontal: 0 inclined: 6 vertical: 129	0 4 14
"B–C/C–D" (BOHRNISCHE V, VI) Total: 700 m	1977	17	horizontal: 2 inclined: 14 vertical: 1	0 0 0
"BL" (LINDAUSTOLLEN) Total: 392 m	1976	21	horizontal: 11 inclined: 10 vertical: 0	4 2 0
Total: 12,510 m	1955 to 1980	255		34

Two supplementary shafts (ÖSTU I / II) and a 460 m long observation tunnel with a diameter of 3 m (observation tunnel Lindau) were excavated to detect the striking of the ore dike and to control the efficiency of its sealing by the cement injections (Fig. 1.1).

In the oblique pit a shaft was sunk up to 72 m depth, with two drilling nitches lying on different levels. The drilling nitches allowed multiple drilling, with a total of 17 boreholes (Fig. 1.2).

From the parallel pit of the observation tunnel 21 boreholes were additionaly drilled into the ore dike. In 25 years more than 12,000 m of drill core were cut, analysed and documented by the SCHLUCHSEEWERKE AG.

About 30 boreholes, several springs and especially the observation tunnel have been used by the AGK since 1987 to investigate the hydraulic conductivity of high permeable fault and fracture zones under in-situ conditions (Fig. 1.3). These investigations were part of the interdisciplinary research programm of the ATH

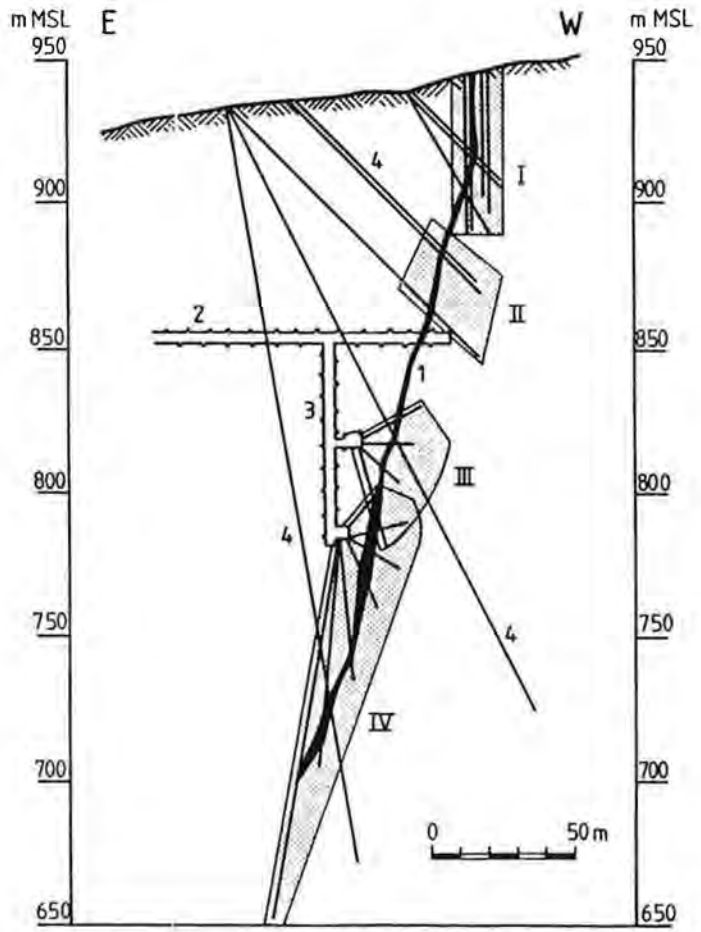

Fig. 1.2: Cross section through the ore dike in the area of the planned dam axis showing the arrangement of the cement injections. 1 ore dike Hermann, 2 oblique pit, 3 shaft with injection nitches, 4 core drillings, I–IV cementations zones.

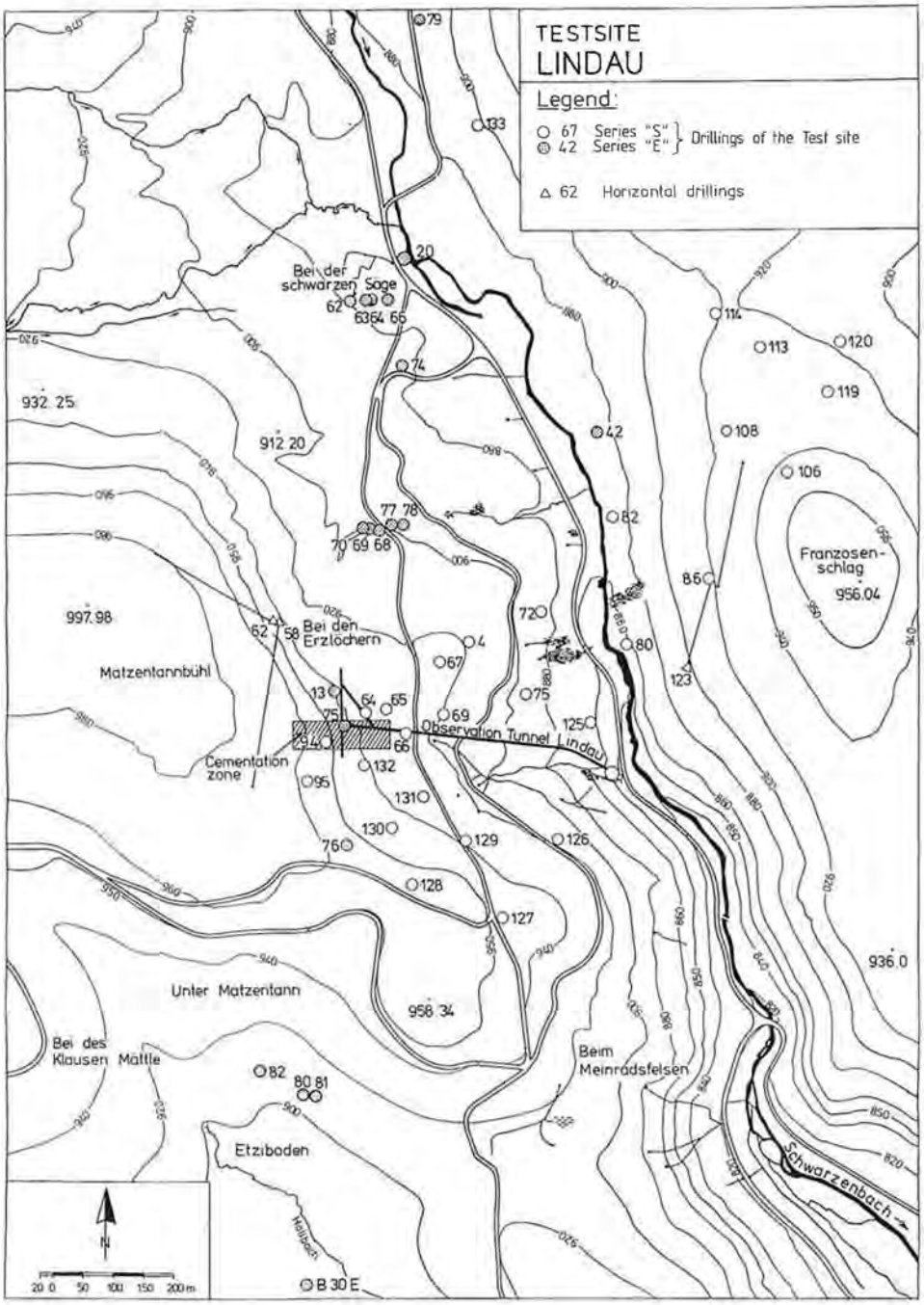

Fig. 1.3: Map of the test site Lindau.

(International Association of Tracer Hydrology) to investigate the subsurface discharge and storage dynamic in a fissured aquifer system.

This implies that,

- most of the boreholes were equipped with mechanical or sensitive electronical water-level recorders for a continuous registration of groundwater level. With this instrumentation even small fluctuations can be registrated, so that the change of groundwater level referring to precipitation could be recorded,
- the discharge and the physical parameters (temperature and conductivity) of four artesian wells (Series"S") and six springs were measured once per week. Supplementary watersamples were taken from the artesian wells and the springs for hydrochemical and isotopical investigations,
- a special test area with 16 porous ceramic suction cups was installed for the investigation of the mean residence time in the unsaturated zone by using the natural isotopes ^{3}H and ^{18}O. The suction cups were installed in two soil profiles in four different depths up to 2 m (approximately 0.50, 1.00, 1.50 and 2.00),
- a rectangular lysimeter having an catchment area of approximately 2.25 m^2, was built for the investigation of the seepage rate,
- additionaly a recording pluviograph and five rain gauges were installed in the test area for the registration of the amount and the frequency of precipitation and for isotopical input measurement,
- and four measuring weirs (V-notch and rectangular weirs) were built for the investigation of the relation between precipitation and surface related runoff in the little catchment area Etziboden.

2. Hydrogeology (T. Himmelsbach, H. Hötzl)

2.1. Hydrogeological Units

2.1.1. Albtal Granite

The test site Lindau is situated in the Southern Black Forest at the north-eastern part of the Albtal granite pluton. This pluton has a total areal outcrop of nearly 125 km^2. The pluton is surrounded by gneisic antexites at its eastern and western border, by paragneises along the southern border and by the Schluchsee-granite and by polymetamorphic gneises at its northern border (R. Metz & G. Rein, 1958). The Albtal granite itself is charaterized by a porphyroblastic structure with large feldspars in a granodioritic matrix (R. Emmermann, 1968).

In general the Albtal granite shows a rather widestanding orthogonally jointing. In hydrogeologic terms this causes a very low average hydraulic permeability. In the tunnel galleries of the test site this permeability is responsable for a generally low percolation rate producing some drop water through the rock walls of the gallery. Over distances lying in the range of tens of meters the bottom of the Lindau tunnel is completely dry. However, in the immediate vicinity of zones affected by intense fracturing due to tectonic shear and normal faulting as well as along the ore dike the Albtal granite shows a distinct higher permeabilty, which produces a noticeable percolation rate through the tunnel walls.

At the ground surface the Albtal granite is weathered to a fine grained granitic grus which is the so called "Berglesand". The thickness of this grus varies generally between a few meters, but in some areas of the test site the Berglesand can reach a thickness up to 15 m and more. Thus, at the higher part of the test site with its flatter slope only at a few locations the Albtal granite pierces through this cover of granitic grus. In the lower part, with the young dissected Schwarzenbach valley, unweathered granites are wider distributed.

2.1.2. Ore Dike Hermann

In the area of the test site Lindau the granite pluton is penetrated by the ore dike Hermann. It belongs to the numerous late variscian hydrothermal dikes in the Southern Black Forest. The mineralization of all these hydrothermal dikes generally happened during three phases, but in the ore dike Hermann only two of them can be observed (R. METZ, 1980). They include the following mineralization:

Phase 1: quartz I,
fluorite,
galena,
pyrite,
baryte.
Phase 2: quartz II,
pseudomorphism of quarz to
fluorite and baryte of phase 1.
Phase 3: quartz III.

The matrix of the ore lode is dominated by quarz I and baryte. The fluorite was mainly dissolved by descendent aqueous solutions due to percolation processes after phase 1. The resulting solution cavities are partly refilled by subsequent cristallization of quarz II as a pseudomorphism to fluorite, but still a relatively high cavernousity exists in parts of the ore dike; this can be observed in many of the drilled cores of the test site. In the test site Lindau the ore dike Hermann shows a generally northbound striking, lying in the range of 5° N (Fig. 2.1). Its angle of dip is very steep, varying between 75° E and 85° E depending on the general depth. Near the surface the angle of dip is more gentle and lies in the range of 75° E. However, with increasing depth it increases as well and the ore lode becomes more and more upright orientated. The thickness of the ore lode varies between 0.3 m and 3 m within horizontal as well as within vertical distances which are less than a few tens of meters. The average thickness of the vein, however, lies very close to 1 m.

The Albtal granite has been alterated hydrothermally on both sides of the ore dike Hermann. This in total about 10 m wide zone was affected by younger tectonic shear processes causing fracturation and faulting parallel to the dike. Within the dike itself there exists a fault and fracture zone which strikes parallel to the dike. This deformations are presumed to be responsible for the strongly varying thickness of the ore dike (A. RENK, 1980). The ore dike forms the major hydraulic element in the area of the test site. Its permeability is characterized by the secondary solution cavities as well as by the parallel striking faults and fractures. The latter are mainly responsable for the high hydraulic conductivity of this zone being some magnitudes higher than that of the rather widestanding jointed unalterated Albtal granite. Hydraulically the ore dike Hermann can be characterized as a double porosity medium (s. also chap. 5.).

2.1.3. Porphyry Dikes

The Albtal granite as well as its polymetamorphic frame are penetrated by generally NW–SE striking porphyry and rhyolithic dikes (Fig. 2.1). The porphyry dikes are not associated with a definite granitic pluton but form a separate magmatic phase.

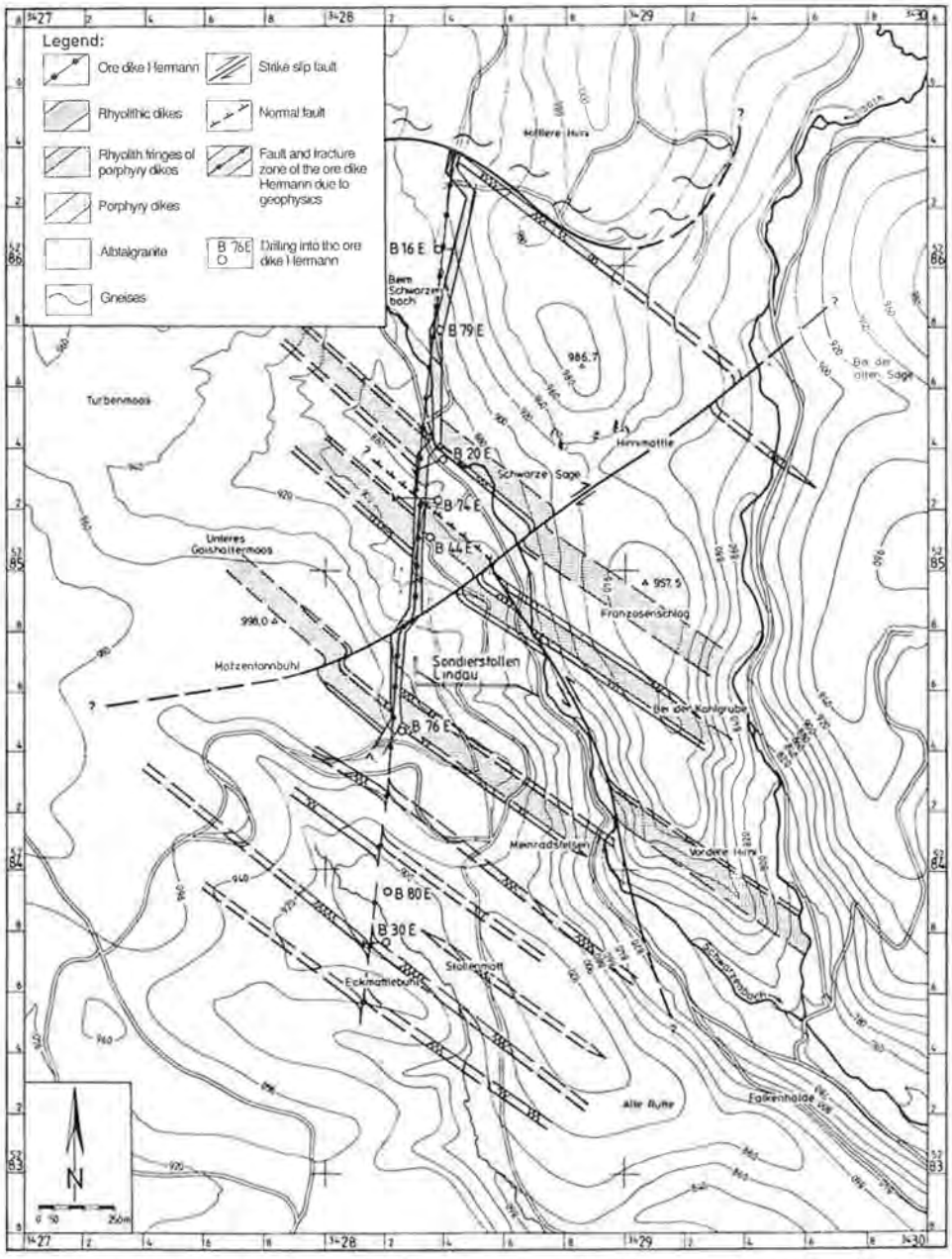

Fig. 2.1: Geological map of the test site Lindau (without the thin quaternary loose rockmasses).

The dikes intruded between late Upper and early Lower Permian times at the end of the Variscian Orogenisis (H. SCHLEICHER, 1984). In the area of the test site Lindau the porphyry dikes reach a thickness up to 100 m but project only at a few locations through the granitic detritus as weathered relicts. At least three porphyry dikes were detected by the numerous drillings of the planned dam site. Others, however, presumed by geophysical investigations, are still surrounded by uncertainities. Generally the angle of dip of these dikes lies in the range of 75° NE. At the lateral margins of the porphyric dikes rhyolith fringes, in the sense of selvages, can be frequently observed. Beside these there also exists just rhyolitic dikes which are not in any contact with a porphyry dike. These "isolated" rhyolithic dikes are assumed to follow major fault zones in the Albtal granite and its polymetamorphic frame. The angle of dip seems to be the same as detected for the porphyry dikes. Although these rhyolithic dikes reach only a thickness lying in the range of a few meters up to 10 m they can be followed over the same distances as the porphyry-dikes (Fig. 2.1).

Both, the porphyry dikes as well as the rhyolithic dikes, are intensly fractured in the vicinity of their contact to adjacent rockmasses formed either by the Albtal granite or by its polymetamorphic frame. This intense fracturing is subparallel to the striking of the dikes and is responsible for the alignment of many springs within the area of the test site. The porphyry dikes, as well as their adjacent rhyolitic dikes, form therefore a hydraulic element which is, however, of subsequent importance in comparison with the ore dike.

2.1.4. Loose Rockmasses

The hard rocks of the test site Lindau are directly outcropping only at a few locations, especially at the steep hill slopes. The cover of loose rockmasses consists of granitic grus and glacial deposits. Only at a few locations this cover does reach a thickness up to 25 m and more. The average thickness, however, lies in the range between 5 m and 10 m. Although the saturated zone of the test site is mainly restricted to the hard rocks the groundwater table lies at some locations within this cover of granitic grus and base moraine. Such locations are generally found at marshy depressions lying at the northern and the southern part of the test site.

2.2. Fault and Fracture Zones

2.2.1. Tectonic Setting

The area of the test site Lindau is affected by the following tectonic systems (Fig. 2.1):

- **N–S directions** are corresponding to the general striking of the ore dike Hermann and other hydrothermal dikes in the Southern Black Forest. The banded cristallization of quartz II may be interpreted from the fault and fracture zone of the ore dike was affected for a long time by an extensional stress regime. However, the observation of fractured fluorites and the occurrence of vein breccia indicate that the ore dike was also subsequently affected by compressional shear processes causing sinistral faults within the ore dike (A. RENK, 1980).
- **NNW–SSE directions** are corresponding to gently dipping slickensides (160°/10°S) which can be observed at some outcrops lying along the little river Schwarzenbach

in the central part of the test site. A lateral movement there along these elements may be responsible for the observed displacement of porphyry dikes in the range of some tens of meters.

- **ENE–WSW directions** are corresponding to faults which were detected during the excavation of the observation tunnel Lindau. Their steep angle of dip lying in the range of 70° N as well as the lack of any slickensides indicate their normal fault character.
- **NW–SE directions** are corresponding to the general striking of the porphyry and rhyolithic dikes. The occurrence of flucan having a thickness up to some centimeters indicates neotectonic movements along these faults which may have a character of lateral displacements.
- **WNW–ESE directions** are corresponding to fault zones having the character of oblique lateral faults. In some drillings of the test site they were detected as crushing zones having an extension of few decimeters. If such crushing zones intersect the ore dike, its mineralization becomes reduced to some veinlets having a thickness of only a few centimeters.

The tectonic displacements of the porphyry dikes within the area of the test site is thought to be restricted to sinistral and dextral lateral faults as well as to steep normal faults. After the intrusion of the late Variscian post- and syntectonic granites of the Southern Black Forest the complex pattern of late Carboniferous-Permian E–W to NE–SW directed extension (F. WICKERT & G. EISBACHER, 1988) caused the intrusion of the porphyry and rhyolithic dikes. This extension was probably related to a continued differential displacement along NNW–SSE trending left lateral strike-slip faults which are responsible for the lateral displacement of the porphyry dikes within the area of the test site. The genesis of the hydrothermal ore dike Hermann may also be related to this magmatic phase and the general extensional patterns.

Due to the continued clockwise rotation of the stress field to the recent direction being approximately 160° as a result of the Alpine Orogenisis (K. GEHLEN et al., 1986) the ore dike Hermann was affected by a left-lateral strike-slip fault which caused minor lateral displacements along the striking of the ore dike lying in the range of a few up to 10 m (Fig. 2.1). During the Neogenic uplift of the Southern Black Forest old Variscian E–W and ENE–WSW trending patterns became reactivated. The ENE–WSW trending patterns are related to an assumed right-lateral strike-slip fault which may be responsible for additional lateral displacements of the porphyry dikes. E–W trending patterns, however, are assumed to be related to normal faults which are responsible for the general slope of the basement towards the Rhine valley in the South.

2.2.2. Hydraulic Effect of Fault and Fracture Zones

Major fault and fracture zone dissecting hard rocks can drain the adjacent rockmasses due to their higher permeability. Such a drainage effect leads to a trough of hydraulic head depression which can be observed in the vicinity of the fault and fracture zone. The flow patterns within this trough of hydraulic head depression are directed towards the fault zone and its extension. Especially in the vicinity of the ore dike Hermann, which is the most effective hydrogeological element at the test site, the zone of the general depression of groundwater table shows steep hydraulic gradients towards the ore dike and its fault and fracture zone. Its lateral

width varies due to hydrogeological as well as due to hydrological conditions. It has an average extension on both sides of the ore lode lying in the range of approximately 50 m.

The whole groundwater affected by this drainage zone flows towards the ore dike and subsequently towards the next base level where the dike is exfiltrating diffusely into natural water courses.

In comparison to the very low average permeability of the hard rocks (k_f = 10^{-9} m/s–10^{-11} m/s) the fault and fracture zones have a permeability which is some magnitudes higher ($k_f = 10^{-6}$ m/s–10^{-5} m/s). The subsurface flow is therefore mainly restricted to the fault and fracture zones. Accordingly, the mean residence time of the mobile water in such a fault and fracture zone has to be much smaller than in other parts of the fissured aquifer which is affected only by the widestanding jointing of the Albtal granite.

The ground water level recorded at such fault and fracture zone follows strong precipitation with a gentle and delayed increase having an amplitude in the range of some meters. In areas of the test site affected by the normal widestanding jointing, however, the groundwater level reacts very rapidly to precipitation. Within a delay being in the range of one to two days the groundwater level increases rapidly with an amplitude up to 10 m.

2.2.3. General Hydraulic Situation

Due to the cement injections to avoid subsurface runoff in the area of the planned dam axis the ore dike Hermann is hydraulically separated into two sections, which do not have any hydraulic interchange.

In the northern part of the test site the flow patterns within the ore dike show a northbound direction towards the location Schwarze Säge. The little stream Schwarzenbach forms there the base level at its intersection with the ore dike. The southern part of the test site is characterized, however, by generally southbound flow patterns. The groundwater affected by the drainage zone of the ore dike flows towards the location Etziboden where the rivulet Höllbach forms the natural base level (Fig. 1.3).

Aside the hydraulic influence of the drainage zone caused by the ore dike Hermann the subsurface flow patterns are assumed to be directed parallel the slope gradient of the test site. The subsurface runoff is related to numerous springs, which are aligned parallel to the Schwarzenbach valley. These springs are mainly restricted to the occurrence of porphyry dikes.

At the northern and southern part of the test site the ore dike Hermann is covered by moraine deposits. The groundwater level recorded at these locations lies very close to the surface. Due to the less permeable moraine deposits, the groundwater in the ore dike can thus be considered lying under confined hydraulic conditions. Especially the latter are responsible for the occurrence of artesian groundwater at these parts of the test site causing an exfiltration of groundwater from the fissured ore dike into its cover of loose rockmasses.

The numerous springs occuring at the northern and southern marsh areas are related to this hydraulic situation. At both locations wells drilled into the ore dike met artesian groundwater, supplying drinking water for a sawmill lying in the northern part of the test site and for a little community which is located in the southern part of the test site.

3. Hydrology

3.1. Investigation of Catchment Areas (T. Himmelsbach, Ch. Leibundgut, T. Meyer)

3.1.1. Hydrological Characterization of the Test Site

A large part of the test site Lindau is drained by the N–S running Schwarzenbach which flows 5 km south of the test site into the Ibach. The Ibach is a tributary of the Alb and finally the Rhein near Albbruck which forms the base level for this part of the Southern Black Forest. The southern part of the test site is drained by the upper Höllbach which flows near the community of Görwihl into the Alb. These two little rivers are supplied by numerous episodic and perennial springs having an average discharge of 0.1–3 l/s. The Ibach catchment encloses an area of 41.9 km^2. It is one of 10 river basins in the Black Forest with fissured rock aquifers. The Ibach basin has been investigated in order to gain knowledge about the general hydrological behaviour. Furthermore, the basin has been selected to get an idea about the representativity of the small catchment "Etziboden" which is located at the southern part of the test site Lindau.

The long-term characteristics of the runoff have been investigated for the period 1955–1976. Only for that period enough data are available. A general feature of these investigations is a relatively homogeneous behaviour in the long-term runoff, although there is a quite broad variation of the catchment parameters. Since 1966 a small part of the runoff of the Ibach river has been diverted for hydro power use. However, a comparison of the time series before and after the introduction of the divertion shows stable mean flow values.

The test site Lindau, which is a part of the Ibach catchment, is affected by a subnival climate which is typical for this hill country. During the wintermonths a snowcap up to 2 m may exist. The geographic location of the investigated area near to the Alps is noticeable because of the dry southern adiabatic winds ("Föhn") that often cause a rapid melting of the snowcap within only a few days. The average annual precipitation within the area of the test site amounts to approximately 1,800 mm but can fluctuate up to ± 500 mm depending on the specific hydrological course of the year. With the exception of single thunderstorms occurring during summer the highest amount of precipitation is generally observed within the period between November until March. In comparison with the Höllbach catchment the long-term mean yearly precipitation in the Ibach catchment amounts to 1,596 mm (s. tab. 3.1).

The recharge of groundwater within the area of the test site depends on the annual distribution of precipitation as well as on the occurrence of the snowmelt and the duration of the vegetation period. Therefore, during the winter and spring time the recharge of groundwater is followed by a subsequent increase of the spring discharge. During the summer months, however, the groundwater discharge is generally decreasing. The surface runoff supplied by the springs shows only short interruptions caused by heavy precipitation which is responsible for sudden changes of the discharge frequency curve.

3.1.2. Hydrology of Small Catchment Areas

To realize a quantification of hydrological parameters as well as their different dependence due to precipitation a small catchment at the southern part of the test

site was investigated. This small catchment, located at the area "Etziboden" was defined according to morphological aspects and is characterized by hill-ranges having an average altitude of 950 m a.s.l. and a difference in elevation up to 110 m. It encloses an area of approximately 1.35 km² and 92% of this area is covered by forest. The non-wooded areas are characterized by swamp meadows which are caused by glacial moraines beneath the surface. The upper part of the Höllbach drains this small catchment and leaves this part of the test site through a narrow valley mouth at the location Stollenmatt (Fig. 3.1).

A hydrological weir (MW 2) was located at the lowest elevation of the Etziboden catchment to control the entire surface related discharge. The weir was constructed in a narrow section of the Höllbach valley. According to the hydrogeological conditions it is assumed that the subsurface runoff is negligible at this location. The latter implies that the entire runoff of the Etziboden catchment can be recorded at this hydrological weir. It enables a continuous record of the discharge ranging up to 200 l/sec. In addition, the discharge of 10 springs occurring in this area was measured with the help of small THOMSON weirs (MB 1–5). The amount of precipitation was recorded once a week by using rain gauges of the typ HELLMANN. For a continuous record of the precipitation, however, a pluviograph was used which was located at the central part of the test site. The fluctuation of the groundwater table was registrated at different wells (B80E, B81E, B82E) which were equipped with automatic gauging devices (Fig. 3.1).

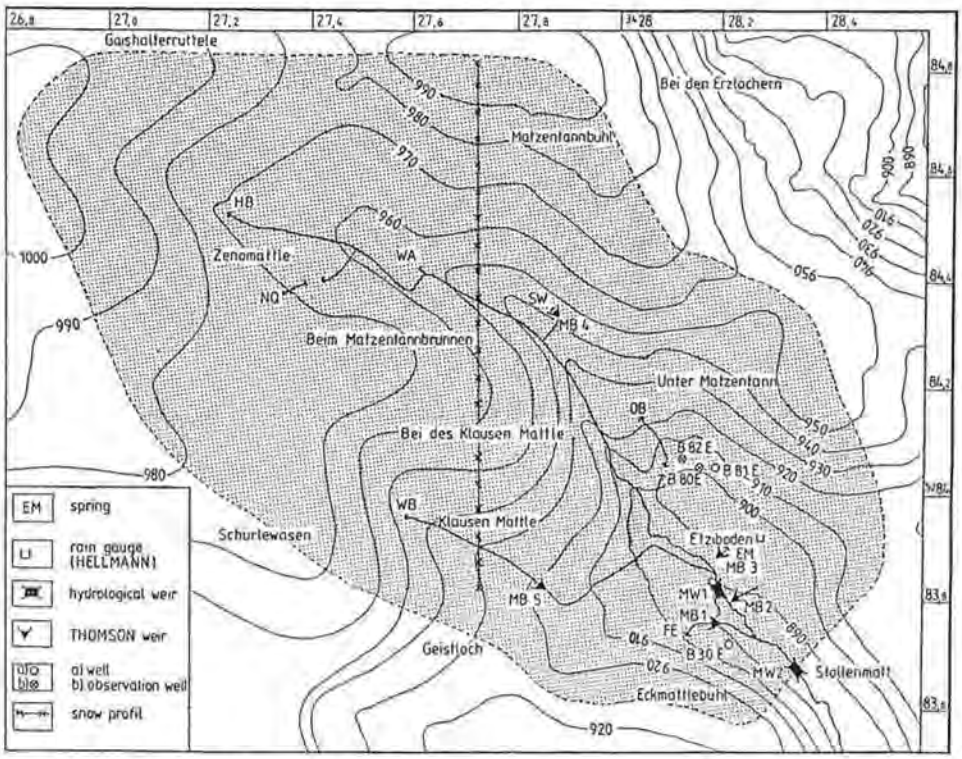

Fig. 3.1: The small catchment area Etziboden.

All calculations of water balances depend on the factor evapotranspiration which is affected with some uncertainities because it is not available by direct measurement. To overcome these problems the equation of W. HAUDE (1955) describing the potential evapotranspiration by

$$ET_p = f \cdot P_{14}(1 - \frac{F_{14}}{100}) \text{ (mm/d)},$$

where

ET_p = potential evapotranspiration,
f = proportionality factor,
P_{14} = degree of vaporsaturation at 2 pm
$= 4{,}525 \times 10^{(7{,}4475 \cdot t)/(234{,}67 + t)}$
with t = air temperatur at 2 pm,
F_{14} = relative atmospheric humidity at 2 pm,

was modified. Instead of conventional factors (f) for different months, as used by W. HAUDE (1955), new factors suggested by H. ERNSTBERGER & V. SOKOLLEK (1984) were involved. The advantage of this modification lies in the consideration of the special vegetation conditions in woodland areas. In tab. 3.1 the factors used for the calculations are listed in comparison with normal HAUDE factors.

Tab. 3.1: Comparison of specific factors from the HAUDE-equation (B. HÖLTING, 1989) and factors suggested by H. ERNSTBERGER & V. SOKOLLEK (1984).

Month	Proportionality factor f	
	HAUDE	ERNSTBERGER & SOKOLLEK
January	0.26	0.01
February	0.26	0.10
March	0.33	0.10
April	0.39	0.23
May	0.39	0.28
June	0.37	0.30
July	0.35	0.35
August	0.33	0.28
September	0.31	0.22
October	0.26	0.10
November	0.26	0.05
December	0.26	0.01

The modified factors, suggested by H. ERNSTBERGER & V. SOKOLLEK (1984), take into account only the amount of transpiration, but they don't consider any interception. Due to this fact the interception had to be evaluated independently. According to these modified parameters it becomes obvious that a significant transpiration, which may reach values up to 30 mm/week, occur only during the months from April until September. When calculating the annual amount of transpiration of the years 1988, 1989 and 1990 under the additional consideration of the specific vegetation factors the amount of the hydrological input being available for the groundwater recharge is generally reduced in the range of 20 up to 30%. The annual changes of transpiration depend, however on the individual course of

temperature development of the specific year. Concerning the hydrological year 1990 a transpiration of 412 mm was calculated for the Etziboden catchment which corresponds to 24% of the total precipitation (1,745 mm) (Tab. 3.2). In comparison to that the long-term mean yearly evapotranspiration of the Ibach catchment calculated from the water balance amounts to 447 mm, which corresponds to 28% of the total precipitation.

The amount of interception was estimated by a comparison between precipitation rates in wooded areas and those measured in open space areas. During the winter 1990/91 a snowprofile consisting of 21 sampling locations was investigated which had a length of about 1 km in N–S direction across the catchment area. The results showed a significant difference for the watercontent of the snowcap in wooded areas compared to the snowcap in non-wooded areas lying in the range of up to 44%. A comparison between liquid precipitation rates, using rain gauges located at wooded areas to those from open space areas yielded differences lying in the range of 10 up to 25%. Detailed investigations referring to the basic hydrological equation

$$P = D + E + (R + C),$$

where

P = precipitation,
D = discharge,
E = (transpiration + interception),
R = reserve,
C = consumption,

yielded for the hydrological year 1990 an interception of approximately 510 mm which corresponds to 29% of the total precipitation (Tab. 3.2).

In fig. 3.2 the general development of surface related discharge within the Etziboden catchment is compared to the seasonal precipitation rate for a 1.5 year lasting period. It is obvious that single precipitation events during the summer months have only a minor influence on the continuous decrease of the discharge rate according to the increasing influence of evapotranspiration. The development of the surface discharge during the summer seems to be controlled only by the storage capacity of the joint aquifer.

To illustrate the short time related interaction between precipitation, surface discharge and fluctuation of the groundwater level all these parameters are shown for a short period lasting only 2.5 days. For better distinction these hydrological parameters were recorded within time steps of only one hour. Already, within four to seven hours since the precipitation event began an increase in the discharge rate could be observed at the measuring weir MW 2 (Fig. 3.3). The groundwater level which was recorded at the boreholes B80E and B82E, however, increased subsequently within a time delay of approximately 27 hours. During the precipitation nearly any surface related direct runoff could be observed. Thus, it is assumed that the precipitation infiltrated directly into the glacial moraines beneath ground surface. However, due to the delay in the response of the groundwater level in the joint aquifer, the precipitation influenced in a direct way only the discharge rate of shallow springs at this location. Accordingly, the shallow springs located in this area drain mainly the moraine deposits. The assumed direct infiltration path as well as the observed subsequent increase in the discharge rate at the springs must therefore be restricted to interflow processes occurring within the glacial moraine and the upper part of

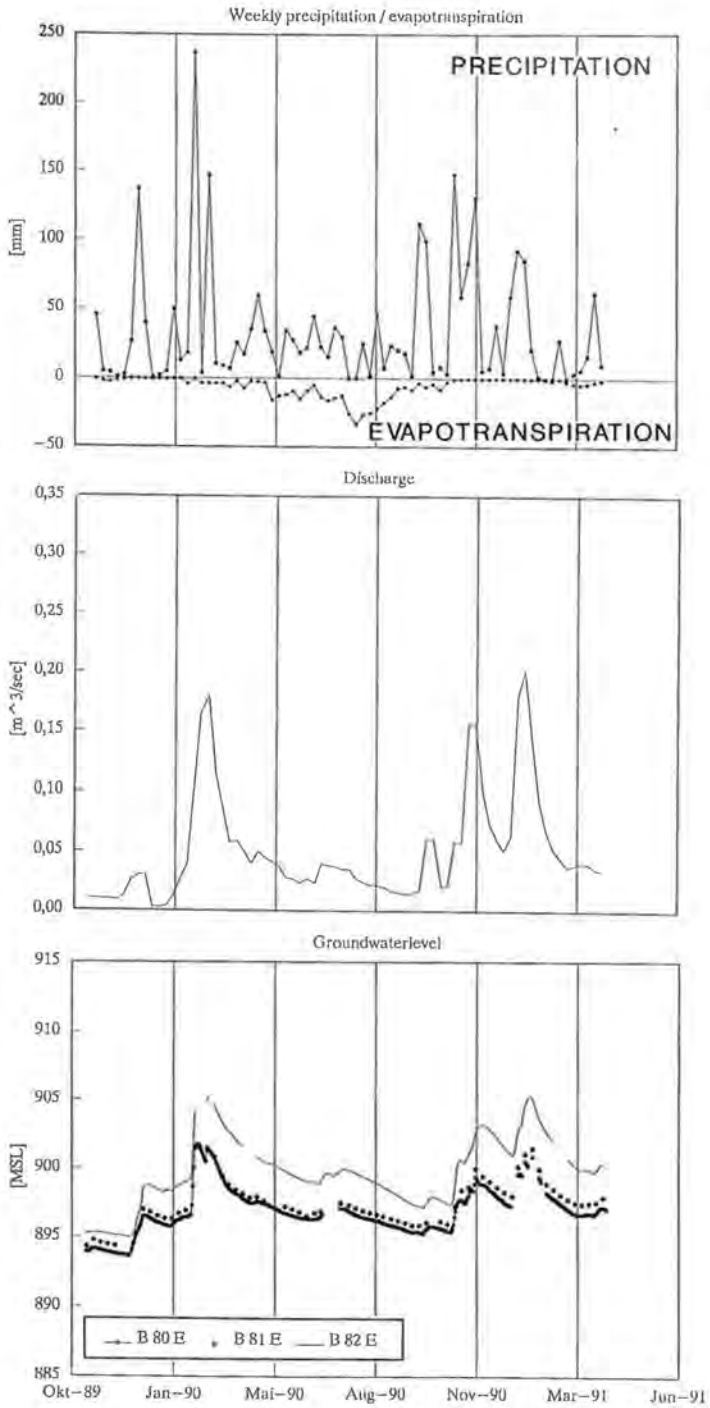

Fig. 3.2: Comparison between precipitation, evapotranspiration, discharge and groundwater level (November 1st, 1989 to March 31st, 1991).

the granitic grus. It is assumed, that these interflow processes may reduce the amount of precipitation contributing to the groundwater recharge of the fissured aquifer lying in the range of 5–10%.

In tab. 3.2 the calculated waterbalance of the Etziboden catchment is presented for the hydrological year 1991. Although the available data base encloses only one hydrological year concerning the runoff measured at the hydrological weirs, the results give a first impression about the hydrological water cycle.

During the hydrological year 1990 a total runoff of 761 mm could be measured at the hydrological weir MW 2. The hydrological input available for groundwater recharge was calculated to 823 mm. The difference between the measured total discharge (761 mm) and the calculated hydrological input (823 mm) is assumed to be related to the groundwater storage due to an increased groundwater level. At the end of the hydrological year 1990 the groundwater level, recorded at the wells B80E and B82E, was 2.1 m higher as at the beginning of the investigations.

By analyzing the discharge curve of the hydrological weir (MW 2) the runoff components were separated. It is assumed that the long-term subsurface runoff amounts 300 mm which refers to 17% of the total precipitation. The surface runoff which also includes the observed interflow was calculated to 369 mm and refers to 21% of the total precipitation. In accordance with field observations a short-term subsurface runoff of approximately 5% was assumed because the drainage of the marsh areas generally shows a delay of a few days due to precipitation. The

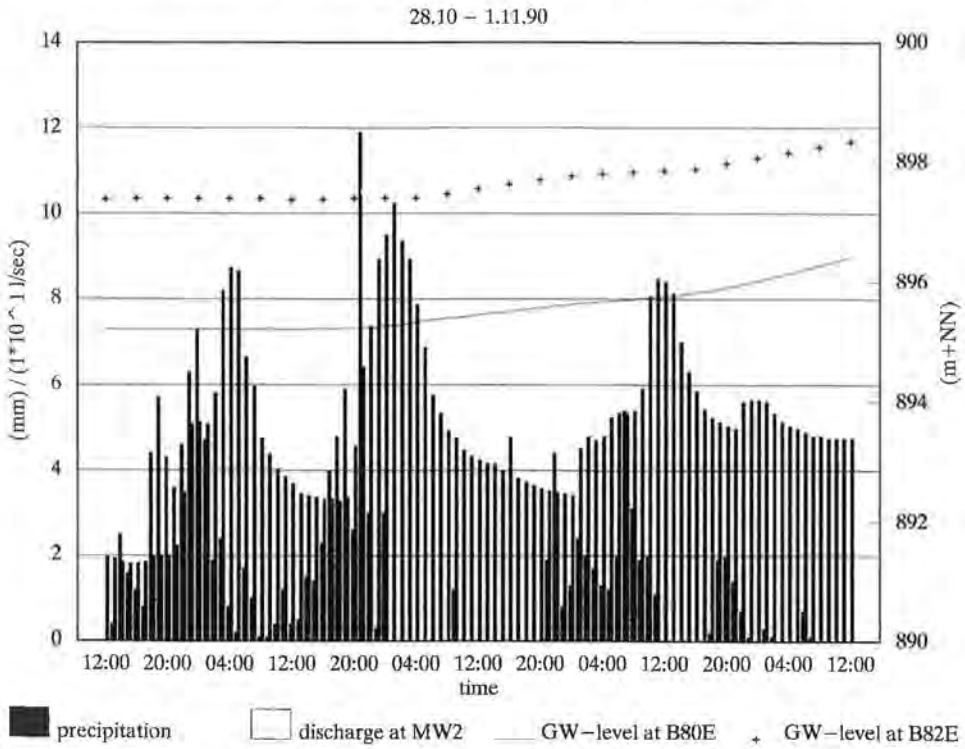

Fig. 3.3: Time related dependence between precipitation, discharge and groundwater level (time steps lasting one hour).

groundwater recharge of the Etziboden catchment, valid for the hydrological year 1990, was calculated to 454 mm which refers to 26% of the total precipitation. It includes the long-term subsurface runoff, the short-term subsurface runoff as well as the storage due to an increased groundwater level (Tab. 3.2).

Tab. 3.2: Test site Lindau: Water balance data of the Etziboden catchment for the year 1990. * *Groundwater recharge = long-term subsurface runoff + short-term subsurface runoff + groundwater storage.*

	[mm]	[%]
Precipitation	1,745	100
Transpiration	412	24
Interception	510	29
Groundwater storage	62	4
Total measured runoff	761	43
Surface runoff and interflow	369	21
Long-term subsurface runoff	300	17
Short-term subsurface runoff	92	5
Groundwater recharge*	454	26

In comparison to that the calculation of the long-term groundwater recharge by means of a modified version of a method proposed by K. KILLE (1979) shows a value of 351 mm for the Ibach catchment which corresponds to 22% of the long-term precipitation. Compared with the 454 mm (26%) of the small catchment Etziboden the difference is not significant. Within the 10 catchments investigated in the Southern Black Forest the values of the Ibach river (11.1 l/s · km²) and the Höllbach (14,4 l/s · km²) are close to the mean value of 12.1 l/s · km², ranging between 7.2–16.9 l/s · km². Further investigations are needed in order to know wether the differences are due to different methods or due to special storage behaviour of the small Etziboden catchment.

3.2. Environmental Isotopes (T. HIMMELSBACH, H. MOSER, V. RAJNER, D. RANK, W. STICHLER, P. TRIMBORN)

3.2.1. Introduction

The environmental isotopes ^3H and ^{18}O occur as constituents of the water molecules ($^3H^1H^{16}O$, $^1H_2{}^{18}O$). Their natural variations in the water cycle could be used as a tool for hydrological studies such as for identification of origin and for estimation of mean residence times in hydrological systems (e.g. IAEA, 1983, H. MOSER & W. RAUERT, 1980).

In the following, preliminary results of a hydrological study carried out at the test site Lindau are presented. The seasonal variations of ^3H- and ^{18}O-contents as well as the long-term trend of ^3H-contents observed in precipitation are used for characterizing the input into the hydrological system of the test site Lindau. The distribution of these isotopes was studied by carrying out a comprehensive sampling and measuring programme. Hydraulic models were used to evaluate the isotopic input and output functions in terms of characteristic hydraulic parameters such as flow velocity and mean residence time of the water in different subsystems.

3.2.2. Sampling Programme

For the sampling programme the facilities of the test site Lindau were used, which include precipitation stations, a lysimeter, suction cups in the unsaturated zone as well as shafts, boreholes and the observation tunnel to access groundwater in different depths (s. fig. 1.3 and chap. 5.2.). In general, series of samples have been taken over a period of three years.

Table 3.3 gives a survey on the samples available for ^{3}H- and ^{18}O-analyses. The vertical subdivision corresponds to the hydrological subsystems of the hydrological cycle to be investigated in the test field and covers a depth interval from the surface to 150 m below surface. Each suction cup (Tab. 3.3) is connected to a 2 l glass bottle evacuated to about 200 mbar; a water sample of about 0.5 l was collected weekly.

Tab. 3.3: Test site Lindau: Sampling programme for ^{3}H- and ^{18}O-analyses.

System	Sampling points	Sampling period
Precipitation:	Hellmann rain gauge at the test site and weather station Todtmoos	10/1987–06/1991 once per week
Unsaturated zone: Glacial deposits and granitic grus	4 profiles with 4 suction cups at different depths down to 2 m	01/1988–06/1991 once per week
Saturated zone: Granitic grus and fissured granite	Boreholes B58S and B62S (30 to 60 m below surface)	01/1988–06/1991 once per week
	Artesian wells B20E and B30E (60 to 80 m below surface)	11/1987–06/1991 every 6 to 8 weeks
Fissured granite	Boreholes and drains in the observation tunnel Lindau (more than 80 m below surface); Outflow from drilling shaft (depth 150 m below surface)	11/1987–05/1991 every 6 to 8 weeks
Granitic grus and fissured granite	Boreholes B42E, B69E, B80E and B76E; sampled in steps of 5 m depth intervals	one single campaign 09/1991

The boreholes B58S and B62S were drilled into the Albtal granite at a hill slope with an angle of 15° to the horizontal plane. The overburden lies in the range from 30–60 m. Therefore, the samples represent water from the shallow and directly precipitation-influenced part of the fissured aquifer. The artesian wells B20E and B30E intersect the ore dike Hermann at depths from 60–80 m below surface, where minor influence from the surface water on the samples can be assumed.

The boreholes in the observation tunnel, which intersect the ore dike and its adjacent fault and fracture zone, are all situated more than 80 m below surface. A direct influence of surface water on the samples can be excluded. The drilling shaft in the tunnel reaches 150 m (70 m below the tunnel). It is completely filled with water and shows a continuous free outflow of approximately 0.5 l/s into the drainage pit of the tunnel. The drainwater samples mentioned in tab. 3.3 originate mainly from dropwater from the tunnel walls. For the localisation of the boreholes and the drain water sampling points see fig. 5.1, chap. 5.

3.2.3. ^{3}H- and ^{18}O-Analyses

The ^{3}H-analyses were performed in the Geotechnisches Institut, Bundesversuchs- und Forschungsanstalt Arsenal, Vienna. The unit "TU" corresponds to a content of 10^{-18} $^{3}H/H$-atoms in the water sample (= 0.118 Bq/l water). The measuring accuracy (2σ-criterion) corresponds to 10% and the detection limit is 1 TU. The ^{18}O-analyses were performed in the GSF-Institut für Hydrologie, Neuherberg. The ^{18}O-values are given as relative ‰-deviation from the standard water "V-SMOW". The measuring accuracy (2σ-criterion) is equal to 0.15‰ ^{18}O.

As an example of the ^{3}H- and ^{18}O-measurements, fig. 3.4 shows the time series of these isotope contents in the precipitation water of the rain gauges at the test site. The values are monthly means weighted according to H. BERGMANN et al. (1986) with the precipitation amount. The well known sinusoidal trend with the winter minima and summer maxima in the ^{18}O-content and with spring maxima and fall minima in the ^{3}H-content can be recognized. Figure 3.4 also shows the time series of ^{3}H- and ^{18}O-contents in the monthly lysimeter outflow. In comparison with the isotope curves of precipitation, a phase shift and a damping of the amplitudes can be recognized.

As a second example, fig. 3.5 gives a comparison of the time series of monthly mean ^{18}O-contents between precipitation and the outflow of the boreholes B58S and B62S also weighted according to H. BERGMANN et al. (1986) with the monthly amount of water. As a consequence of the situation of the sampling sites of the boreholes (s. chap. 3.2.2.), the $\delta^{18}O$-values of the groundwaters follow the general seasonal and annual trend of the precipitation values with damped and phaseshifted amplitudes. So the direct influence of surface water on these boreholes is obvious. The comparison of the ^{18}O-curves of both boreholes gives for B58S a more direct reaction to changes in the $\delta^{18}O$-values of precipitation, especially after the winter minimum, than in B62S.

As a third example, fig. 3.6 gives a comparison between the time series of monthly mean ^{18}O-contents of two suction cups at different depths. The suction cups SC H and SC K are located at depths of approximately 0.5 m and 1.85 m below surface. As a consequence of increasing depth within the unsaturated zone, the $\delta^{18}O$-values of the water samples show a different damping effect. In addition, the amplitudes are phaseshifted against each other as a result of the generally increasing mean residence time with increasing depth. The phase shift between the amplitudes amounts 10 to 12 weeks which refers to an average seepage velocity of 1.2–1.5 cm/day.

3.2.4. Preliminary Evaluation of ^{3}H- and ^{18}O-Analyses

3.2.4.1. Model Approaches

The preliminary evaluation of the measured ^{3}H- and ^{18}O-time series and depth profiles is still limited to rough estimations of mean residence times and, in the case of the unsaturated zone, of seepage velocities. Because of that, the measured output-functions of ^{3}H- and ^{18}O-contents in the depth profiles of the unsaturated zone and in the time series of the lysimeter outflow, as well as of groundwater sampling points, are compared with the inputfunctions of ^{3}H- and ^{18}O-contents in precipitation. For the time period 1987–1990, the measurements of precipitation at the test site were used. For long-term evaluations, the inputfunction was taken from ^{3}H-contents of precipitation in comparable sites measured under the guidance of national and international networks (e.g. IAEA, 1960–1990).

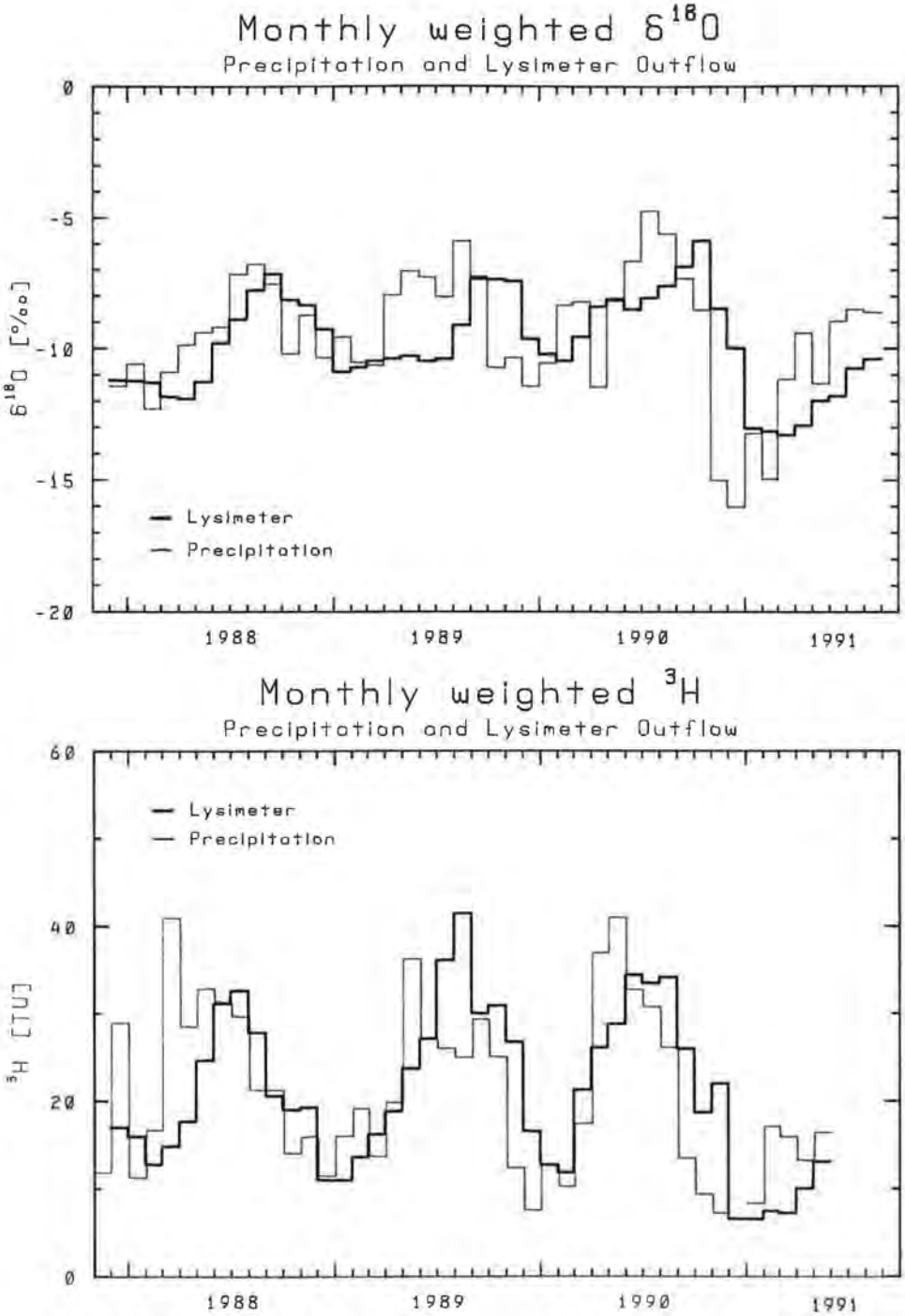

Fig. 3.4: Weighted monthly ^{18}O- (above) and ^{3}H-contents (below) of precipitation (rain gauge at the test site) and lysimeter outflow.

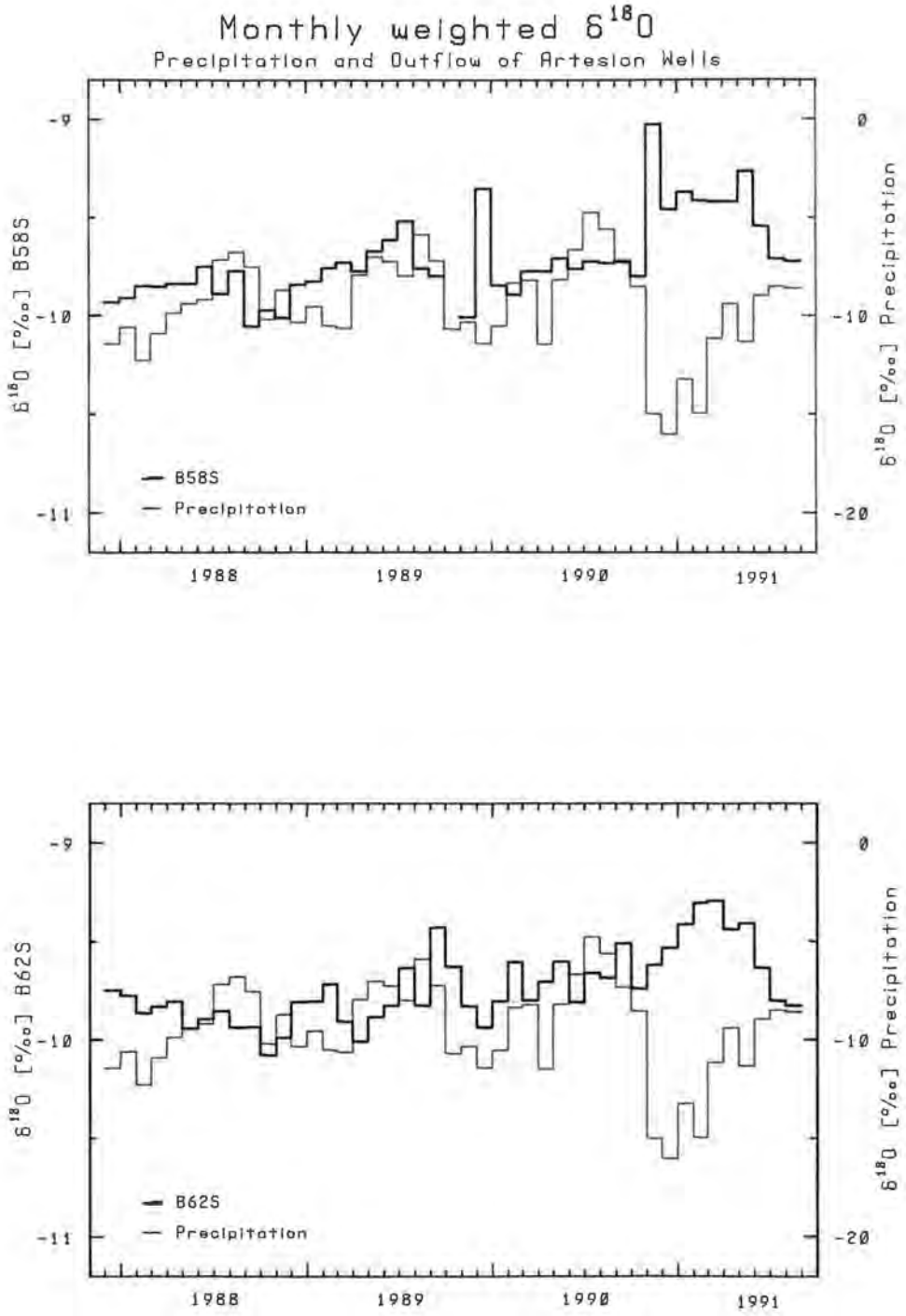

Fig. 3.5: Weighted monthly ^{18}O-content of outflow from horizontal wells B58S (above) and B62S (below) in comparison with corresponding values of precipitation.

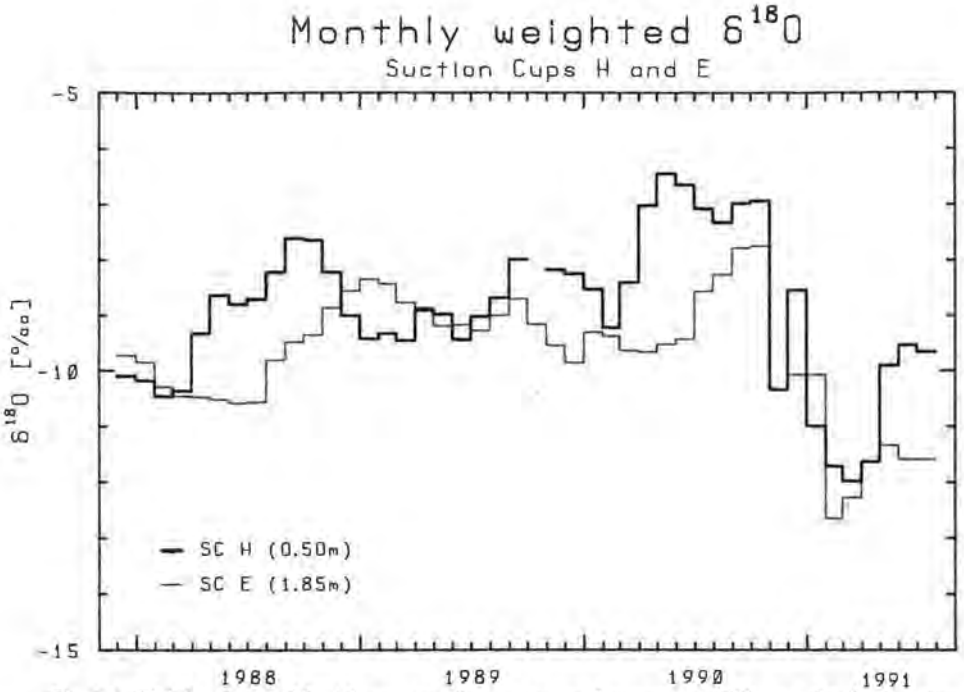

Fig. 3.6: Weighted monthly ^{18}O-content from two suction cups at different depths (suction cup SC H at 0.5 m and suction cup SC E at 1.85 m below surface).

The mathematical approach for the input-output-comparisons was done by simple hydraulic models (s. e.g. H. MOSER & W. RAUERT, 1980):

a) Piston-Flow-Model (PFM)

Using this model, the "peak-peak-method" was applied, comparing extrema in the input- and output functions, or in depth profiles sampled at different times, for a direct estimation of the residence times and the seepage velocities respectively.

b) Exponential-Model (EM)

For this model, a complete mixing with exponentially weighted age distributions at the outflow is assumed. In the case of a ^{18}O-sinusoidal inputfunction, with nearly constant period and amplitudes, the ratio (f) of the amplitudes of the output- and inputfunction can be used to estimate the mean residence time according to the formula

$$T_{0e} = \frac{1}{2\pi} \cdot \sqrt{\frac{1}{f^2} - 1}.$$

For the calculation of T_{0e} applying ^{3}H-data, an inputfunction based on annual mean values was used.

c) Dispersion-Model (DM)

For this model, a dispersive age distribution is assumed. The model is more realistic for seepage processes through the unsaturated zone than the PFM but requires the additional parameter D/vx, where D/v is the longitudinal dispersivity and x the length of the flow path. In the case of the sinusoidal ^{18}O-inputfunction with nearly constant

period and amplitudes, the ratio (f) of the amplitudes of the output- and inputfunction can be used to estimate the mean residence time T_{0d} by the formula

$$T_{0d} = \frac{1}{2\pi} \cdot \sqrt{\frac{-\ln f}{D/vx}}.$$

3.2.4.2. Unsaturated Zone

Suction cups

The depth profiles of ^{18}O-contents in the samples from the suction cups have been treated by means of PFM, EM, and DM. Using the PFM with peak-peak-method, flow times from two to three months result for the 2 m-depth profile corresponding to a mean seepage velocity of 7–12 m/year.

Figure 3.7 gives a survey on the results gained from the application of EM and DM respectively. The detailed residence times between the suction cups in the different profiles and depths are in the range of three to nine months. As expected, the mean residence time increases with depth; the inverse trend of the suction cups SC G and SC C (Profiles 1 and 3 between 0,5 and 1,0 m) may be due to a local increase of the seepage velocity caused by macropores. The mean seepage velocity through the unsaturated zone results from the mean velocity gradient over the distance between 0.5 m and 2.0 m below surface at 1.5 cm up to 3.0 cm/day.

Lysimeter

The evaluation of the mean residence time within the lysimeter, using the ^{18}O-contents in precipitation (input) and in the lysimeter outflow (output) – see fig. 3.4 – led to values of 11 weeks for the EM and of 15 weeks for DM. The dispersion parameter D/vx used in DM was independently determined to 0.15 from the moisture distribution, measured by means of a neutron gauge.

The mean amount of seepage water in the lysimeter outflow corresponds to a precipitation height of 2.7 mm/day. From the lysimeter depth of 1.35 m and the mean residence time of 11 to 15 weeks, a seepage velocity from 1.4–1.7 cm/day results. These seepage velocities correspond quite well with measurements in other lysimeters (e.g. W. STICHLER et al., 1984) and with peak-peak evaluations using extrema of isotope values in the precipitation and lysimeter outflow curves (e.g. the minimum of ^{3}H-content in precipitation in November 1990 which appears in the lysimeter outflow in January 1991).

3.2.4.3. Saturated Zone

The preliminary evaluation of mean residence times of groundwater in the different aquifer subsystems was mainly done by means of EM, using the time series of ^{3}H- and ^{18}O-contents in these subsystems.

Boreholes B58S and B62S (25–45 m below surface)

The time series of ^{18}O-contents (Fig. 3.5) leads to mean residence times of 1.7 years for B58S and 2.3 years for B62S. The evaluation of the available ^{3}H-measurements are not in contradiction with these results.

Artesian wells B20E and B30E (40–60 m below surface)

The mean residence times evaluated from the ratio of amplitudes in time series of ^{18}O-contents in precipitation and in the water samples from B20E and B30E are close to three years for both wells.

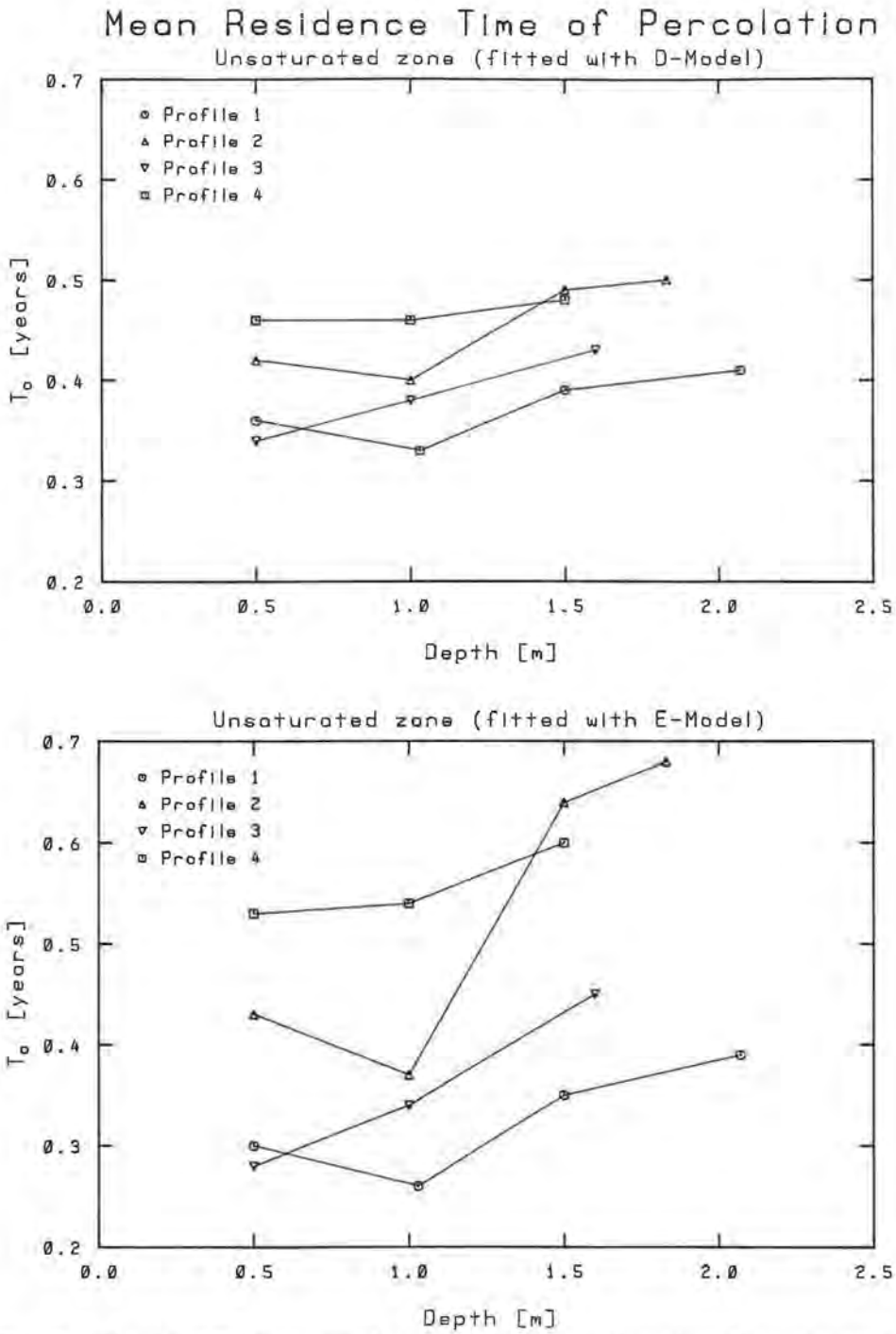

Fig. 3.7: Evaluation of ^{18}O-contents with regard to the mean residence time of water in suction cups situated in different depth profiles.

Sampling points in the observation tunnel (more than 80 m below surface)

The evaluation of mean residence times in the deepest aquifer level under investigation is mainly based upon ^{3}H-data, because of the ^{18}O-content does not show any more seasonal variations in most of these groundwaters. For the determination of mean residence times, the measured time series of ^{3}H-contents in the groundwater samples were fitted with calculated output curves of different mean residence times using the EM. As an example, fig. 3.8 shows the measured time series of ^{3}H-contents (1987–1990) in water samples from the shaft and from the borehole BL5 in the tunnel, as well as calculated curves for groundwaters of different mean residence times by means of EM, based on inputfunctions described in chap. 3.2.4.1. The best fit gives a mean residence time of 5.5 to 6 years for the water in the shaft and 3.5 to 4 years for the samples from BL5.

Table 3.4 presents the evaluated mean residence times for all sampling stations in the tunnel. It can be seen that the waters from the boreholes in the southern part of the tunnel (BL17, BL19) have the lowest values with two to four years; that was confirmed by the rough evaluation of ^{18}O-contents based on EM using the amplitude ratio of seasonal variations.

In the central part of the parallel pit along the ore dike with the boreholes BL6, BL8 and BL10, mean residence times of four up to five years occur. That confirms the hydraulic separation of this part from the other parts of the ore dike (s. chap. 5.).

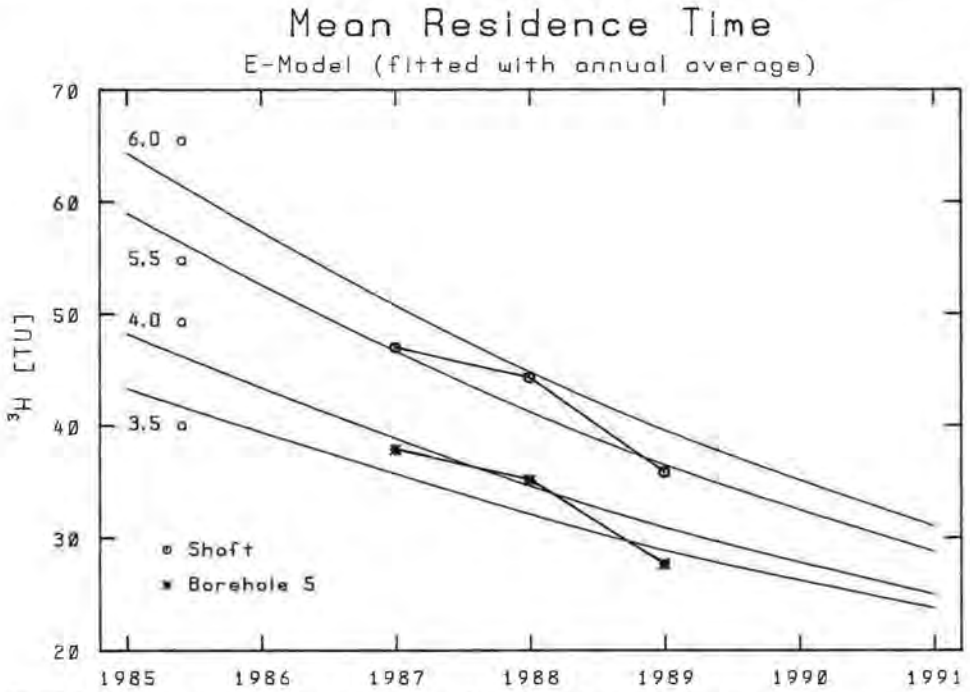

Fig. 3.8: Demonstration of fitting procedure for the evaluation of mean residence times from measured time series of ^{3}H-contents. The calculated curves for different mean residence times are based on the exponential model and an inputfunction for the test site using the time series of ^{3}H-contents of precipitation from Lindau, Konstanz and Vienna (s. chap. 3.2.4.1.).

Tab. 3.4: Test site Lindau: Evaluation of mean residence times for all sampling locations in the observation tunnel Lindau; ^{3}H-data fitted with calculated output curves of different mean residence times using the EM.

Sampling point	Location	Mean residence time from EM based on mean annual ^{3}H-data of water samples in years
Drain 2	half-way into tunnel	1.5 ± 1
Drain 3	two-third-way into tunnel	3.5 ± 1
Drilling shaft	oblique pit	5.5 ± 1
BL12	northern parallel pit	4.0 ± 1
BL2	northern parallel pit	3.5 ± 1
BL5	northern parallel pit	3.5 ± 1
BL6	central parallel pit	4.0 ± 1
BL8	central parallel pit	4.0 ± 1
BL10	central parallel pit	4.5 ± 1
BL14	southern parallel pit	2.0 ± 1
BL17	southern parallel pit	2.0 ± 1
BL19	southern parallel pit	4.0 ± 1
BL20	southern parallel pit	4.5 ± 1

In the southern part of the parallel pit with the boreholes BL2, BL5 and BL12, residence times are evaluated in the range of three to four years. The relatively low value for the samples from the nearby located sampling point "dike" can be explained by a leakage through the tunnelwall in front of the ore dike. This leakage causes a percolation rate of about 1 l/s, which promotes an admixture of recent water.

The relatively high value of mean residence time for the water in the drilling shaft and the relatively low values for the waters of drain 2 and drain 3 can be explained by the different thickness of the overburden of these sampling points. The shaft reaches the deepest aquifer part under investigation. The drains are located at the half-way and two thirds of the tunnel length, where the overburden is relatively thin.

3.2.4.4. Vertical Isotope Profiles of Boreholes

Figure 3.9 shows the ^{3}H- and ^{18}O-contents in water samples taken from different depths in the boreholes B42E, B69E, B79E and B80E. The ^{3}H-profiles of the boreholes B42E, B69E and B80E show a significant jump in depths of 20, 30 and 35 m respectively, which indicates also a jump in the mean residence time. The different waters above and below these jumps are also characterized by different electrolytical conductivities (less than 35 µS/cm and more than 60 µS/cm respectively). This phenomenon can not be observed in the borehole B79E.

^{3}H-contents of about 15 TU, as observed in the upper part of the boreholes B42E, B69E and B80E, correspond to mean residence times of equal to or less than one year, whilst in deeper parts, and in the whole B79E profile with ^{3}H-contents of about 30 TU, mean residence times of more than five years can be expected.

The δ^{18}O-profiles show a general decrease in the upper layers down to a depth of 30 m and further no more significant variations. Due to the lack of knowledge on the development of these profiles with time (only one sampling campaign), it is impossible to differentiate between seasonal variations or waters of different origin, which could explain the variations in the δ^{18}O-profiles.

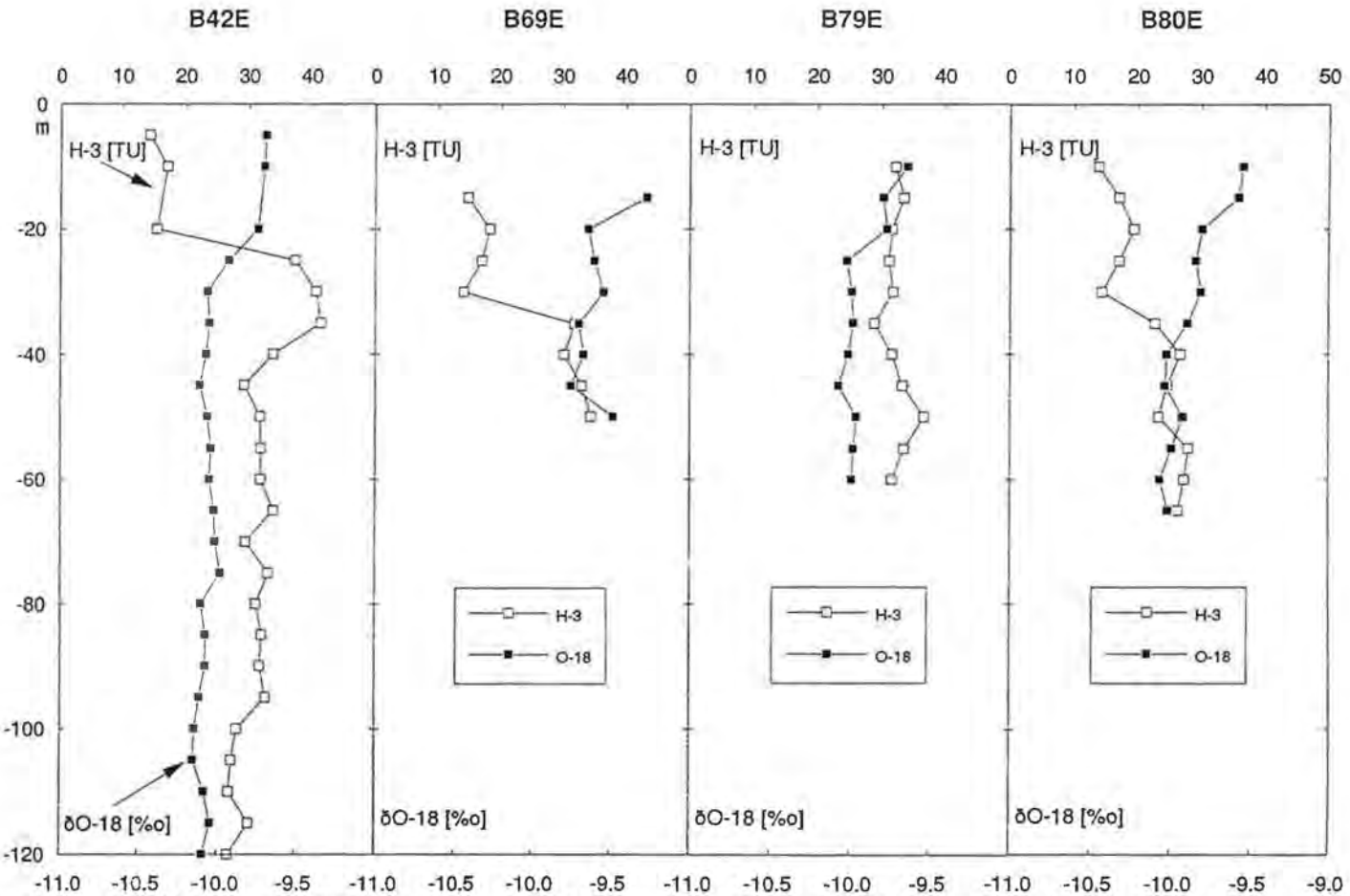

Fig. 3.9: Depth profiles of ^{3}H- and ^{18}O-contents in boreholes. Sampling by means of a submersible electric sampler in steps of 5 m depth intervals.

3.2.5. Preliminary Conclusions

The preliminary evaluation of the ^{3}H- and ^{18}O-analyses on the basis of very simplified hydraulic models (e.g. EM) doesn't consider a system consisting of water components with different mean residence times. For such a consideration the data basis is not yet sufficient. One should bear this in mind in the following conclusions.

As it is to be expected, the mean residence time in the saturated zone generally increases with increasing depth. However, a comparison of mean residence times from the shallow boreholes (B58S and B62S) with those from the artesian wells (B30E and B20E), or with samples from the observation tunnel Lindau, indicates a probable age related stratification of the fissured aquifer under investigation. This vertical stratification is assumed to be responsible for the observed significant differences in the vertical isotope profiles in the boreholes.

All this indicates that the fissured aquifer under investigation at the test site Lindau is divided into two vertical parts. The upper part can be characterized by mean residence times in the order of two years or less. Obviously, this part does not extend towards depths of more than 30 m. The lower part of the aquifer seems to be characterized by mean residence times in the order of up to five years or more. The significant jump in the ^{3}H-content in the vertical profiles indicates that the two parts of the aquifer do not have a direct interchange between each other. The stratification of the aquifer seems to occur within a vertical depth interval of less than 10 m and can be assumed to be characteristic for the test site.

Only in aquifer parts, which are located close to the hydraulic influence of the observation tunnel, this stratification might be disturbed. The tunnel affects the adjacent fissured aquifer in hydraulic terms as a sink due to its permanent, but still not investigated leakage effects. The change of the drainage conditions due to hydraulic experiments carried out in the observation tunnel (s. chap. 5.) may explain the observed relatively high scattering of ^{3}H-values in some tunnel waters.

4. Tracer Experiments under Natural Flow Conditions

(T. Himmelsbach, H. Hötzl, W. Käss, Ch. Leibundgut)

4.1. Purpose and Scope of the Experiments

In the Southern Black Forest old Variscian fault patterns and fracture zones became the ascent path for hydrothermal mineralizations. The resulting ore dikes have been regarded as nearly impermeable geological units for a long time, but recent research has shown that their accompanying fault and fracture zone may have a high permeability (A. Blinde et al., 1982). This relative high permeability is a result of fracturing by tectonic shear processes and by weathering through descendent aquateous solutions as can be observed in the ore dike Hermann. The single, nearly vertical orientated fracture zone of the ore dike with a permeability being some magnitudes higher than the permeability of the adjacent rockmasses creates a specific flow pattern. The draining function of the high permeable fault and fracture zone developes a trough of hydraulic head depression. The hydraulic behaviour of such a system is quite similar to that of a set of discrete parallel fractures (G.P. Kruseman & N.A. De Ridder, 1991).

The thickness of the ore lode Hermann varies between 0.3 m and 3.0 m. It is accompanied by a subparallel fracture zone in the hydrothermal alterated Albtal granite extending a few meters up to 10 m on both sides of the ore dike. The drainage zone has an average width up to 50 m on both sides of the ore lode. Therefore the ore dike Hermann can be characterized as a nearly vertical plane sink whose hydraulic behaviour was specially studied in the recent investigations.

The aim of the tracer experiments which were recently carried out was to provide detailed hydraulic information about the general flow directions, the effective width of the draining zone, the flow velocities and about the mean residence time of water in different parts of the ore lode. The intention of the experiments was to investigate transport processes under natural flow conditions, which means that the natural hydraulic gradient in the ore dike was not affected by pumping or other artificial hydraulic influences. This implies that all boreholes of the Lindau tunnel were closed at this stage of the experiments. Due to the assumption that in a certain distance to the cement plug natural undisturbed hydraulic gradients might exist, the experiments were carried out in two sections of the ore lode which are situated within a sufficient distance to the cement plug.

4.2. Hydraulic Situation in the Test Sections

The permeability of the ore dike stems from uniformly distributed fractures as well as from solution cavities. The fracture aperture and fracture density are reduced with increasing depth so that the ore dike can be regarded as more or less tight up to a depth of approximately 80 m below surface. The ore dike is covered at its top by moraine deposits which are less permeable. In the northern and southern part of the test area, where the ground water level is close to the surface, this causes confined hydraulic condition.

The cement injections carried out in the central part of the test site to avoid underflow of the planned dam axis separate the ore dike hydraulically into two parts. The flow patterns in the northern section are directed towards the location Schwarze Säge which forms the lowest elevation in the northern part of the ore dike. This section was chosen for the first tracer experiment. Several wells which penetrate the ore dike provided the opportunity to inject tracers directly into the dike. The collecting of tracer samples was additionally very easy, because the main probe location was the artesian well B20E which is used for the water supply of the nearby saw mill (Fig. 4.1).

The flow patterns of the ore dike in the S of the cement plug were assumed to have a generally southbound direction. A combined tracer experiment was carried out using the wells B80E and B82E for the injection of the dyes. This boreholes also pentrates the ore dike and its fault and fracture zone. At the location Etziboden, the artesian well B30E, which supplies drinking water for a little village nearby, could be used for collecting tracer samples from the dike (Fig. 4.1).

4.3. Experiments

4.3.1. Tracing in the Northern Ore Dike Section

The first tracer experiment was carried out in 1988. The tracer was injected on October 4th into the ore dike and its adjacent fault and fracture zone using the oblique

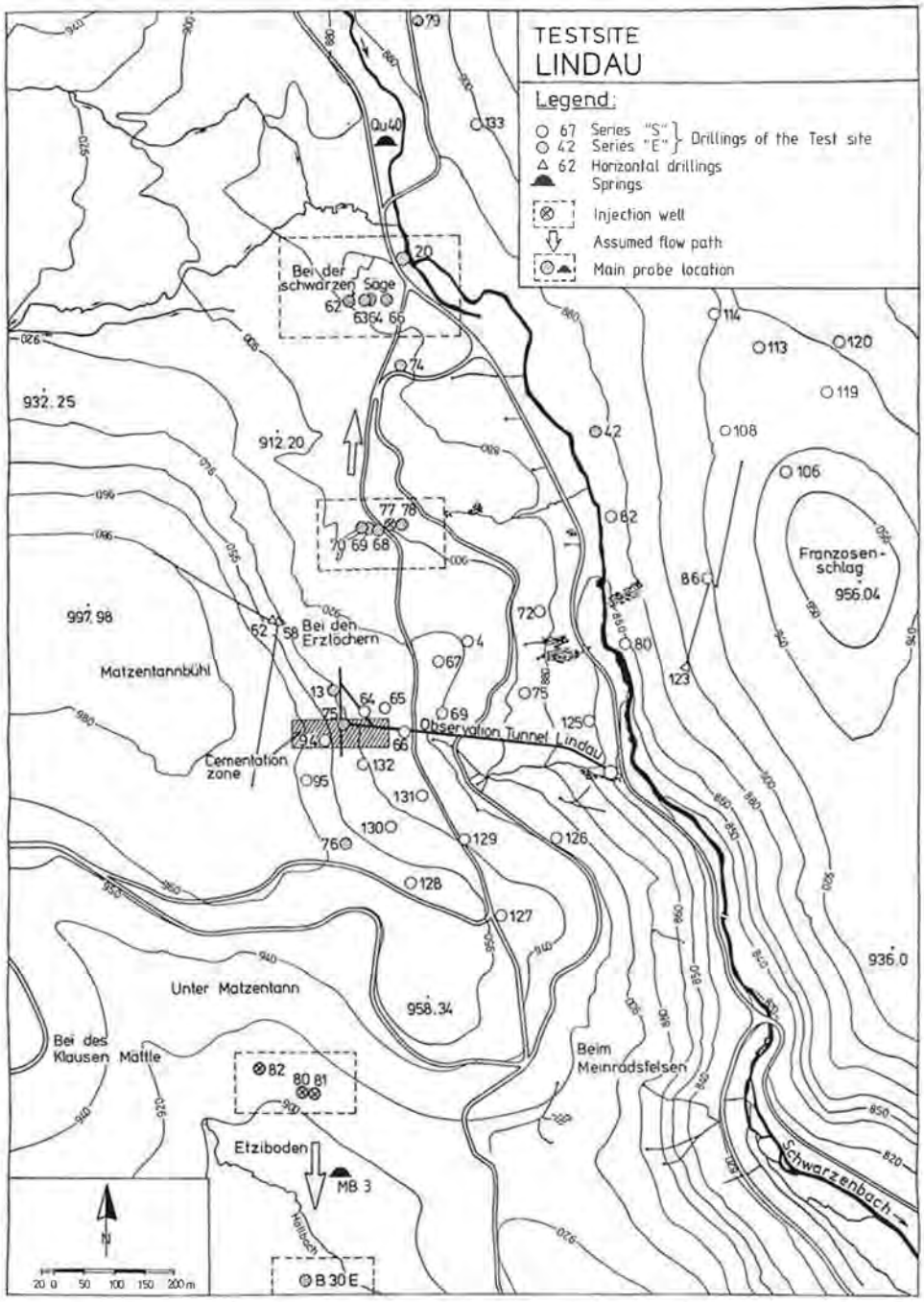

Fig. 4.1: Assumed flow directions and injection and main probe locations for the tracer experiments.

45° declined borehole B77E which intersects the ore dike Hermann at depths between 50 m and 80 m below surface (Fig. 4.2). As tracer 2 kg of EOSIN was used after being dissolved within 80 l of water. The tracer solution was injected using an injector at the end of a thin plastic hose which was placed within the fractured part of the ore dike to prevent any losses of tracer into the unsaturated zone. After the injection of the tracer 2 m^3 of water was pumped into the borehole to flush the fluorescent dyes into the fractures. Together with the fluorescent tracer a suspension of 2×10^6 microspheres (diameter 0.98 µm) made of polystyrene was injected. The suspension of the microspheres, consisting of a 1 ml ampoule, was diluted before with 1 l of water containing some drops of a detergent to reduce the surface tension of the water.

The main emphasis of tracer sampling was laid upon the artesian well B20E which is situated north of the injection well B77E (Fig. 4.1). The oblique 45° declined probe well B20E penetrates the ore dike as well as the fault and fracture zone completely at a depth of approximately 100 m below surface. The interwell distance between the injection well (B77E) and the artesian probe well (B20E) is 346 m, referring to the piercement of the wells through the ore dike. In advance of the tracer injection

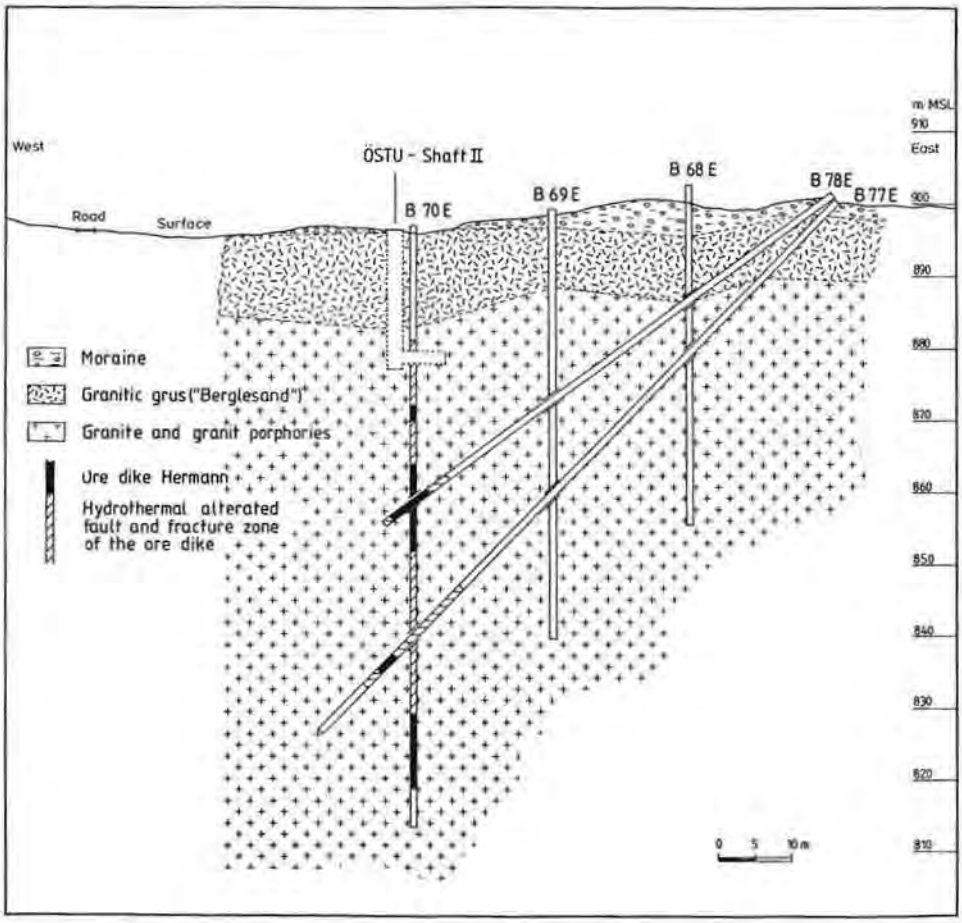

Fig. 4.2: Cross section through the ore dike Hermann, injection well B77E (T. Himmelsbach, 1992).

the artesian probe well was opened to a free discharge rate of about 3.5 l/s to enhance the interwell hydraulic gradient between the wells. According to the assumption that the breakthrough of tracer would occur first at this location the well was equipped with an automatic sampling device whose time interval was set at first to four hours and was later increased up to 12 hours. The wells B62E, B63E and B64E intersecting the ore dike and its adjacent fault and fracture zone as well as the probe well B20E were additionally equipped with small electric submersible pumps which were located within the fractured part of the ore dike Hermann (Fig. 4.1). The vertical observation wells intersect the ore dike at depths ranging between 20 m and 50 m below surface.

For the detection of patterns other than the assumed main flow patterns the springs in the vicinity of the above cited wells and in the valley of the Schwarzenbach were also monitored during the experiment. The samples from the springs were collected at the beginning of the experiment twice a day and later on once a week (Fig. 4.1).

The hydraulic heads at the observation wells B62E and B64E were monitored continuously using automatic water level recorders to calculate the hydraulic interwell gradient valid for the experiment. The injection of tracer was carried out under general low ground water conditions. At the beginning of the experiment the interwell hydraulic gradient was in the range of up to 0.5%, but raised, due to an high amount of precipitation during November and December, up to 1.5%. The average hydraulic gradient during the whole experiment was about 1%.

Fifteen days after the injection first traces of EOSIN could be found in the artesian well B20E. Within 41 days after the injection the breakthrough of tracer reached its maximum concentration (Tab. 4.1). Within another 80 days it decreased to an amount of only 20% of the measured peak concentration and changed into a long tailing effect of continuously decreasing concentrations. The tailing effect of the tracer breakthrough can still be observed even three years after the injection and is assumed to last at least for the next few years (Fig. 4.3).

Six months after the injection of EOSIN first traces of the fluorescent dye could also be observed in samples of two springs lying 240 m north of the artesian well B20E (Qu 40, Qu 41). These springs are located at a marshy area where the ore dike Hermann infiltrates into the moraine deposits overlaying the granitic grus (Fig. 4.1). The observed concentration at the springs, however, reached only 15% of the concentration observed at the artesian well B20E and changed very rapidly due to precipitation. During periods of general low water level conditions generally occuring during the summer months, the springs became nearly dry. It can be assumed that under these hydrological conditions the dike infiltrated diffusely into the Schwarzenbach (Tab. 4.1).

Even though the wells B62E, B63E and B64E penetrate the ore dike Hermann as well as its adjacent fault and fracture zone, never any fluorescent dye could be observed in samples from these wells. Obviously the migration of the tracer the ore dike was restricted to depths below the level explored by the wells. In the springs along the right slope of the Schwarzenbach valley no traces of EOSIN could be proved. This fact may be interpreted in the way that the migration of tracer occurred only within the trough of hydraulic head depression caused by the ore dike and its fault and fracture zone. Therefore the crossing NW–SE striking rhyoloitic dikes and granite-porphyries did not cause any hydraulic losses of tracers into other flow paths than the presumed flow patterns.

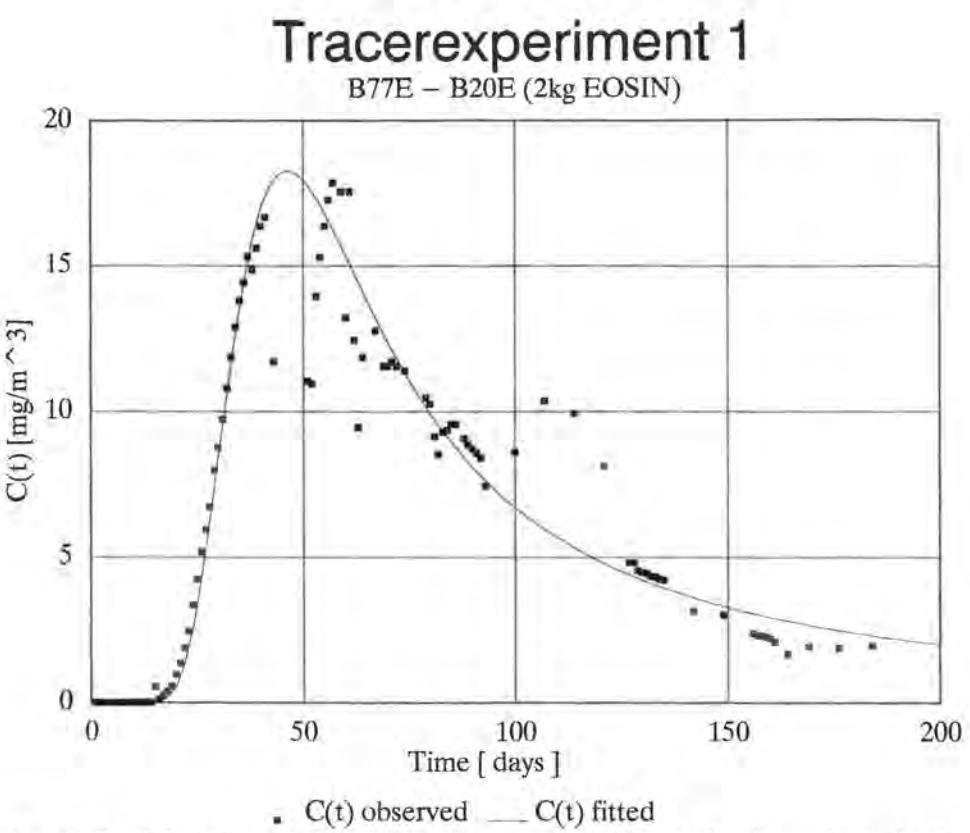

Fig. 4.3: Breakthrough curve of the first tracer experiment with EOSIN at the artesian well B20E (Northern ore dike section).

The microspheres of polystyrene which were injected together with the fluorescent dye could be observed only in samples of the artesian well B20E. However, their breakthrough occurred with a delay of about six months in comparison to the breakthrough of the EOSIN. Even though the detection of flow patterns using microspheres is possible the principal suitability of this method in fractured aquifers could not be proved. However, a quantitative interpretation of the results of the microspheres, especially with regard to transport modelling, is impossible (Tab. 4.1).

4.3.2. Tracing in the Southern Ore Dike Section

The second tracer experiment was carried out in the ore dike section lying 500 m south of the cement plug near the location Etziboden (Fig. 4.1). In a combined tracer experiment 2 kg EOSIN and 2 kg PYRANIN were injected on April 27th directly into the ore dike and its adjacent fault and fracture zone. The injection was done using the boreholes B80E (EOSIN) and B82E (PYRANIN) which both penetrate the ore dike as well as its fracture zone. Each tracer was diluted within 80 l of water and was subsequently injected using the same injector device as already described in chap. 4.3.1. The injector was placed in each borehole at the most fractured part of the ore dike at varying depths between 20 m and 40 m below ground surface.

After the injection 2 m^3 of water was pumped into each borehole to flush the dyes into the fractures.

According to the presumed flow paths the tracer sampling was focused upon the artesian well B30E which is situated south of the injection wells. The oblique 45° declined borehole B30E penetrates the ore dike at depths between 45 m and 50 m below ground surface. The distance between the injection wells and the probe wells amounts 280 m, referring to the location where the wells pierce the ore dike. The artesian well B30E, which supplies drinking water to a nearby village, has an average outflow of 3.5 l/s, varying only within narrow ranges.

For the detection of patterns other than the presumed flow paths the springs in the vicinity of the injection wells as well as the springs along the rivulet Höllbach were monitored throughout the experiment. The tracer sampling was carried out once a week according to the results of the first tracer experiment. The groundwater levels at the boreholes B80E and B82E were monitored during the experiment to calculate the interwell gradient between the injection and the main probe location. Due to the assumption that the breakthrough of tracer would occur first at the artesian well B30E its well shaft was equipped with an automatic sampling device whose time interval was set at first to 12 hours and later to once a day.

Twelve days after the injection of the fluorescent dyes first traces of EOSIN could already be observed in one spring (MB 3) lying 171 m south of the borehole B80E (EOSIN). The measured concentration of EOSIN reached its maximum within only 48 days after injection and decreased later within a further 60 days to a tracer concentration in the range of 25% of the observed peak concentration. The breakthrough curve of the measured tracer concentration changed into a long tailing effect similar to the breakthrough curve of the first tracer experiment at the northern ore dike section (Fig. 4.4). However, this tailing showed a strong correlation with the general groundwater level (B80E and B82E). As the groundwater level increased the tracer concentration always decreased within a short time. Obviously, an increasing infiltration caused a dilution of the tracer in the groundwater of the granitic grus. The total recovery of EOSIN at the probe location MB 3 reached an amount of only 2% during the first two years.

Even though the wells B80E and B82E were assumed to penetrate the same fault and fracture zone, no traces of EOSIN (B80E) could be yet observed in tracer samples derived from the artesian well B30E. The breakthrough of EOSIN at only one spring (MB 3) may be explained by an oblique orientated fracture zone intersecting the borehole B80E at shallow depths between 20.4 m and 21.4 m below the ground surface (B. TROSCHKE, 1990, T. MEYER, 1991). This fracture intersects the borehole B80E close to the border between the Albtal granite and its overlaying granitic grus. The fracture extends into the granitic grus and favours the further migration of the EOSIN in the granitic detritus. This may explain the observed flow pattern towards the probe location MB 3 (EOSIN) lying a little aside the presumed direction of migration within the ore dike.

In samples of others than the above cited spring as well as in the samples of the artesian well B30E neither any traces of EOSIN nor of PYRANIN could ever be observed throughout the whole experiment lasting more than two years. Although tracer samples were taken six months after injection from the wells B80E and B82E, indicating that the injected dyes had been flushed completely into the ore dike system, their further migration, obviously, followed other than the presumed flow patterns. Subsequent detailed geological investigations pointed out the probable existence

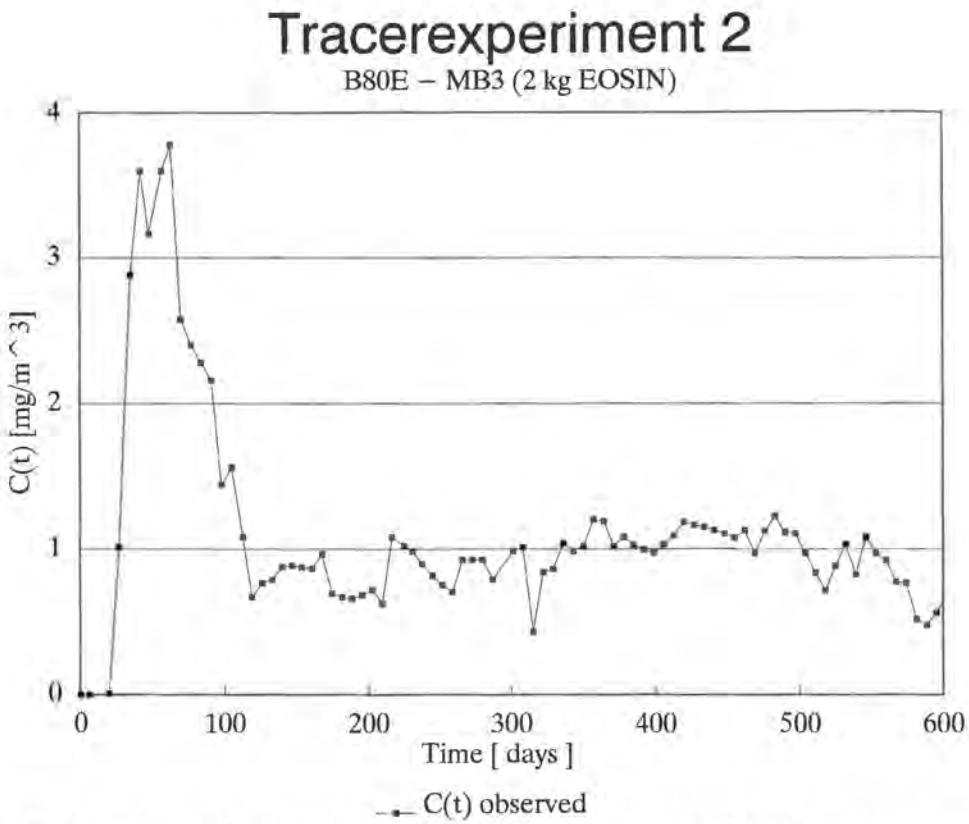

Fig. 4.4: Breakthrough curve of the second, combined tracer experiment at the spring MB 3 (EOSIN, southern ore dike section).

of a thin NW–SE striking porphyry dike, which might intersect the presumed flow path towards the artesian well B30E (J. MELLERT, 1989). Although, the existence of such a porphyry dike is still surrounded by uncertainties, it might be a plausible

Tab. 4.1: Test site Lindau: Results of the tracer experiments within the fault and fracture zone of the ore dike Hermann.

Probe location	Distance [m]	First arrival [days]	Maximum [days]	Mean residence time [days]
B20E (Eosin)	346	15	57	35
B20E (Microspheres)	346	225	310	–
Qu. 40 Eosin)	540	163	233	–
MB 3 (Eosin)	171	12	46	–

explanation for the "loss" of an amount of nearly 4 kg fluorescent dyes. If the migration of the dyes became restricted to deep levels within such a porphyry dike their detection at springs would be nearly impossible due to the high mean residence time expected in such a system.

4.4. Conclusions

The tracer experiments at the test site confirmed the significant role of the anisotropy as well as the valuacy of the joint system controlling the migration processes in a fissured aquifer. This fact implies that a detailed hydrogeological investigation is requested in advance of the injection of the dyes to detect all probable flow patterns in the area of investigation. However, even when the main fault patterns as well as the general striking of dikes seem to be well known, like at the test site Lindau with its numerous drillings, there still exists a relatively high probability to loose artificial tracer in parts of a fissured aquifer having a very slow exchange with the surface.

The mean residence time of artificial tracer in a fissured aquifer is directly controlled by the specific flow rate through a single fracture:

$$q = \frac{g\,(2\,b)^3\,i}{12\,\nu},$$

with

q = specific flow rate,
ν = dynamic viscosity,
i = hydraulic gradient,
2b = fissure aperture,
g = gravity acceleration.

It becomes obvious that the mobile water in a fissured aquifer is restricted to fractures having a sufficient fracture aperture. However, the immobile water content of the aquifer can only be affected by the relatively slow processes of matrix diffusion which is responsible for the generally observed tailing effect of breakthrough curves (s. also chap. 5.). Although the flow velocities in a fault and fracture zone may reach values being much higher than the velocities in porous aquifers, the overall time required for the reliable observation and evaluation of a tracer experiment in a fissured aquifer is often much greater than for porous aquifers. This "time effect" must be kept in mind, especially when performing tracer experiments in fissured rocks.

The tracing of groundwater in narrow fracture systems requires long running experiments. The overall time, necessary for the sufficient detection of the breakthrough curve, is then likely in the range of a few years. In addition, a detailed programm concerning the tracer sampling is necessary to avoid a vast amount of tracer samples. Furthermore, automatic sampling devices are recommended to reduce the financial costs of such an experiment.

In the present case only the tracer experiment at the northern test section between the wells B77E and B20E allowed a quantitative interpretation (s. also chap. 5.), because some of the hydraulic boundary conditions, which were valid for the experiment, could be fixed sufficiently well. Especially the constant discharge rate at the artesian well B20E and the direct hydraulic contact between the injection well

and the probe well by a dominant fracture system favoured the migration of the tracers. However, the measured recovery rate of tracer, lying near 8%, reveals that a high amount of tracer followed other than the presumed flow paths. Beside the problems due to the quantification of matrix diffusion effects, it seems that the migration of tracer was restricted likely to depths which were not explored by the test wells.

The tracer experiment carried out at the southern test section, however did not allow any attempts to apply mathematical transport. The main problem for the evaluation of this experiment lies in the superposition of the deep fracture flow by a fast subsurface discharge in the granitic grus.

5. Tracer Tests and Hydraulic Investigations in the Observation Tunnel Lindau (T. HIMMELSBACH, P. MALOSZEWSKI)

5.1. Introduction

One of the most important preconditions for a quantitative analysis of tracer experiments using mathematical models is the definition of the hydraulic boundary conditions valid for the experiment. Fortunately, in the Lindau observation tunnel a test site could be established which allows to determine the hydraulic boundary conditions. The great advantage of the experimental site lies in the possibilty to induce the hydraulic gradient in the test section. The latter can be influenced artifically in a wide range by changing the discharge and recharge rate at the test wells. With the help of an electric pump the interwell flow field can be forced to steady-state conditions, thereby supplying another important precondition for the later quantitative analysis of the experiments. The tracer experiments can be executed over different distances by involving different well pairs which explore different sections of the ore dike.

5.2. Site Description

5.2.1. Lindau Observation Tunnel

The observation tunnel Lindau, which was used for the tracer experiments, has a length of about 460 m and bifurcates near its end into two pits both penetrating the ore dike Hermann. The oblique pit as well as the main tunnel enter into the parallel pit which is aligned parallel to the striking of the ore dike. The parallel pit was excavated a few meters beside the ore dike which is nearly upright orientated and shows a northbound striking (5/85E). The thickness of the ore dike varies between 0.3 m and 3 m.

From the parallel pit 21 boreholes were drilled into the ore dike. The drillings are located at borehole galleries, lying within an average distance of 10 m to each other. The boreholes were drilled as vertically orientated, fan shaped profiles, consisting of one borehole in the centre and two inclined boreholes 45° up- and downward. All the drillings were made using a rockbit of 2" diameter and penetrated the ore dike completely. They detect the ore dike Hermann over a horizontal distance of approximately 150 m (Fig. 5.1). The wells are closed by stainless steel shut-in

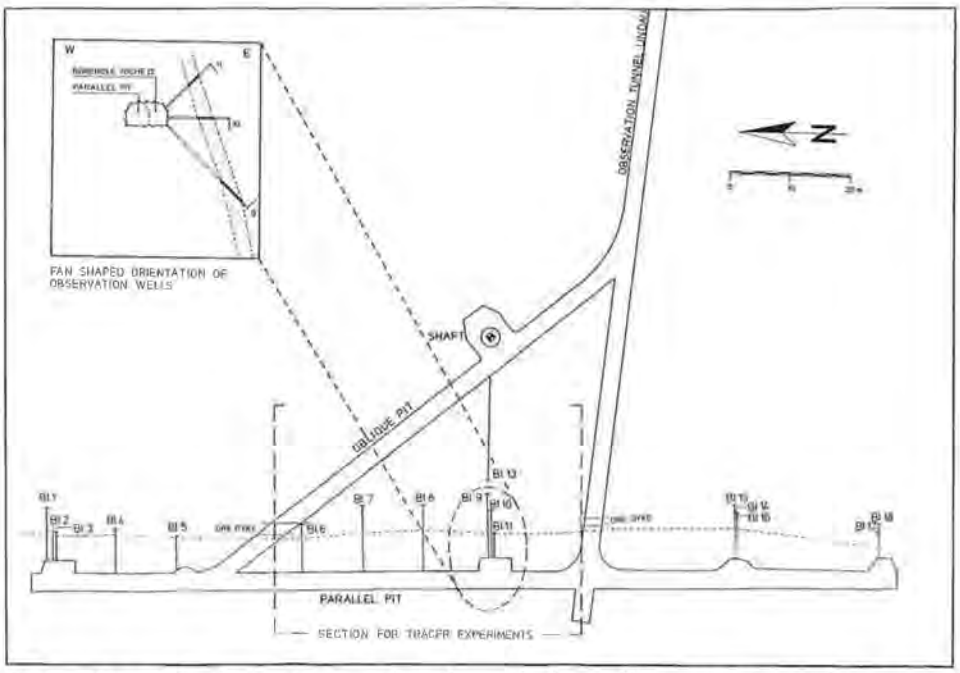

Fig. 5.1: Map of the observation tunnel Lindau with the ore dike section choosen for the tracer experiments (T. HIMMELSBACH, 1992).

valves. The well heads are equipped with pressure gauges to measure the hydraulic head in the ore dike.

5.2.2. Hydraulic Characterization of the Ore Dike Hermann

The permeability of the dike is a result of secondary solution cavities and a set of faults and fractures striking within and parallel to the ore dike. Due to this fact the ore dike has a much higher permeabilty in comparison to the adjacent rockmasses formed by the Albtal granite. During the excavation of the Lindau tunnel and during the later drilling campaigns, some nearly impermeable sections of the ore lode were detected lying very close to other parts of the ore dike having a high permeability. These "transmissive" sections of the ore dike are considered to exist of discrete parallel fractures which are intersecting the wells. Due to the observed changes in permeabilty within horizontal distances lying in the range of few tens of meters, these discrete fractures are assumed to have only a finite lateral extension. Accordingly, the lateral extension of such "transmissive" fractures is a magnitude smaller than the scale of the experimental site.

The sealing of the cavernous ore lode by the cement injection seperated the ore dike hydraulically into two sections showing different hydraulic heads. The southern part of the ore lode has a hydraulic head up to 60 m. The section of the ore dike lying north of the cement plug only shows hydraulic heads in the range of 25 m. The difference in hydraulic head occurs within a horizontal distance of less than 20 m. During the experiments never any hydraulic exchange between these two sections could be observed. In addition, the distribution of the hydraulic head is

uniform for each section of the ore dike, leading to the assumption that the natural hydraulic gradient must be close to zero. Hence, with a natural hydraulic gradient being negligible, the natural flow field in the test section can be assumed to ly under stagnant water conditions. This assumption can be proved easily by coupling the wells through a pressure hose and a sensitive flow meter. The lack of any detectable flux confirms the above assumption of stagnant water conditions. Accordingly, the hydraulic interwell gradient may now be influenced artificially.

5.3. Hydraulic Investigations

5.3.1. Preliminary Pulse Interference Tests

The detection of hydraulic contacts between different parts of the ore dike was an important precondition for the further tracer experiments. The aim of these qualitative, early hydraulic investigations was to evaluate the length as well as the orientation of "transmissive" sets of parallel fractures to choose an appropriate test section. For this purpose pulse interference tests were carried out between different well pairs to determine an ore dike section, supplying a sufficient hydraulic contact between the test wells. The pulse interference tests were done by opening the shut-in valve of a test well for a short time (between five and 20 seconds). The decrease as well as the recovery of hydraulic head were measured by electronic pressure transducers and monitored continuously for the test well and the observation wells. The experiments were performed for different cross hole arrangements affecting different parts of the ore lode. An example of the results of a pulse interference test is given in fig. 5.2.

The pulse interference tests were evaluated only in a qualitative way by interpreting the phase shift of the maximum head decrease between the test and the observation wells. In addition, the damping effects of the recorded pressure signals at the observation well were interpreted. During the pulse interference tests, generally two different types of hydraulic response could be observed. If the phase shift between the maximum head decrease for the test and the observation wells became nearly negligible, the drawdown effect extended obviously directly towards the observation well. Accordingly, the assumption was made that a discrete set of parallel fractures intersect both the test well and the observation well.

However, if a zone of decreasing permeability was detected between the test well and the observation well, the phase shift of head decrease became evident and the pressure signals at the observation well were reduced so extremely they became difficult to be determined. Hence, the test well and the observation well do not intersect the same set of parallel fractures.

The pulse interference tests confirmed a previous assumption, based upon geological data, that the ore dike of the central section of the parallel pit is hydraulically separated from all other parts of the ore lode. Any hydraulic contact was never detected, neither towards the northern part nor towards the southern part of the ore dike. Due to its hydraulic separation the central section of the parallel pit was chosen as a migration test site for the further tracer experiments.

The hydraulic pulse interference tests carried out for different cross hole arrangements allowed in addition a first rough estimation about the lateral extension of a discrete set of parallel fractures. Obviously, the drillings BL8, BL9, BL10 and BL11 intersect the same discrete set of parallel fractures. However, this assumed

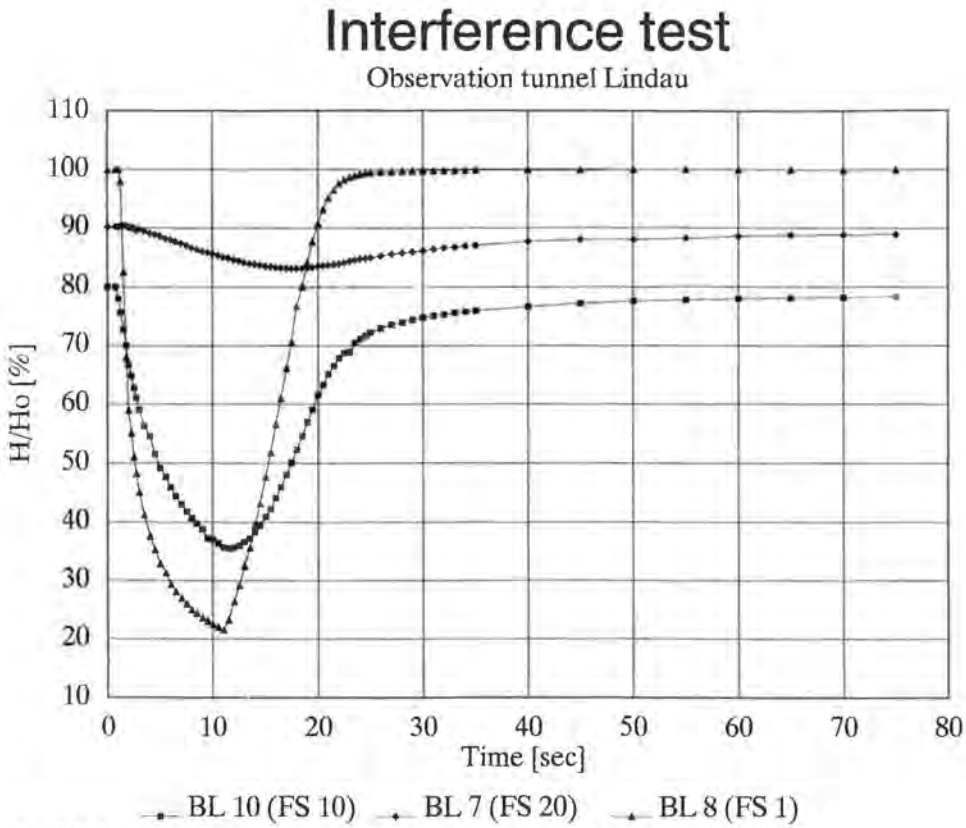

Fig. 5.2: Interference test in the centre part of the observation tunnel Lindau.

set of parallel fractures does not extend towards the wells BL7 and BL6. The wells of the central part of the parallel pit are generally located within a horizontal distance between 10 and 15 m to each other. In conclusion the extension of a discrete set of fractures must have the same magnitude.

5.3.2. Hydraulic Tests in Boreholes

In preparation of the tracer tests several hydraulic tests were carried out to evaluate the transmissivity of the ore dike section under investigation. The objective of these early hydraulic testing was to predict the groundwater flow velocities and to investigate wether the fissures may change their hydraulic behaviour due to the imprinted artificial flow field. The hydraulic tests were generally performed as constant head tests. A constant injection or withdrawal head was applied for a flow period of approximately 15 minutes. During the entire test series the water for injection was taken from the central part of the ore dike Hermann. This means that no additional water was allowed to enter the flow system to avoid any alteration of the fissure system due to hydrochemical interactions.

First of all different well pairs were coupled by a MOHNO-pump and the standpipes of the drillings were equipped with pressure tranducers to record the hydraulic head. The MOHNO-pump was used to impress a steady-state dipol flow

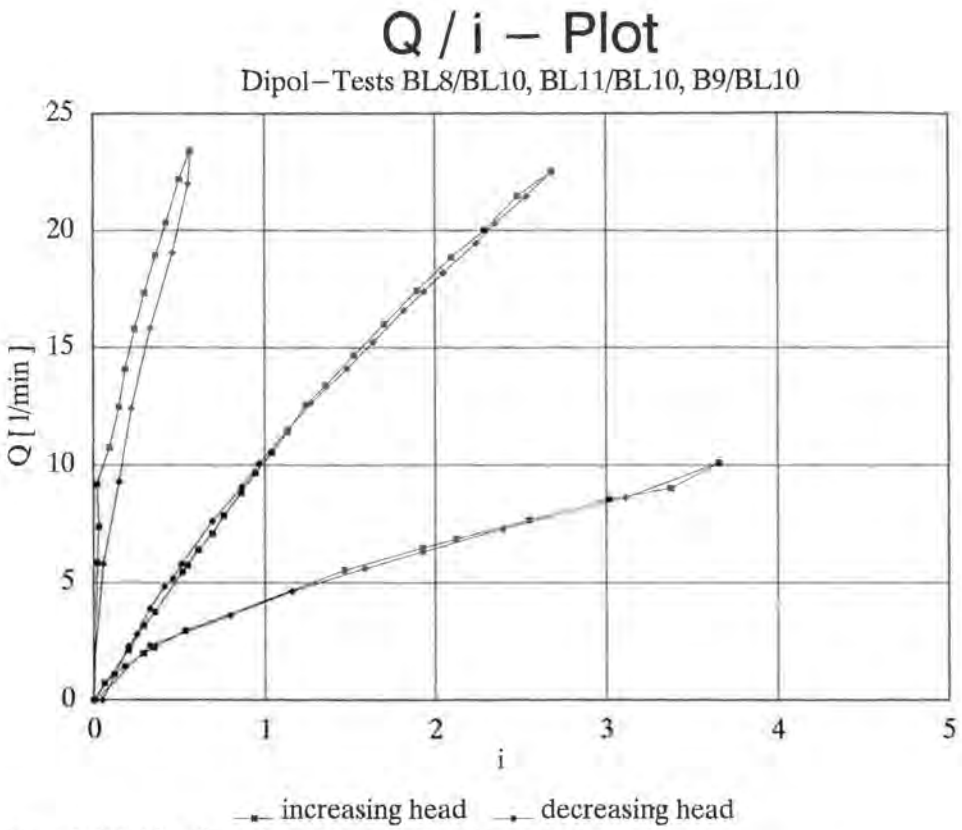

Fig. 5.3: Q/i-Plot of steady-state injection-withdrawal tests.

field of equal strength (s. chap. 5.4.) between the test wells. The flow rate through the MOHNO-pump was increased subsequently by steps of equal time intervals. As to be expected after a few minutes the steady-state flow conditions were achieved and the flow rate and the resulting hydraulic heads were recorded.

During the hydraulic testing the MOHNO-pump did not show any measurable fluctuations in its flow rate and the tests were performed for several cross hole arrangements. A plot of the realized pumping rate against the resulting hydraulic gradient shows that the values for the increasing hydraulic head as well for the decreasing hydraulic head are aligned along a nearly straight line (Fig. 5.3). Although the flow rate was increased in several steps up to approximately 25 l/s neither any erosion nor any obstruction of the fissures due to the imprinted flow field could be observed.

Due to the nearly straight alignement of the experimental data it is further assumed that the resulting flow field was laminar and no turbulent flow conditions occured within the tested ore dike section (W. KOPPELBERG, 1986).

The steady-state injection and withdrawal tests were evaluated according the following relation

$$T = \frac{Q}{H\,m}\,C,$$

where T is the steady-state transmissivity (m/s^2), Q is the flow rate through the MOHNO-pump (m^3/s), H is the injection head at the end of the flow period (m) and m is the thickness of the ore dike (m). The constant factor C depends on the approach whatever is choosen and involves the radius of influence (R) (e.g. S.W. LOHR, 1969) or the length of the flow line (L) (USBR, 1963) for the calculation of the transmissivity. The radius of influence (R) is a potential source of error, because it was estimated with the help of the previous hydraulic interference tests. However, the transmissivity is proportional to the logarithmus of R and is, therefore not very sensitive to incorrect assumptions. The length of the flow line was assumed to be equivalent to the thickness of the ore dike drilled by the test well, because during the drilling a worth mentioning percolation occured only within the fractured ore dike Hermann.

In tab. 5.1 the average transmissivities (T) from the hydraulic tests are listed. The transmissivity of the ore dike Hermann in the central part of the parallel pit (Fig. 5.1) is in the order of 5×10^{-6} m^2/s up to 1×10^{-4} m^2/s. The transmissivities calculated for the boreholes BL8, BL9 and BL10 lie relatively close to each other and differ only in the range of half a magnitude. The well pair BL8 and BL10 was therefore assumed as an ideal test section for the later tracer experiments. Much larger differences concerning the transmissivity occur towards the other test wells BL11 and BL7.

The vertical orientated borehole profile BL9 – BL10 – BL11 was therefore choosen as the second test section for tracer experiments. With regard to the later strained quantitative analyses of the tracer experiments a "mean transmissivity" of the test section had to be determined because the transmissivity determined by hydraulic tests in single wells are assumed to be valid only for the direct vicinity around the test well. The "mean transmissivity" of the test sections, however, was determined by involving the hydraulic head relationships of a dipol flow field. According to R.J.M. DE WIEST (1965) and D.S. WEBSTER (1970) the "mean transmissivity" of the test sections was estimated as

$$T \approx \frac{Q}{\pi \Delta H} \ln \frac{X}{r_w},$$

where T represents the "mean transmissivity" (m^2/s), Q is the discharge-recharge rate (m^3/s), X is the distance between the wells, ΔH is the difference in hydraulic head (m) and r_w is the radius of the test wells.

For the planned main test sections (BL8 – BL10, BL9 – BL11) this approach yielded a "mean transmissivity" of 1.36×10^{-5} m^2/s and 2.47×10^{-5} m^2/s respectively.

Tab. 5.1: Test site Lindau: Average transmissivities calculated from single well, hydraulic recharge and discharge tests.

Borehole	Thickness of ore dike (m)	Transmissivity (m^2/s)
BL7	0.85	1.3×10^{-4}
BL8	1.05	6.5×10^{-6}
BL9	3.07	2.5×10^{-5}
BL10	2.00	4.7×10^{-5}
BL11	1.35	5.4×10^{-4}

5.4. Tracer Tests

The tracer experiments in the central part of the parallel pit were carried out under artificially induced hydraulic gradients to force the interwell flow field to steady-state conditions. The use of different well pairs during different experiments allowed to conduct the tracer experiments over different distances. Generally, two different flow-field geometries were realized. The experiments were carried out under radial-convergent flow-field conditions (monopol tests) and under injection-withdrawal flow-field conditions (dipol tests). For the latter an injection-withdrawal well pair was required. The monopol tests, however, required only one discharge well. The instantaneous pulse injection of the tracer into the cone of hydraulic head depression was realized by a second well lying within a certain distance to the discharge well.

5.4.1. Experimental Set-up for Dipol Tests

Approximately 1,500 l of groundwater was stored in a 2,000 l steel pressure reservoir to provide water for the subsequent injection. The groundwater was extracted from the hydraulically separated southern part of the ore dike which does not have any exchange with the test section. The pressure reservoir was kept under nitrogen gas at 2.5 atm above ambient pressure to minimize any hydrochemical alteration of the oxygen unsaturated formation water. The pressure of the reservoir corresponds to the mean hydraulic head of the tested ore dike section. In addition, the nitrogen pressure reduced any possible changes in the pumping rate which might influence the interwell flow field.

In advance of the experiments all boreholes of the migration test site (BL6, BL7, BL8, BL9, BL10, BL11) were equipped with a thin 12 mm diameter PVC-tubing to reduce the residence time in the whole flow line to a minimum. Each PVC-tubing ended in an injector of 1" diameter having small radial outlets. This injector was placed at the centre of the ore dike at each test well. The thin flow line was mounted to the shut-in valves of the stand pipes and was connected to little turbine flow meters to continuously control the discharge and recharge rates during the experiments. For control purposes of the hydraulic interwell gradient, the standpipes of the test wells (2" diameter) were equipped with electronic pressure transducers.

Before the tracer was injected, it was stored in a pressure hose having a volume of approximately 1 l. This reservoir could be coupled for a short time as a bypass into the flow line. The tracer injection needed generally less than a few minutes and therefore the injection of tracer followed a Dirac pulse boundary condition sufficiently well.

The dipol tracer tests were carried out generally as an "open dipol" implying that a reinjection of the withdrawn water into the test section was avoided. The extracted water from the discharge well was led through an automatic sampling device containing a set of 100 ml glass bottles for the later quantitative analysis in the laboratory. With the help of an additional bypass a field fluorimeter was coupled into the flow line to optimize the length of the sampling intervals. Finally, the contaminated water was led out of the experimental site using a sewage pipe to avoid any contamination of the test area.

Due to the assumed stagnant water conditions the hydraulic interwell gradient in the ore dike could be influenced by a MOHNO-Pump. This pump has very low fluctuations in its pumping rate, while the flow rate depends directly on the number

of revolutions per minute. The pumping rate can be changed over a range of 5 up to 25 l/min. Figure 5.4 shows the technical set-up which was used for the dipol tests.

5.4.2. Experimental Set-up for Monopol Tests

The technical set-up described above could also be used for the monopol tests which needed only minor modifications to the technical set-up. For the monopol tests the injection of the fluorescent dyes was achieved, using the pressure reservoir which was kept under a pressure of 4 atm above ambient pressure.

The water of the reservoir was necessary to flush the dyes into the formation, providing a radial convergent homogeneous spreading of the tracer cloud around the injection well. The injection of the tracer dyes needed only a few minutes and, as the injection was finished, the shut in valves of the injection well were closed again. At the withdrawal well the discharge rate was controled continuously with the help of a little turbine flow meter.

The discharge rate was set to a constant value with the help of several valves in the flow line. In the same way as described for the dipol tests the hydraulic interwell gradient was monitored continuously (Fig. 5.4).

5.4.3. Flow-Field Geometries

The flow field of a dipol experiment is symmetric and has an equal strength if the injection rate (Q) is equal to the withdrawal rate (–Q). The withdrawal well is on the x-axis at the distance x = X/2 and the recharge well is at the distance x = –X/2. If the aquifer is confined, infinite in its lateral extension, and is not affected by any

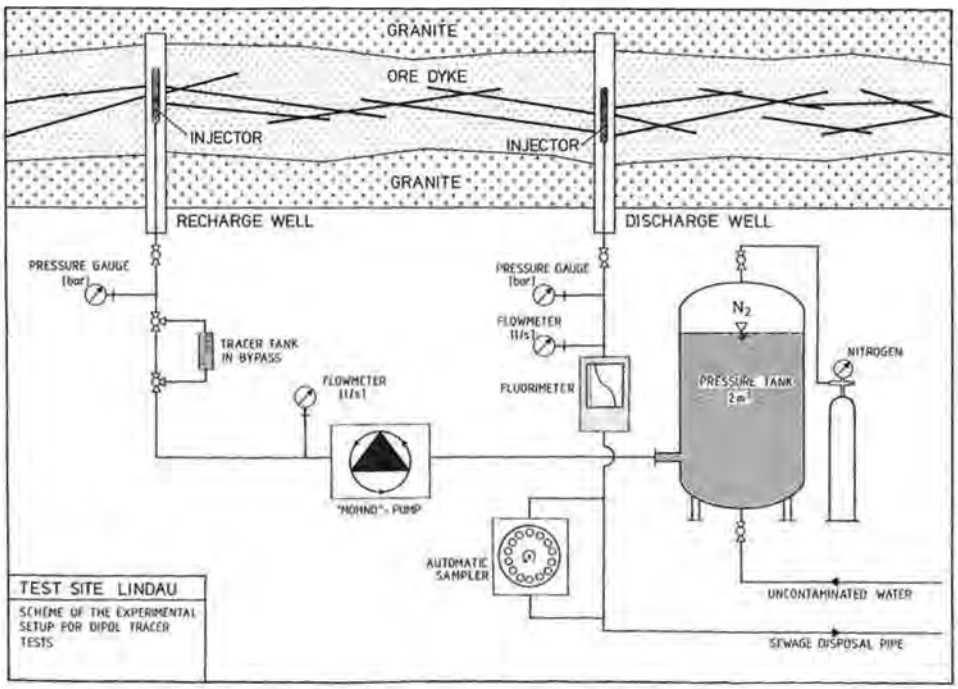

Fig. 5.4: Experimental set-up used for the tracer experiments (T. HIMMELSBACH, 1991).

natural hydraulic gradient the hydraulic head is given by a superposition of the THIEM-equation for a sink and source term

$$h = \frac{Q}{4\,\pi\,k\,m}\ \ln\frac{(x - X/2)^2 + y^2}{(x + X/2)^2 + y^2} + C. \qquad (5.1)$$

For a very large distance the hydraulic head H is not any longer affected by the injection-withdrawal well pair. Therefore C = H, which also implies that h = H for x = 0 and y = 0, being the intersection of the y-axis with the x-axis at the symmetry point. Since the equipotential lines h = constant eq. (5.1) can be rearranged to (R.J.M. DE WIEST, 1965):

$$e^{\frac{4\,\pi\,k\,m}{Q}} = \frac{(x - X/2)^2 + y^2}{(x + X/2)^2 + y^2} = C \qquad (5.2)$$

or

$$x^2 + y^2 - 2\,x\,(X/2)\,\frac{1 + C}{1 - C} + (X/2)^2 = 0. \qquad (5.3)$$

Equation (5.3) represents a set of circles which have their centre at the coordinates

$$\left[(X/2)\,\frac{1 + C}{1 + C}\,,\,0\right],\ \text{with radii}\ \frac{2\,(X/2)\,\sqrt{C}}{1 - C}\,. \qquad (5.4)$$

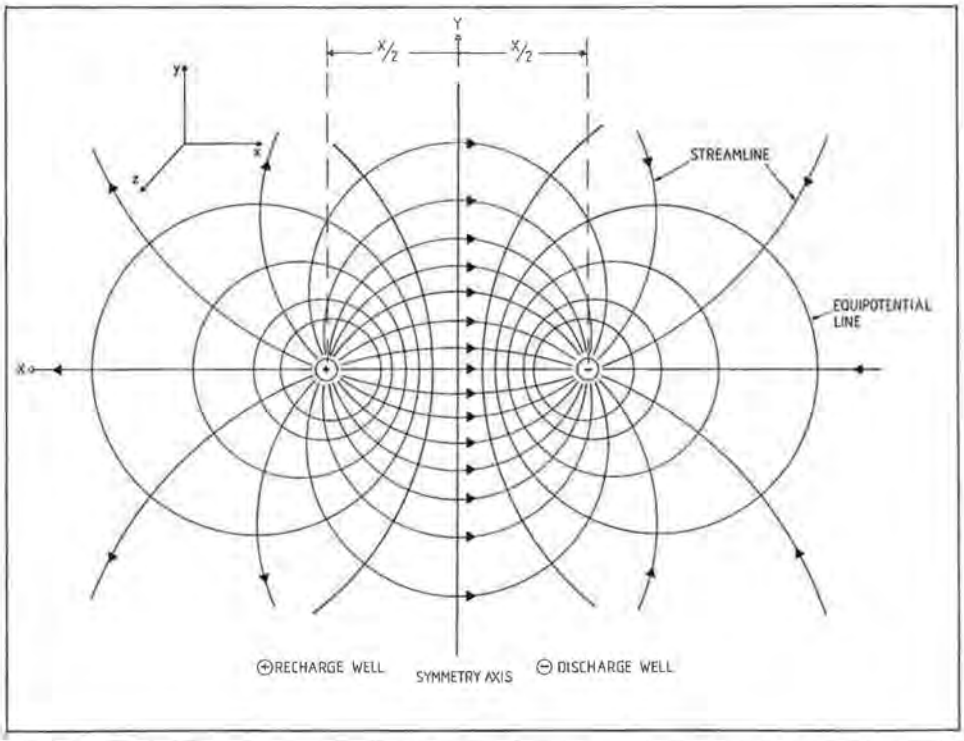

Fig. 5.5: Flow-field geometry of a dipol experiment of equal strength and negligible natural hydraulic gradient.

Since the movement of groundwater is always perpendicular to the equipotential lines their centres have to be on the symmetry axis (Fig. 5.5). Therefore, the flow paths from an injection to a discharge well form arcs of circles intersecting both the injection as well as the withdrawal well. Only in case of a higher withdrawal rate as the injection rate, the dipol becomes asymmetric. If the injection rate is negligible in comparison to the withdrawal rate, the flow field converges towards a pure radial convergent character.

Due to the lack of any natural hydraulic gradient a superimposed artificial symmetric dipol flow field is not limited in its lateral extension, as it does not have any dividing streamline. Accordingly, a water particle which is leaving the injection borehole under an angle φ_i ($\varphi \varepsilon [0 \rightarrow \pi]$) enters the withdrawal borehole under the same angle φ_i. If one regards two adjacent streamlines leaving the injection well under the angle φ_1 and φ_2 and takes into account the thickness of the ore dike (m), a streamtube can be determined representing a certain portion of the total flux between injection and withdrawal well (Fig. 5.6). As flux condenses to an infinite narrow streamtube between two streamlines the time required to fill up such a streamtube is a function $F(\varphi)$. The transit time for a water particle throughout such a streamtube is equivalent to the time required for filling up the streamtube and can be given analytically (D.S. WEBSTER et. al, 1970)

$$t_{0i} = n_f m \frac{\pi X^2}{Q} \left[\frac{1 - \varphi_i \operatorname{ctg} \varphi_i}{\sin^2 \varphi_i} \right] \tag{5.5}$$

where

X = distance between wells,
Q = pumping rate,
n_f = fissure porosity,
m = thickness of aquifer,
t_{0i} = mean transit time of water,

for any streamline leaving the injection well under an angle with $\varphi > 0$. This term, however, is not defined for a streamline connecting the injection and withdrawal well directly. For small values of the angle φ the expression in the brackets as well as its first derivation trends towards the same limit

$$\left[\frac{1 - \varphi_i \operatorname{ctg} \varphi_i}{\sin^2 \varphi_i} \right] \rightarrow \frac{1}{3} \quad \text{for } \varphi_i \rightarrow 0. \tag{5.6}$$

Therefore eq. (5.5) can be simplified to

$$t_{01} = \frac{1}{3} n_f m \frac{\pi X^2}{Q} \tag{5.7}$$

with t_{01} being the mean transit time of water following the direct interconnecting streamline between the injection and the withdrawal well.

A combination of eq. (5.5) and (5.7) leads to an expression for the relation of mean transit times between any arbitrary streamline and the direct connecting streamline. It can be written as (D.S. WEBSTER et al., 1970, F. HERZOG, 1990)

$$\frac{t_{0i}}{t_{01}} = 3 \left[\frac{1 - \varphi_i \operatorname{ctg} \varphi_i}{\sin^2 \varphi_i} \right]. \tag{5.8}$$

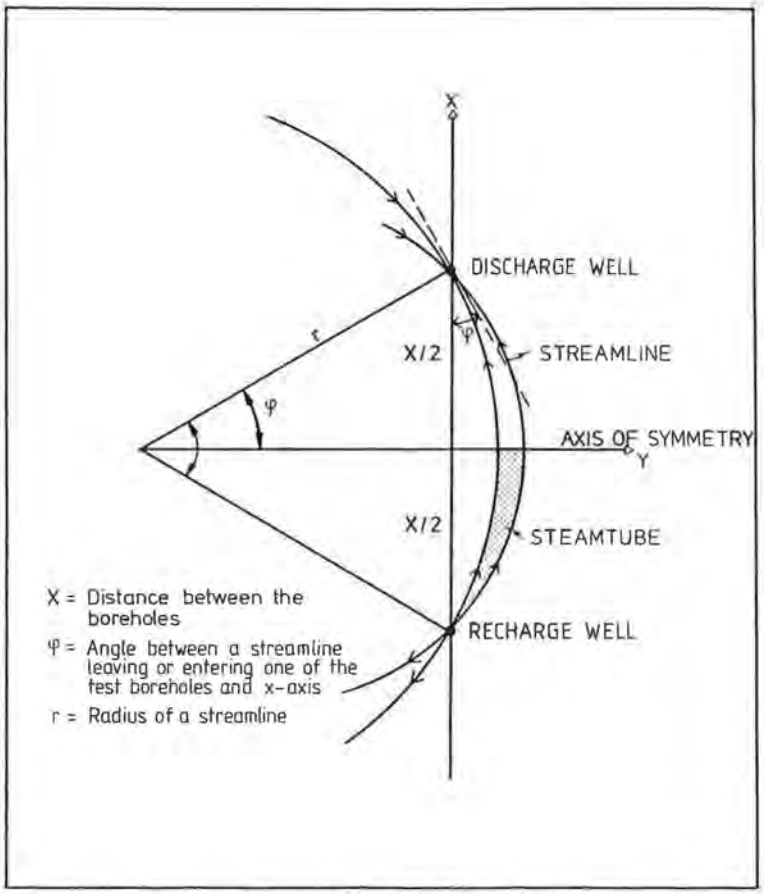

Fig. 5.6: The stream tube approach chosen for the evaluation of dipol tracer experiments.

If the relation of transit times is plotted as a funktion F(φ) it becomes obvious that for an angle $\varphi > \pi/2$ streamlines are entering the withdrawal well which have been injected "backward" in relation to the direct streamline. As the angle π increases the transit time of the "backward" injected streamlines also increases rapidly. The latter must kept in mind for the practical use, especially when analysing recovery rates for dipol tracer experiments.

Assuming a radial convergent, homogenous spreading and dilution of the tracer cloud around the injection well, it becomes obvious that for a certain time after the pulse injection of the tracer only a certain recovery rate can be observed, because only a distinct portion of streamlines will reach the withdrawal borehole at this time. Under practical field conditions, using an injection-withdrawal set-up of equal strength, recoveries close to 100% are impossible, rather lying in the range of 60 up to 75%. Under the additional assumption that the movement of the tracer cloud only occurs along opened fractures being parallel to the ore dike section, eq. (5.7) can be rearranged

$$n_f m = \frac{3\,Q\,t_{01}}{\pi\,X^2}\,, \tag{5.9}$$

describing the "effective thickness" of the tested ore dike section. This "effective thickness" ($n_f m$) of the aquifer is supposed to be equivalent to the integration of all fracture apertures which are parallel to the x-axis and represent the mobile flux of the system. Under the assumption that all flux contributing fissures intersect both the test wells, the mean residence time of water in a streamtube can now be used to derive a first estimation about the fissure aperture.

Knowing very well that flow processes in the ore dike are somewhat far beyond the previously assumed homogenous conditions like in a porous aquifer, the transit times for arbitrary streamlines can also be written as a function $F(\pi)$ by using a discontinuum approach and involving POISEUILLE's law (K.S. NOVAKOWSKI et al. 1985). The discontinuum approach means that the fluid movement occurs only along fractures representing the mobile water content of the ore dike. The matrix, however, is thought to represent the immobile water phase which can only be affected by processes of matrix diffusion. For the injection-withdrawal set-up eq. (5.5) can be rearranged to the form

$$t_{0i} = \frac{X^2\, 12\nu}{\Delta H\, (2b)^2\, g} \ln\left(\frac{X}{r_w}\right) \left[\frac{1 - \varphi_i \operatorname{ctg} \varphi_i}{\sin^2 \varphi_i}\right], \tag{5.10}$$

where

g = gravity acceleration,
ν = dynamic viscosity,
ΔH = difference of hydraulic head between wells,
X = distance between wells.

Accordingly the transit time for the shortest flow path can also be rearranged to

$$t_{01} = \frac{1}{3} \frac{X^2\, 12\nu}{\Delta H\, (2b)^2\, g} \ln \frac{X}{r_w}. \tag{5.11}$$

Rearrangement of eq. (5.11) leads to an estimation of the fracture aperture 2b representing the effective hydraulic aperture and has the form

$$2b = \sqrt{\frac{1}{3} \frac{X^2\, 12\nu}{\Delta H\, t_{01}\, g} \ln \frac{X}{r_w}}. \tag{5.12}$$

The use of eq. (5.12) for the estimation of fracture aperture has the principle advantage that the thickness of the ore dike (m), which is surrounded by some uncertainities, is no longer involved in the calculation of the fracture aperture.

5.5. Experiments

5.5.1. Injection-Withdrawal Flow (Dipol Tests)

Due to the results of the preliminary hydraulic tests the first tracer tests were restricted to sections of the ore dike Hermann supplying a sufficient hydraulic contact between the injection and withdrawal wells. The previous hydraulic interference tests had indicated, that the test wells within these sections might be interconnected by a discrete set of parallel fractures.

According to this assumption the dipol experiment I was carried out between two wells lying within a horizontal distance of 11.2 m to each other. For the injection

and the withdrawal of water two horizontal wells were used which intersect the ore dike Hermann completely (BL8 – BL10). The well BL8 was used as injection well (2 g EOSIN) and the well BL10 was used as withdrawal and observation well. During the experiment, which was carried out as an "open dipol" of equal strength, a constant flow rate of 1.26×10^{-4} m³/s could be realized. In contrast to the first dipol experiment the dipol experiment III was carried out between two wells lying within a vertical distance of approximately 16.2 m to each other (BL11 – BL9). The 45° upward inclined well BL11 was chosen as the injection well (2 g PYRANIN). The well BL9, which is 45° downward declined was used as the observation well. Similar to the first experiments this dipol test was carried out as an "open dipol" of equal strength, having a constant flow rate of 1.1×10^{-4} m³/s.

During the dipol experiments I and III first traces of the fluorescent dyes could be observed within approximately 35 minutes after the injection of the tracer. In both cases the peak of the measured tracer concentration was reached within only one hour, having a sharp and well defined maximum. The measured tracer concentration decreased subsequently very fast and changed within a further three hours into a long tailing effect. During both experiments the measured concentrations decreased within less than eight hours to a level lying below 5% of the observed peak concentration. Although the dipol experiments lasted generally about 12 hours a still existing tracer concentration of approximately 3% of the peak concentration could be observed at the end of the experiments. Due to this tailing effect traces of fluorescent dyes could be even observed more than six weeks after the experiments, although the wells had been opened to a free outflow to flush the dyes out of the tested ore dike section.

The results of the dipol experiments I and III are shown in fig. 5.11 (chap. 5.8.). The experimental data are depicted as triangle symbols for the observed tracer concentrations and rectangular symbols for the observed relative recovery. The best fit for the experimental data obtained with the help of the Single Fissure Dispersion Model (SFDM, s. chap. 5.6.) is depicted as solid lines. For a better comparison the measured tracer concentrations are normalized to the injected mass of tracer, while the relative recovery is the ratio between the injected mass and the integration over the breakthrough curve (eq. 5.34).

5.5.2. Radial Convergent Flow (Monopol Tests)

In contrast to the dipol experiments the monopol experiments were conducted under radial convergent flow conditions. The injection of the fluorescent dyes was carried out as a short Dirac pulse respectively. During each experiment the observation well was opened to a constant flow rate to force the interwell flow field to steady-state conditions.

The monopol experiment I was carried out between the same wells which were already used for the dipol experiment I (BL8 – BL10). The well BL8 was used as the injection well for the fluorescent dyes (2 g PYRANIN) and the well BL10 was used as the withdrawal and observation well (Fig. 5.1). During the experiment a constant flow rate of 0.98×10^{-4} m³/s could be realized. The monopol experiment IV was carried out over the same vertical orientated distance which was already used for the dipol experiment III (BL9 – BL11). The 45° upward inclined well BL11 was used as injection well (2 g URANIN) and the 45° downward declined well BL9 was used as withdrawal well (Fig. 5.1). Similar to the first monopol experiment a constant flow rate of 1.27×10^{-4} m³/s was achieved.

During the monopol experiments I and IV which lasted about 20 hours first traces of the fluorescent dyes could be measured within 67 minutes (Monopol I) and 30 minutes (Monopol IV) after the injection. The breakthrough curves of the tracer experiments showed a well defined maximum of tracer concentration which was reached within 155 minutes (Monopol I) and 75 minutes (Monopol IV). As already observed during the dipol experiments the breakthrough curves changed subsequently into a long tailing effect of slowly decreasing tracer concentrations. Although the observation wells were opened to a free outflow at the end of the experiments to flush the test sections a remaining tracer concentration could be even measured more than eight weeks after the experiments.

The following monopol experiment V was carried out over twice the horizontal distance as used for the monopol experiment I. The well BL10 was chosen again as observation well and was opened to a constant discharge rate of 1.27×10^{-4} m³/s. The tracer (10 g PYRANIN) was injected into the well BL7 which is located within a horizontal distance of 21.4 m from the observation well BL10 (Fig. 5.1). The preliminary hydraulic interference tests had indicated a reduced hydraulic contact between these test wells. Accordingly the experiment lasted more than 300 hours and the first traces of PYRANIN could be observed not before 8.5 hours. The peak of the breakthrough curve was three decades below the observed maximum concentration of the other monopol experiments and it was reached not before 42 hours after the injection of the PYRANIN. In addition, the relativ tracer recovery reached only 0.3% which is very poor in comparison to the recovery rate derived from the other monopol tests. Hence, the assumption of a radial convergent flow field is rather unlikely, because the test wells (BL7 – BL10) obviously did not intersect the same set of parallel fractures.

The last tracer experiment, the monopol experiment VI, was carried out as a combined one, to evaluate the diffusion coefficient of the PYRANIN (s. also chap. 5.8.). It was conducted over the same distance as already used for the monopol experiment I (BL8 – BL10) and the discharge rate at the observation well BL10 was set to 0.96×10^{-4} m³/s. As tracers 2 g PYRANIN and 300 g D_2O (DEUTERIUM 99.9%) were injected. The breakthrough of the tracers occured within nearly the same time as observed during the monopol experiment I because the discharge rate at the observation well BL10 was quite similar to the first monopol experiment. As to be expected, the peak concentration of the DEUTERIUM and the PYRANIN occured at the same time, but the slight different shape of the breakthrough curves of the PYRANIN and the DEUTERIUM is due to a different diffusion coefficient of the tracers (Fig. 5.10).

5.6. Mathematical Modelling of Tracer Transport in Fissured Aquifers

5.6.1. Introduction

Tracer transport in fissured rocks has attracted a lot of attention because hard rocks were considered in several countries as the best place for radioactive waste disposal. The hard rocks due to their low permeabilities, some orders of magnitude smaller than those usually observed in porous media, were assumed to be nearly impermeable. A possible migration of pollutants by diffusion from a depository was not expected to be a serious menace to groundwater resources. First experimental and theoretical work of G.E. GRISAK & J.F. PICKENS (1980, 1981), G.E. GRISAK et

al. (1980), and E. GLUECKAUF (1981) have shown that pollutants which may flow quickly through interconnected fissures are delayed by diffusion into a microporous matrix. Since the earliest works on flow in fissured rocks the main problem has been how to deal with a very strong anisotropy of hard rocks. Fissures have different apertures and spacings, and are oriented in different directions and intersect one another D.T. SNOW (1969, 1970). Due to these facts the solute transport is treated as either the transport in systems having different distributions of fissure spacing and aperture (I. NERETNIEKS, 1981, A. RASMUSON, 1985, Y.W. TSANG & C.F. TSANG, 1987, Y.W. TSANG et al., 1988, and L. MORENO et al., 1988), or the convective-dispersive flow through a very simple fissure system with molecular diffusion into the stagnant water in the micropores of the matrix (D.H. TANG et al., 1981, E.A. SUDICKY & E.O. FRIND, 1982, P. MALOSZEWSKI & A. ZUBER, 1984, 1985, 1989, 1990). In the present work the latter approach is taken. However, whichever approach is taken, the mathematical model of the tracer transport is so complicated that the inverse problem cannot be easily solved. The inverse problem is understood here as finding the flow and/or rock parameters from tracer experiments. In such a case the mathematical model has to be as simple as possible with reduced number of fitting parameters but at the same time it should yield the proper values of the transport parameters needed for the prediction of the pollutant movement.

5.6.2. Mathematical Model

The mathematical model developed by E.A. SUDICKY & E.O. FRIND (1982) is followed here. The fissured aquifer is approximated by the system of parallel fissures having the same aperture and being equally spaced in a porous matrix (Fig. 5.7).

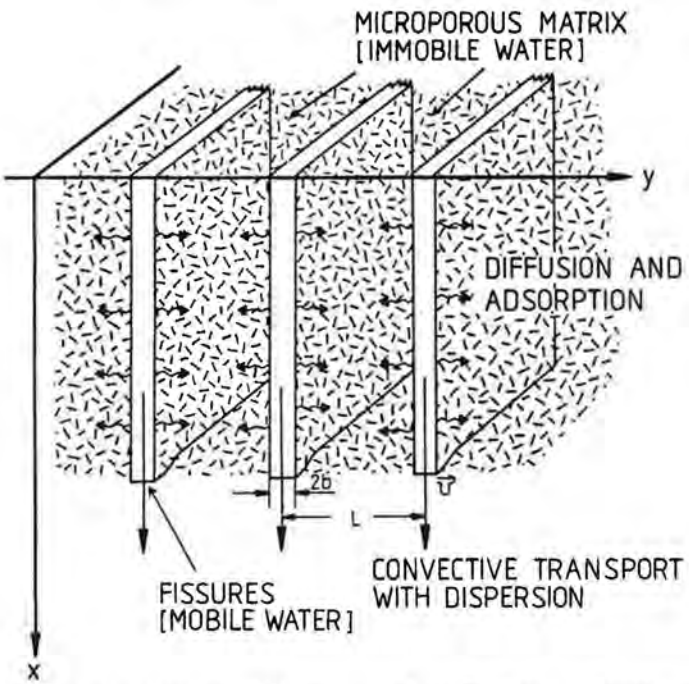

Fig. 5.7: Solute transport processes within a system of parallel fractures (conceptual model).

The tracer is injected into the water entering the fissures, and is transported along the fissures by groundwater flow. The microporous matrix is assumed to be impermeable. The tracer distribution across the fissure width is assumed to be constant due to a sufficient transverse dispersion and diffusion. The movement of the tracer in the porous matrix is governed by molecular diffusion. For such assumptions the transport equations for a conservative tracer are as follows:

$$\frac{\partial C_f}{\partial t} + v\frac{\partial C_f}{\partial x} - D\frac{\partial^2 C_f}{\partial x^2} - \frac{n_p D_p}{b}\frac{\partial C_p}{\partial y}\bigg|_{y=b} = 0 \quad \text{for } 0 \le y \le b \qquad (5.13)$$

$$\frac{\partial C_p}{\partial t} - D_p\frac{\partial^2 C_p}{\partial y^2} = 0 \qquad \text{for } b \le y \le L/2 \qquad (5.14)$$

where C_f and C_p are the tracer concentrations in water in the fissures and in the matrix, respectively, v is the mean water velocity in the fissures, x is spatial coordinate taken in the direction of flow, y is the spatial coordinate perpendicular to the fissure extension, D is dispersion coefficient in the fissures, 2b is fissure aperture, t is time variable, n_p is matrix porosity, D_p is the molecular diffusion coefficient in the porous matrix, and L is the fissure spacing.

Equation (5.13) describes dispersive-convective tracer transport in fissures and eqation (5.14) the diffusive transport in the matrix in the direction perpendicular to the fissures. The analytical solution of the eq. (5.13) and (5.14) for the continuous injection was given by E.A. SUDICKY & E.O. FRIND (1982), whereas for instantaneous injection by P. MALOSZEWSKI & A. ZUBER (1984). The solution for instantaneous injection is called by P. MALOSZEWSKI & A. ZUBER (1985) as the Parallel Fissure Dispersion Model (PFDM). That model consists of six physical parameters: v, D, 2b, L, n_p and D_p, which can be combined into four nondisposable fitting (model) parameters. P. MALOSZEWSKI & A. ZUBER (1985) have shown that in short-term tracer experiments the tracer flow through the system of parallel fissures can be approximated with a sufficient accuracy by the transport through a single fissure in infinitely extended matrix (mathematically it means: $L \approx \infty$). This implies that, if the mean transit time of water is sufficiently short (up to a few weeks), the tracer has no time to diffuse into the matrix deep enough to be affected by adjacent fissures. This condition is satisfied in most practical cases in tracer tests performed at small time and space scales. Then, the initial and boundary conditions are as follows:

$$C_f(x,0) = 0, \qquad (5.15.1)$$
$$C_f(0,t) = M/Q\,\delta(t), \qquad (5.15.2)$$
$$C_f(\infty,t) = 0, \qquad (5.15.3)$$
$$C_p(y,x,0) = 0, \qquad (5.15.4)$$
$$C_p(b,x,t) = C_f(x,t), \qquad (5.15.5)$$
$$C_p(\infty,x,t) = 0, \qquad (5.15.6)$$

where M is the mass of tracer instantaneously injected, Q is the volumetric flow rate through the system and $\delta(t)$ is the Dirac delta function. The solution to (5.13) and (5.14) with the above given boundary and initial conditions, describing the tracer concentration as a function of time for a given distance (X) was given by P. MALOSZESKI & A. ZUBER (1985, 1990). It reads as follows:

$$C_f(t) = \frac{aM}{2\pi Q}\sqrt{Pet_0}\int_0^t \exp\left[-\frac{Pe(t_0-u)^2}{4ut_0} - \frac{a^2u^2}{t-u}\right]\frac{du}{[u(t-u)^3]^{1/2}}, \qquad (5.16)$$

with

$$t_0 = X/v \text{ or } V/Q, \tag{5.17}$$

$$Pe = vX/D, \tag{5.18}$$

$$a = n_p \sqrt{D_p}/(2b), \tag{5.19}$$

where X is the distance between injection and detection wells, V is the the mobile water volume in the system, Pe is the Peclet number, t_0 is the mean transit time of water and a is the diffusion parameter. The solution (5.16) is called the Single Fissure Dispersion Model (SFDM). The solution for a continuous injection was given by D.H. TANG et al. (1981).

5.6.3. Model Parameters

The SFDM model has three nondisposable (fitting) parameters: a, t_0 and Pe , defined by eq. (5.17) to (5.19). They are the combination of five physical parameters v, D, 2b, n_p and D_p. In the calibrating procedure (fitting of solution (5.16) to the tracer concentration measured) the three model parameters can be relatively easily found. If the matrix porosity, n_p, and diffusion coefficient in the water in the matrix, D_p, are known from separate laboratory experiments on core samples, the fissure aperture, 2b, is directly found from eq. (5.19).

5.7. Determining of Model Parameters

5.7.1. Natural Flow Conditions

The volumetric flow rate through the system of fissures is equal to:

$$Q = n_f \, v \, S, \tag{5.20}$$

where S is the cross-section area perpendicular to the flow and n_f is the fissure porosity defined for the system of parallel fissures as:

$$n_f = 2b/L. \tag{5.21}$$

In most cases the cross-section area remains unknown and Q has to be eliminated from eq. (5.16). To overcome this difficulty the tracer breakthrough curve has to be normalized to the maximum concentration C_{max} measured in time $t = t_{max}$. The same has to be done with the theoretical output concentration, $C_f(t)$. Then, instead of eq. (5.16), for the calibration of the SFDM model the following function is used:

$$F(t) = \frac{C_f(t)}{C_{max}} = \frac{\int_0^t \exp\left[-\frac{Pe(t_0-u)^2}{4ut_0} - \frac{a^2u^2}{t-u}\right] \frac{du}{[u(t-u)^3]^{1/2}}}{\int_0^{t_{max}} \exp\left[-\frac{Pe(t_0-u)^2}{4ut_0} - \frac{a^2u^2}{t-u}\right] \frac{du}{[u(t-u)^3]^{1/2}}}. \tag{5.22}$$

If the distance X between injection and detection wells is known the mean water velocity v and longitudinal dispersivity α_L can be estimated from the fitting parameters t_0 and Pe by using eq. (5.17) and (5.18):

$$v = X/t_0, \tag{5.23}$$

$$\alpha_L = X/Pe. \tag{5.24}$$

As mentioned, the a-parameter can be used for determining the fissure aperture when the matrix porosity and the difusion coefficient of tracer in porous matrix are known:

$$2b = n_p\sqrt{D_p}/a. \tag{5.25}$$

5.7.2. Radial Convergent Flow (Monopol Test)

If tracer experiment is performed together with pumping test, i.e. in the case of radial convergent flow, the volumetric flow rate through the system, Q, is equal to the pumping rate. Then, from eq. (5.17), the volume of the mobile water in the system is:

$$V = Q\, t_0. \tag{5.26}$$

If the volume of depression cone is negligible in the comparison with the volume of water in the investigated part of the system i.e., water in cylinder of radius X and height m (thickness of the aquifer), the fissure porosity n_f can be calculated as follows (A. ZUBER, 1974):

$$n_f = Q\, t_0/(\pi m X^2). \tag{5.27}$$

As the hydraulic conductivity, k, is also known from the pumping test, the fissure aperture may be estimated. For a system of tortuous fissures of the same aperture one obtains (A. ZUBER, 1974):

$$2b = 4.29 \times 10^{-6}\, \tau_f\, (k/n_f)^{1/2}, \tag{5.28}$$

where 2b is expressed in meters and k in meters per day. τ_f is the tortuosity factor for fissures (≈ 1.5). Finally, if the molecular diffusion coefficient of a tracer in the free water, D_m, is known and the constrictivity factor is equal to one, the matrix porosity, n_p, can be found by combining the formula for D_p (I. NERETNIEKS, 1980) with eq. (5.19) (P. MALOSZEWSKI & A.ZUBER, 1990):

$$n_p = [(2ba)^2\, \tau_p/D_m]^{1/2}, \tag{5.29}$$

where τ_p is the tortuosity factor for the matrix (≈ 1.5). Equation (5.29) is well suited for carbonate rocks where the constrictivity factor is probably equal to one for the majority of typical tracers. For magmatic rocks of low matrix porosity the constrictivity factor is smaller than 1 (K. SKAGIUS & I. NERETNIEKS, 1986) and then eq. (5.29) is not applicable.

5.7.3. Injection-Withdrawal Flow (Dipol Tests)

In some practical situations it is not possible to perform a tracer test in the convergent radial flow (monopol test) due to a high hydraulic water pressure. Some authors like K. NOVAKOWSKI et al. (1985) or K.G. RAVEN et al. (1988) proposed to use in such a situation injection-withdrawal tracer test. The steady-state groundwater flow is induced by injection-withdrawal pair of wells. If the volumetric flow rates in the injection and withdrawal wells are the same, the natural gradient between wells is neglegible, and the groundwater system is homogeneous and isotropic, the

streamlines are in form of a symmetrical dipol (s. fig. 5.5 in chap. 5.4.2.). The tracer is injected into the recharging well and its concentration is observed in the withdrawal well. The water from the pumping well is not reinjected into recharging well (so called "open dipol test"). Assuming that there is no exchange of tracer between the streamlines the unidimensional tracer transport can be considered for each streamline (stream tube) separately as described by eq. (5.16). It should be mentioned that the water velocities vary spatially in the vicinity of the wells. Therefore, the unidimensional transport model described by eq. (5.16) approximates the natural flow conditions with the average constant velocity in each stream tube. The output concentration $C_f(t)$ observed in the pumping well is the weighted sum of the stream tube flows:

$$C_f(t) = \frac{1}{Q} \sum_{i=1}^{2N} [q_i C_{fi}(t)], \tag{5.30}$$

where Q is the pumping rate, q_i and $C_{fi}(t)$ are the partial volumetric flow rate and the output concentration from the i-th stream tube, respectively, and 2N is the number of all stream tubes. One may assume, that partial volumetric flow rates, q_i, are the same

$$q_i = Q/(2N). \tag{5.31}$$

Taking into account the symmetry of the hydrodynamic field the weighted output concentration of tracer is

$$C_f(t) = \frac{1}{2N} \sum_{i=1}^{2N} C_{fi}(t) = \frac{1}{N} \sum_{i=1}^{N} C_{fi}(t). \tag{5.32}$$

Assuming, according to A. ZUBER (1974), that the mass of tracer transported in the each stream tube M_i is proportional to partial volumetric flow rate q_i:

$$M_i/q_i = M/Q \tag{5.33}$$

and that the dispersivity α_L is constant and the same for all the stream tubes, the output concentration from the i-th stream tube, $C_{fi}(t)$, is equal to:

$$C_{fi}(t) = \frac{aM}{2\pi Q} \sqrt{Pe_i t_{0i}} \int_0^t \exp\left[-\frac{Pe_i(t_{0i}-u)^2}{4ut_{0i}} - \frac{a^2u^2}{t-u}\right] \frac{du}{[u(t-u)^3]^{1/2}}, \tag{5.34}$$

where t_{0i} and Pe_i are the mean transit time of water and Peclet number through the i-th stream tube, respectively, which according to D.B. GROVE & W.A. BEETEM (1971) are then equal to:

$$t_{0i} = \frac{\pi BX^2}{Q} \frac{1-\varphi_i \cot\varphi_i}{\sin^2\varphi_i}, \tag{5.35}$$

$$Pe_i = \frac{X}{\alpha_L} \frac{\varphi_i}{\sin\varphi_i}, \tag{5.36}$$

where φ_i varies positively from 0 to π:

$$\varphi_i = \pi(i-1)/N \text{ with } i = 2, N. \tag{5.37}$$

The stream tube connecting both wells rectilinearly with the shortest way (for $i = 1$, $\varphi_1 = 0$) has the mean transit time and the Peclet number equal to:

$$t_{01} = \frac{\pi B X^2}{3Q}, \tag{5.38}$$

$$Pe_1 = \frac{X}{\alpha_L}. \tag{5.39}$$

B is equal to the fissure aperture for a tracer experiment performed in a single fracture

$$B = 2b, \tag{5.40}$$

whereas for a densely fissured system

$$B = n_f m. \tag{5.41}$$

The calibration of the model, eq. (5.32) with (5.34), is possible only numerically for an assumed number of stream tubes, 2N. K. NOVAKOWSKI et al. (1985) have shown that acceptable results of calculation can be obtained using only 48 stream tubes. In the present work 120 stream tubes (N = 60) were taken. The fitting parameters of the model for dipol tracer test are t_{01} (eq. 5.38), Pe_1 (eq. 5.39) and diffusion parameter a (eq. 5.19). From the t_{01} parameter one can easily find B by making use of eq. (5.38) for the known distance, X, and pumping rate, Q. Consequently, for a single fracture the B factor is directly equal to the fissure aperture, 2b, whereas for a densely fissured system by combining eq. (5.38) and (5.41) the fissure porosity, n_f, is obtained:

$$n_f = 3\,Q\,t_{01}/(\pi\,m\,X^2). \tag{5.42}$$

In that latter case the mean fissure aperture 2b and the matrix porosity n_p may be calculated identically as it was described for the monopol tracer test.

5.8. Results of Model Calculation

The SFDM model described by eq. (5.16) was derived for unidimensional flow, whereas the model is also used to interpret the data in convergent-radial flow (monopol test) and symmetrical dipol flow which becomes radial in the vicinities of injection and withdrawal wells.

However, A. LENDA & A. ZUBER (1970), A. ZUBER (1974) and P. MALOSZEWSKI & A. ZUBER (1985, 1990) and many others have shown that this approximation works properly yielding the average parameters for the distance X between the injection and detection wells.

The monopol or dipol radial flows are especially suitable for tracer experiments because they allow the inclusion of the concept of the tracer mass recovery. The mass recovery curve or the relative mass recovery curve as a function of time can be included in the fitting procedure, which improves the model calibration (D. KLOTZ et al., 1988, P. MALOSZEWSKI & A. ZUBER, 1990). The relative tracer recovery RR(t), is defined as follows:

$$RR(t) = Q \int_0^t C_1(t)\,dt/M \tag{5.43}$$

and is calculated from either the tracer experimental tracer curve or theoretical one (eq. (5.16) for the monopol test or eq. (5.32) for the dipol test).

5.8.1. Tracer Experiment in Natural Flow Conditions

This experiment is described in chap. 4. The best fit curve, shown in fig. 4.3, was obtained with the following parameters: $\tau_0 = 35$ days, Pe = 33 and $a = 0.41 \times 10^{-3}\ s^{-1/2}$. The distance between injection and detection points is X = 346 m which yields from eq. (5.23) and (5.24) the mean water velocity of 9.9 m/d and the longitudinal dispersivity of 10.4 m. Any additional interpretation may be questionable because no data about fissure aperture or matrix porosity exist. Assuming that the fissure aperture is about 360 μm (from the hydraulic tests in the gallery) and that the coefficient of molecular diffusion for the Eosine is equal to that of Uranine, i.e. $D_m = 4.5 \times 10^{-10}\ m^2/s$ (K. SKAGIUS & I. NERETNIEKS, 1986), the mean matrix porosity $n_p = 0.9\%$ can be estimated by applying eq. (5.29) with $\tau_\rho = 1.5$.

The tracer experiment performed between wells BL7 and BL10 which had been intended as a monopol test (X = 21.4 m and Q = 0.127 l/s) was similarly interpreted, which is of course highly questionable. The relative tracer recovery obtained after 300 hours of pumping (10 times longer than the time in which the maximal concentration appeared) reached only 0.3%. It means that the pumping of the water from the system did not produce the radial convergent flow between both wells. The wells were too remote for the pumping rate used, or, they were not in the same fracture zone, or, what is more probable, another fracture zone exists which intercepts the flow field between the both wells. The best fit curve (Fig. 5.8) was obtained with $\tau_0 = 20$ hours, Pe = 20 and $a = 4.17 \times 10^{-3}\ s^{-1/2}$. The mean water velocity obtained in that case was 25.7 m/d and the longitudinal dispersivity 1.1 m. The matrix porosity

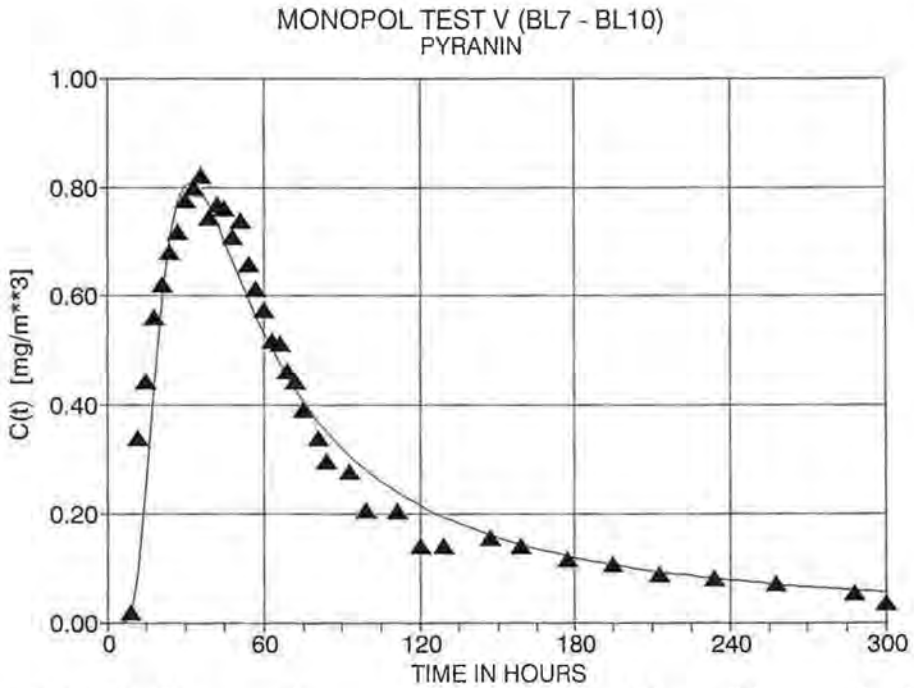

Fig. 5.8: Results of the monopol tracer test V in the central part of the parallel pit (considered as a flow in "natural conditions"). Triangle – tracer concentration.

of 5.2% was estimated by assuming fissure aperture and the tortuosity factor for the porous matrix the same as before and by taking the coefficient of molecular diffusion for Pyranine as equal to 1.3×10^{-9} m²/s (s. next chap.).

5.8.2. Radial Convergent Flow

The tracer monopol tests performed with the radial convergent flow are described in details in chap. 5.4.

Monopol test IV was performed between wells BL11 and BL9 for the distance of 16.2 m with the pumping rate of 0.127 l/s. The calibration of the SFDM was obtained for $t_0 = 1.25$ hour, Pe = 13.3 and $a = 5.66 \times 10^{-3}$ $s^{-1/2}$ in simultaneous fitting of the tracer concentration and recovery curves (s. fig. 5.9 a). For the known mean thickness of the water bearing layer of 2.15 m, the fissure porosity was calculated from eq. (5.27) to be 0.05%. The hydraulic conductivity of 1.1×10^{-5} m/s (0.95 m/d) found from the hydraulic test (transmissivity, $T = 2.47 \times 10^{-5}$ m²/s) yields (eq. 5.28) the mean fissure aperture of 280 µm. By using eq. (5.21) the mean fissure spacing of 0.56 m can be estimated from the 2b and n_f values. It means that for m = 2.15 m the water bearing layer between these two wells consits of three or four parallel fissures. Finally, the relatively high matrix porosity of 9.3% is estimated from eq. (5.29) for assumed $D_m = 4.5 \times 10^{-10}$ m²/s (Uranine). If the molecular diffusion coefficient for Uranine in this formation is greater, the matrix porosity calculated is smaller.

An interesting monopol test was performed two times between wells BL8 and BL10 for a distance of 11.2 m. In the first experiment (monopol test I with Q = 0.098 l/s) Pyranine was applied (Fig. 5.9 b), whereas in the second experiment (monopol test VI with Q = 0.096 l/s) Pyranine and Deuterium were injected simultaneously (Fig. 5.10 a and Fig. 5.10 b). The calibration of the SFDM was performed for Pyranine using simultaneously tracer concentration and recovery curves. In both experiments it was not possible to fit both concentrations and recoveries without the additional assumption that the part of tracer (Pyranine) was lost. In monopol test I it was about 15% whereas in monopol test VI about 10%. The fitting parameters obtained for Pyranine were nearly the same in both experiments ($t_0 = 1.58$ and 1.62 hours, Pe = 33 and 50, $a = 11.6 \times 10^{-3}$ and 10.3×10^{-3} $s^{-1/2}$ for monopol test I and VI, respectively). The best fit curves for Pyranine are shown in fig. 5.9 b and 5.10 a. The fissure porosity calculated for the aquifer thickness of 1.53 m was in both cases the same and equal to about 0.1%. Similarly, the mean fissure aperture calculated for $k = 0.89 \times 10^{-5}$ m/s (found for the injection well from the hydraulic tests) was nearly the same (184 µm). The matrix porosities calculated for $D_m = 1.3 \times 10^{-9}$ m²/s and $\tau_p = 1.5$ were insignificantly different (7.3% and 6.5%, respectively). The mean fissure spacing of 19.8 cm was obtained from the 2b and n_f values. This fissure spacing yields about six parallel fissures for the observed thickness of fractured zone, which poorly agrees with three fissures observed visually on the drill core.

The modelling of Deuterium was only possible for the tracer concentration curve normalized to the maximum concentration (s. fig. 5.10 b). The main problem which appeared was that the maximal concentration measured (about 200 ppm) was only 30% higher than the natural background concentration (about 150 ppm). This low signal probably caused a large part of the tracer curve to be undetectable. In other words, the mass of tracer injected was approximately 10 times too small. However, the fitting parameters obtained $t_0 = 1.52$ hour and Pe = 50 agree very well with those

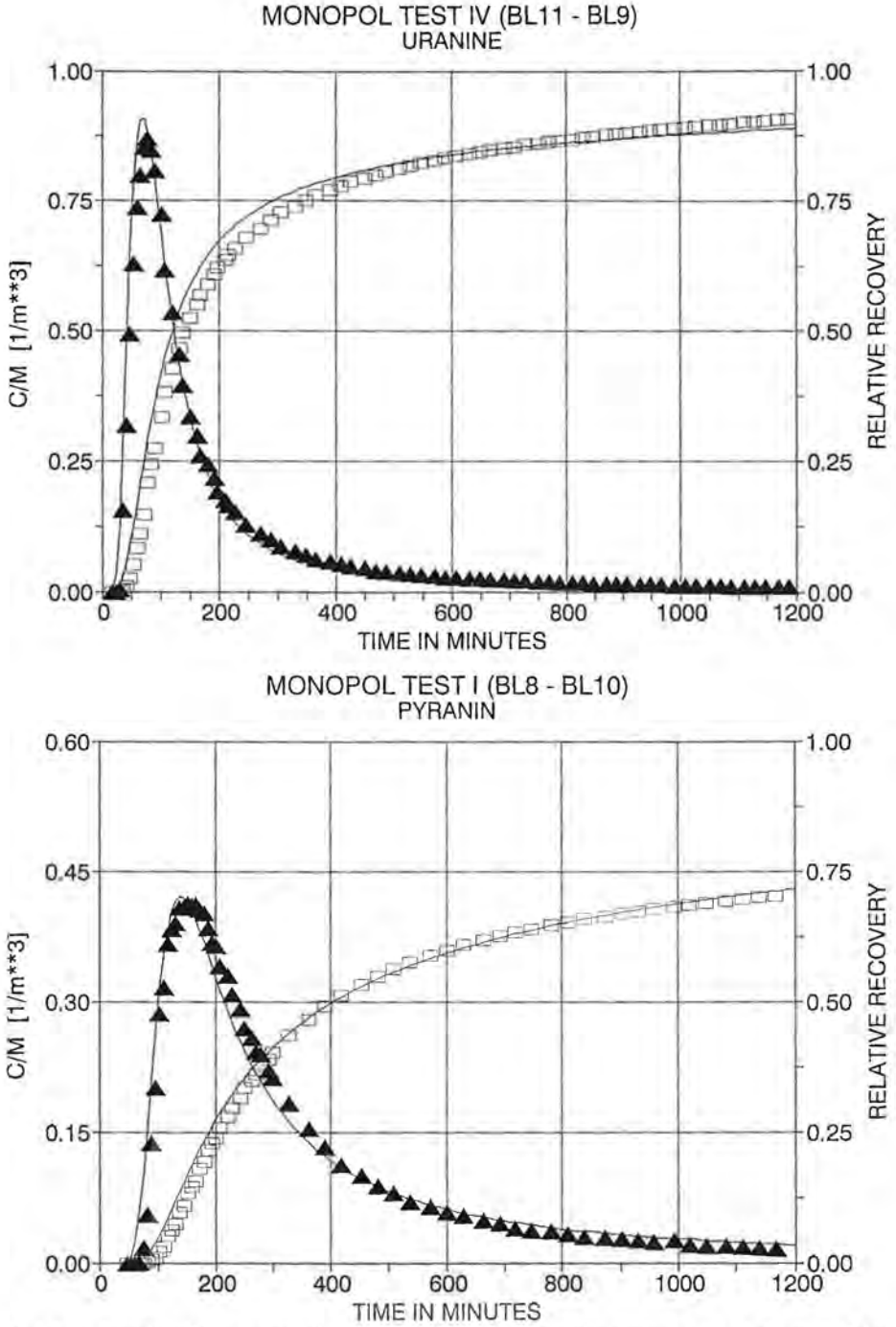

Fig. 5.9: a) Results of the monopol tracer test IV (above) in the central part of the parallel pit. b) Results of the monopol tracer test I (below) in the central part of the parallel pit. Triangle – tracer concentration, square – relative tracer recovery, measured.

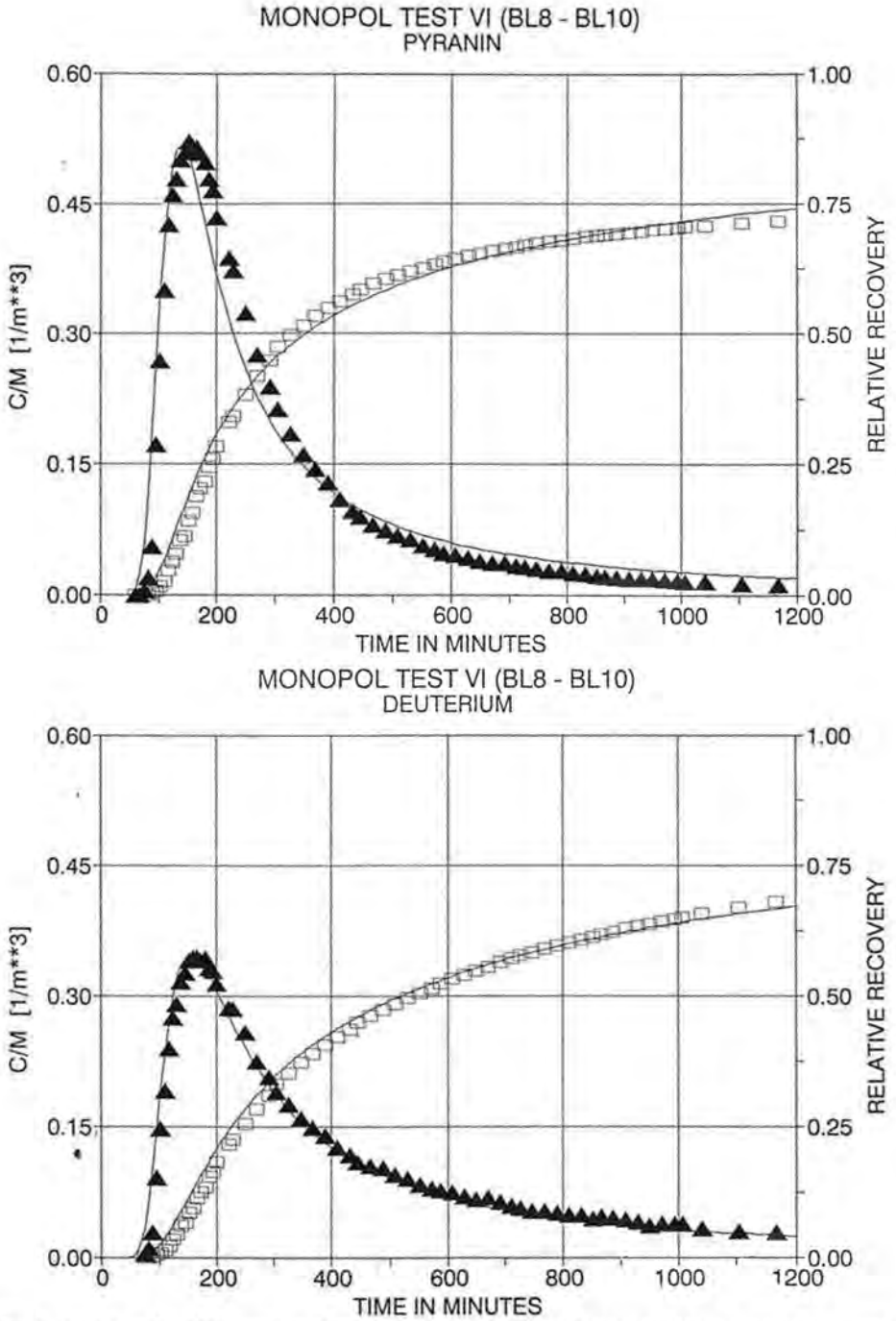

Fig. 5.10: a) Results of the combined monopol tracer test VI with PYRANIN (above) in the central part of the parallel pit.
b) Results of the combined monopol tracer test VI with DEUTERIUM (below) in the central part of the parallel pit.
Triangle – tracer concentration, square – relative tracer recovery, measured.

found for Pyranine. The diffusion parameter, $a = 14.2 \times 10^{-3} s^{-1/2}$, found for Deuterium is about 1.4 times greater than that found for Pyranine in the same experiment. Equation (5.19) shows that the ratio of a^2 for both tracers is equal to the ratio of molecular diffusion coefficients of both tracers. In this way (s. P. MAŁOSZEWSKI & A. ZUBER, 1989), the molecular diffusion coefficient for Pyranine could be easily estimated from the known molecular diffusion coefficient for Deuterium, i.e. $D_m = 2.5 \times 10^{-9}/(1.4)^2 = 1.3 \times 10^{-9}$ m²/s. This value was used to interpret all the experiments performed with Pyranine in this study. The results of modelling of the monopol tracer experiments are summarized in tab. 5.2.

Tab. 5.2: Results of the monopol tracer experiments.

Experiment (Tracer)	Distance X [m]	Mean thickness of the ore dike [m]	Transit time t_0 [hr]	Matrix porosity n_p [–]
Monopol I BL8 – BL10 (PYRANIN)	11.2	1.53	1.58	0.073
Monopol IV BL11 – BL9 (URANIN)	16.2	2.15	1.25	0.093
Monopol V BL7 – BL10 (PYRANIN)	21.4	1.30	20.0	0.052
Monopol VI BL8 – BL10 (PYRANIN)	11.2	1.35	1.62	0.065
Monopol VI BL8 – BL10 (D_2O)	11.2	1.35	1.52	0.065

5.8.3. Injection-Withdrawal Flow

The tracer experiments in injection-withdrawal flow fields are described in details in chap. 5.4. These tests were performed between two different pairs of wells (BL8 – BL10 for dipol test I and BL9 – BL11 for dipol test III), i.e. between wells where the monopol tracer tests (monopol test I, VI and IV) were done but with other tracers.

Dipol test I was performed using Eosine with the pumping rate of 0.127 l/s. The distance between the wells was 11.2 m. The best fits obtained for tracer concentration and relative recovery curves are shown in fig. 5.11 a. The parameters obtained were: $t_{01} = 0.6$ hour, $Pe_1 = 67$ and $a = 11 \times 10^{-3}\ s^{-1/2}$.

The fissure porosity of 0.29% (eq. 5.42) and the fissure aperture of 105 μm (eq. 5.28) obtained were similar to those found from the monopol tests. However the fissure spacing of 4.3 cm found was nearly five times smaller. The matrix porosity of 6.6%, calculated assuming the diffusion coefficient for Eosine to be the same as for Uranine, agrees well with the 6.5% and 7.3% found in monopol tests VI and I.

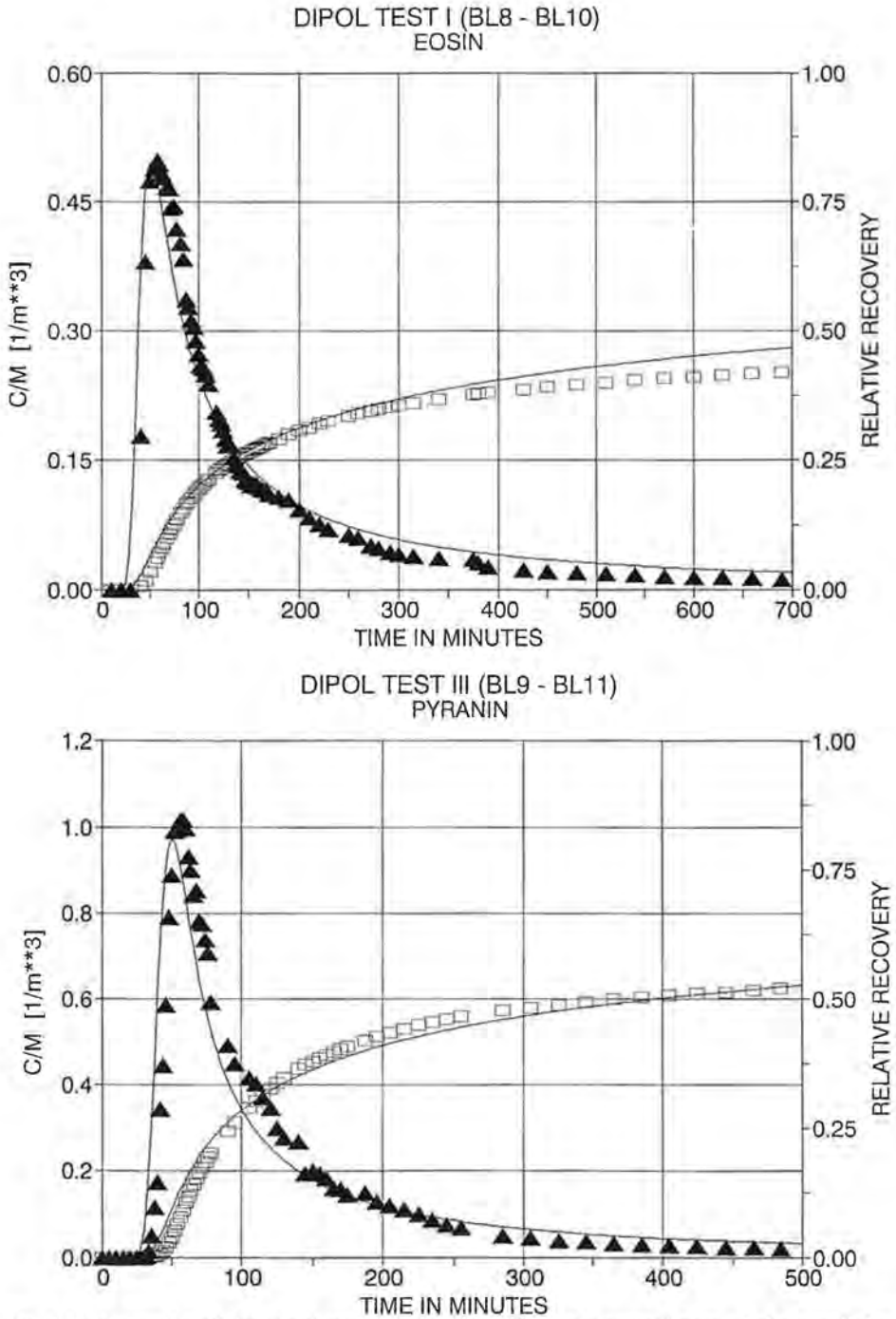

Fig. 5.11: a) Results of the dipol tracer test I (above) in the central part of the parallel pit. b) Results of the dipol tracer test III (below) in the central part of the parallel pit. Triangle – tracer concentration, square – relative tracer recovery, measured.

Dipol test III was performed between the wells BL9 and BL11 (X = 16.2 m) for the flow rate of 0.11 l/s. The tracer used was Pyranine. The best fit (Fig. 5.11 b) was obtained for both the tracer concentration and relative recovery curves. The fitting parameters were: $t_{01} = 0.7$ hour, Pe = 67 and $a = 4.91 \times 10^{-3}\ s^{-1/2}$. The calculated fissure porosity and aperture ($n_f = 0.05$ % and 2b = 280 μm) were exactly the same as in monopol test IV. The matrix porosity of 4.8%, calculated taking D_m for Pyranine as above, was smaller and more realistic than in the monopol test with Uranine. The results of modelling of the dipol tracer experiments are listed in tab. 5.3.

Tab. 5.3: Results of the dipol tracer experiments.

Experiment (Tracer)	Distance X [m]	Mean thickness of the ore dike [m]	Transit time t_{01} [hr]	Matrix porosity n_p [–]
Dipol I BL8 – BL10 (EOSIN)	11.2	2.15	0.70	0.066
Dipol III BL9 – BL11 (PYRANIN)	16.2	1.30	0.60	0.048

Table 5.4 shows the calculated fissure apertures which were evaluated from the results of the dipol experiments by applying eq. (5.26). These calculations depend on the hydraulic conductivity, k, which has to be known and upon the fissure porosity which has to be evaluated with the help of the mean residence time. The application of eq. (5.12), however, depending upon the measured differences in hydraulic head and upon the mean residence time, yields also a quite good evaluation of the fissure aperture. If one compares the values based upon the different approaches, it is obvious that the differences are negligible.

Tab. 5.4: Fissure apertures calculated from the results of the dipol tracer experiments.

Experiment	Hydraulic parameters		Calculated parameters from tracer experiments		
	Distance X [m]	Difference of hydraulic head [m]	Transit time t_{01} [hr]	Fissure aperture 2b (eq. 5.12) [μm]	Fissure aperture 2b (eq. 5.28) [μm]
Dipol I (BL8 – BL10)	11.2	20.83	0.70	88	105
Dipol III (BL9 – BL10)	16.2	6.64	0.60	250	280

6. Conclusions (T. Himmelsbach, H. Hötzl, P. Maloszewski)

The fissured aquifer under investigation at the test site Lindau is divided into two vertical parts which seems to have only minor interchange between each other. The uppermost part of the aquifer, which does not extend towards depths of more than

30 m below the ground surface, is characterized by mean residence times of approximately two years or less. It is affected by a fast infiltration of precipitation causing rapid changes in the discharge of springs and small rivulets as well as strong fluctuations of the groundwater level in the test site.

The underlying lower part of the aquifer is characterized by mean residence times rather lying in the range of five years or more. In boreholes which are located at aquifer parts lying far away from the hydraulic influence of the observation tunnel Lindau a significant increase of the ^{3}H-content in the vertical borehole profil can be observed. This increase occurs in several profiles in which the ^{3}H-changes take place within a depth intervall of approximately 10 m. The observed stratification is assumed to be relatively stable unless it is not disturbed by artificial hydraulic influences. In the direct vicinity of the observation tunnel Lindau, however, this stratification is disturbed due to its permanent leackage effects. The tunnel causes a permanent drainage of the fissured aquifer. Due to a fissure porosity of the main fault and fracture zone of the ore dike Hermann lying in the range of 0.1% up to 0.5% this permanent leackage may be responsible for the observed scattering of the ^{3}H-values in some tunnel waters. Due to this scattering of the ^{3}H-content, it is assumed that a breakthrough of a young water component likely at high groundwater stages occur down to the tunnel level. Hence, the water samples of the observation tunnel must represent a mixture of at least two age related components, although the relation between this components can not be quantified at the present stage of investigation. To derive a quantification of these age related components the data base is yet not sufficient, because it would require at least a weekly sampling programme.

The results of the tracer experiments carried out at the test site Lindau confirm again the relatively high probability to "loose" artificial tracers into deeper fracture systems of the aquifer, because the latter have only a reduced exchange with the surface. If the fluorescent dyes are injected into such deep lying fracture systems the tracing of groundwater in fissured aquifers over distances in the range of a few 100 m requires always long running experiments lying in the range of a few years. This "time effect" must be kept in mind, especially when planing or performing tracer experiments in natural fissured flow systems. Even when the flow patterns seem to be well known the further migration of the dyes is directly controled by the fissure aperture and by the relatively slow processes of matrix diffusion. Especially, if narrow fissure systems are involved the latter cause a rapid increase of the mean residence time. A high mean residence time, however, is always associated with a relatively high dilution effect which may render more difficulties in the detection of artificial tracers despite the meanwhile reached low detection limits.

At the present stage tracer experiments are not any longer restricted to simple flow path detections. For a quantitative analyses of a tracer experiment the hydraulic boundary conditions valid for the experiment have to be fixed sufficiently. The use of mathematical transport models to obtain hydraulic parameters like fissure apertures and fissure and matrix porosities requires the knowledge about the hydraulic gradient, the discharge or pumping rate at the main probe location as well as the knowledge about the direction of the flow path.

In the present study till now only one tracer experiment in natural flow conditions which was carried out in 1988 at the northern test section allowed a quantitative interpretation. The analytical approach was possible, because the injection and probe wells were interconnected by a direct hydraulic contact and the artesian probe well

had a nearly constant discharge rate. In comparison to that an analytical evaluation of tracer experiments carried out in other aquifer parts was impossible because there was a superposition of deep fracture flow by a faster discharge in the surface weathered zone.

Fortunately, in the observation tunnel Lindau a test site could be established which allowed to fix the hydraulic boundary conditions sufficiently. Within a fault and fracture zone of the ore dike Hermann the interwell flow field between the injection and probe well could be forced to steady-state conditions, thereby supplying an important precondition for the later quantitative analyses. By involving different flow-field geometries (e.g. dipol- and monopol-experiments) the suitability of the **Single-Fissure-Dispersion-Model** (SFDM) could be proved. The analyses of the tracer experiments carried out at the observation tunnel Lindau indicated that the fissure porosity n_f of the aquifer under investigation is very small lying in the range between 0.1% and 0.3%. The fissure porosity n_f represents the total mobile flux whereas the matrix porosity n_p is assumed to represent the immobile water content of the aquifer. The matrix porosity represents the "dead-end-fissures" of the fault and fracture zone as well as the solution cavities within the ore dike Hermann and was determined to be in the order of 5% up to 10%. It is responsible for the observed long tailing effects of the tracer due to the matrix diffusion processes. The fissure apertures were calculated to be in the range of 100 µm up to 300 µm. With the help of combined tracer experiments using D_2O and Pyranine the diffusion coefficiant of this tracer could be determined.

References

ACKERMANN, G, A. BLINDE & H. HÖTZL (1982): Anwendung der Markierungstechnik zur Untersuchung der Entwässerungsfunktion eines Erzganges. – Beiträge z. Geologie der Schweiz – Hydrologie, **28/II**, 423–434, Bern.

BERGMANN, H., B. SACKL, P. MALOSZEWSKI & W. STICHLER (1986): Hydrological investigations in a small catchment area using isotope data series. – Proc. 5th Intern. Symp. Underground Water Tracing (SUWT) 1986, 255–272, Athens.

BLINDE A., E. FABIAN & H. HÖTZL (1982): Insitu investigations and sealing of a cavernous ore load in the foundation area of a dam site. – Comm. Intern. Grand Barrages, **Q 53, R 16**, 289–307, Rio de Janeiro.

DE WIEST, R.J.M. (1965): Geohydrology.– 366 p., New York (John Wiley & sons).

EMMERMAN, R. (1968): Differentiation und Metasomatose des Albtalgranites (Südschwarzwald). – N. Jb. Miner. Abh., **109**, 94–130, Stuttgart.

EMMERMAN, R. (1977): A Petrogenetic Model for the Origin and Evolution of the Hercynian Granite Series of the Schwarzwald. – N. Jb. Miner. Abh., **128**, 219–253, Stuttgart.

ERNSTBERGER, H. & V. SOKOLLEK (1984): Der Einfluß land- und forstwirtschaftlicher Bodennutzung auf die Absickerung aus dem durchwurzelten Bodenraum. – Z. dt. geol. Ges., **8**, 723–734, Hannover.

GEHLEN, K., G. KLEINSCHMIDT, R. STENGER, H. WILHELM & W. WIMMENAUER (1986): Kontinentales Tiefbohrprogramm der Bundesrepublik Deutschland – Ergebnisse der Vorerkundungsarbeiten Lokation Schwarzwald. – 2. KTB-Kolloquium, Seeheim/ Odenwald 19.9.–21.9.1986.

GLUECKAUF, E. (1981): The movement of solutes through aqueos fissures in microporous rock during borehole experiments. – UKAEA Rep., AERE-R-10043.

GRISAK, G.E. & J.F. PICKENS (1980): Solute transport through fractured media, 1. The effect of matrix diffusion. – Water Resour. Res., **16**, 719–730, Washington.

GRISAK, G.E. & J.F. PICKENS (1981): An analytical solution for solute transport through fractured media with matrix diffusion. – J. Hydrol., **52**, 47–57.

GRISAK, G.E., J.F. PICKENS & J.A. CHERRY (1980): Solute transport through fractured media, 2. Column study of fractured till. – Water Resour. Res., **16**, 731–739, Washington.

GROVE, D.B. & W.A BEETEM (1971): Porosity and dispersion constant calculations for a fractured carbonate aquifer using two well tracer method. – Water Resour. Res., **7**, 128–134. Washington.

HAUDE, W. (1955): Zur Bestimmung der Verdunstung auf möglichst einfache Weise. – Mitt. d. DWD, **11**, 23 p., Bad Kissingen.

HERZOG, F. (1990): Transport modelling for the Grimsel Migration Experiments: Stream tube approach, first results and predictions. – Paul Scherrer Institute, **TM-41-90-18** (unpubl.), Würrenlingen, Switzerland.

HIMMELSBACH, T. (1991): Dipoltests zur Untersuchung des Stofftransportes in Kluftgrundwasserleitern. – Steir. Beitr. z. Hydrogeologie, **42**, 131–149, Graz, Austria.

HÖLTING, B. (1989): Hydrogeologie: Einführung in die allgemeine und angewandte Hydrogeologie. – 3. neu bearb. Aufl., 396 p., Stuttgart (Ferdinand Enke).

IAEA (1960–1990): World Survey of Isotope Concentration in Precipitation, Environmental Data. – No.1–No.9, Vienna, Austria.

KILLE, K. (1979): Das Verfahren MoMNQ, ein Beitrag zur Berechnung der langjährigen mittleren Grundwasserneubildung. – Z. dt. geol. Ges., Sonderheft Hydrologie und Hydrochemie, 89–95, Hannover.

KLOTZ, D., P. MALOSZEWSKI & H. MOSER (1988): Mathematical modelling of radioactive tracer migration in water flowing through saturated porous media. – Radiochimica Acta, **44/45**, 373–379.

KOPPELBERG, W. (1986): Numerische und statistische Untersuchungen zur Durchlässigkeit geklüfteter geologischer Körper und ihrer Bestimmung durch Wasserdruckversuche. – Mitt. Ing.- u. Hydrogeol., **23**, 299 p., Aachen.

KRUSEMAN, G.P. & N.A. DE RIDDER (1991): Analysis and Evaluation of Pumping Test Data. – IInd Ed., 377 p., Intern. Inst. f. Land Reclamation and Improvement, Wageningen, The Netherlands.

LENDA, A. & A. ZUBER (1970): Tracer dispersion in groundwater experiments. – Isotope Hydrology **1970**, 619–641, IAEA, Vienna.

LOHR, A. (1969): Beitrag zur Bestimmung des KH-Wertes durch hydraulische Feldversuche. – Das Gas- und Wasserfach, **110** (**14**), 369–376.

MALOSZEWSKI, P. & A. ZUBER (1984): Interpretation of artificial and environmental tracers in fissured rocks with a porous matrix. – Isotope Hydrology **1983**, 635–651, IAEA, Vienna.

MALOSZEWSKI, P. & A. ZUBER (1985): On the theory of tracer experiments in fissured rocks with a porous matrix. – J. Hydrol., **79**, 333–358.

MALOSZEWSKI, P. & A. ZUBER (1989): Mathematical models for interpreting tracer experiments in fissured aquifers. – In: The Application of Isotope Techniques in the Study of Hydrogeology of Fractured and Fissured Rocks, 287–301, IAEA, Vienna.

MALOSZEWSKI, P. & A. ZUBER (1990): Mathematical modelling of tracer behaviour in short-term experiments in fissured rocks. – Water Resour. Res., **26**, 1517–1528, Washington.

MELLERT, J. (1989): Geologische Kartierung im Gewann Etziboden. – Unveröff. Diplomarbeit, Univ. Karlsruhe, Teil **I**, 45 p., Karlsruhe.

METZ, R. & G. REIN (1958): Erläuterungen zur geologisch petrographischen Übersichtskarte des Südschwarzwaldes 1 : 50,000. – Lahr, Schwarzwald (Schauenburg).

METZ, R. (1980): Geologische Landeskunde des Hotzenwaldes. – Lahr, Schwarzwald (Schauenburg).

MEYER, T. (1991): Hydrologische, hydrochemische und radiologische Untersuchungen im oberen Höllbachtal (Gewann Etziboden im Testgebiet LINDAU, Südschwarzwald). – Unveröff. Diplomarbeit, Univ. Karlsruhe, Teil **II**, 92 p., Karlsruhe.

MORENO, L., Y.W. TSANG, C.F. TSANG, F.V. HALE & I. NERETNIEKS (1988): Flow and tracer transport in a single fracture: a stochastic model and its relation to some field observations. – Water Resour. Res., **24**, 2033–2048, Washigton.

MOSER, H. & W., RAUERT (1980): Isotopenmethoden in der Hydrologie. Lehrbuch der Hydrogeologie Band 8. – 400 p., Berlin/Stuttgart (Geb. Bornträger).

NERETNIEKS, I. (1980): Diffusion in the rock matrix. An important factor in radionuclide retardation? – Journal of Geophys. Research, **85** (**B8**), 4379–4397.

NERETNIEKS, I. (1981): Prediction of radionuclide migration in the geosphere: is the porous-flow model adequate? – IAEA Symposium, Knoxville, IAEA-SM-257/19, 635–657, IAEA, Vienna.

NOVAKOWSKI, K.S., G.V. EVANS, D.A. LEVER & K.G. RAVEN (1985): A field example of measuring hydrodynamic dispersion in a single fracture. – Water Resour. Res., **21**, 1165–1174, Washington.

RASMUSON, A. (1985): Analysis of hydrodynamic dispersion in discrete fracture networks using method of moments. – Water Resour. Res., **21**, 1677–1683, Washington.

RAVEN, K.G., K.S NOVAKOWSKI & P.A LAPCEVIC (1988): Interpretation of field tracer tests of a single fracture using a transient solute storage model. – Water Resour. Res., **24**, 2019–2032, Washington.

RENK, A. (1980): Zum Mineralinhalt des Hermannganges (Südschwarzwald). – Unveröff. Rep. GLA Baden-Württemberg, 39 p., Freiburg.

SCHLEICHER, H. (1984): Die Granitporphyre des Schwarzwaldes. – DMG-ÖMG-SMPG-Tagung 1984. – Fortschr. d. Miner., **62**, Beiheft **2**, Stuttgart.

SKAGIUS, K. & I. NERETNIEKS (1986): Porosities and diffusities of some nonsorbing species in crystalline rocks. – Water Resour. Res., **22**, 389–398, Washington.

SNOW, D.T. (1969): Anisotropic permeability of fractured media. – Water Resour. Res., **5**, 1273–1289, Washington.

SNOW, D.T. (1970): The frequency and apertures of fractures in rock. – Int. J. Rock Mech. Min. Sci., **7**, 23–40.

STICHLER, W., H. MOSER & M. SCHROEDER (1984):Measurements of seepage velocity in a sand lysimeter by means of ^{18}O-content. – Proc. Intern. Symp. Munich, October 1984: Recent Inevstigations in the Zome of Acration, 191–204, Munich.

SUDICKY, E.A. & E.O. FRIND (1982): Contaminant transport in fractured porous media: analytical solutions for a system of parallel fractures. – Water Resour. Res., **18**, 1634–1642, Washington.

TANG, D.H., E.O. FRIND & E.A. SUDICKY (1981): Contaminant transport in fractured porous media: analytical solutions for a single fracture. – Water Resour. Res., **17**, 555–564, Washington.

TROSCHKE, R. (1990): Quantifizierung der Durchlässigkeiteigenschaften geklüfteter Granite und deren Störungszonen mittels hydraulischer Testverfahren (Albtalgranit, Sürschwarzwald. – Unveröff. Diplomarbeit, Univ. Karlsruhe, Teil **II**, 63 p., Karlsruhe.

TSANG, Y.W. & C.F. TSANG (1987): Channel model of flow through fractured media. – Water Resour. Res., **23**, 467–479, Washington.

TSANG, Y.W., C.F. TSANG, I. NERETNIEKS & L. MORENO (1988): Flow and tracer transport in fractured media: a variable aperture channel model and its properties. – Water Resour. Res., **24**, 2049–2060, Washington.

U.S. BUREAU OF RECLAMATION (1963): Earth Manual. – 783 p., Denver, USA.

WEBSTER, D.S., J.F. PROCTOR & I.W. MARINE (1970): Two-well tracer test in fractured crystalline rock. – In: General Ground-Water Techniques, Geological Survey Water-Supply Paper, **1544-I**.

WICKERT, F. & G.H. EISBACHER (1988): Two-sided Variscian thrust tectonics in the Vosges Mountains, northeastern France. – Geodinamica Acta, **2/88**, 101–120, Paris, France.

ZUBER, A. (1974): Theoretical possibilities of the two-well pulse method. – In: Isotope Techniques in Groundwater Hydrology **1974**, 277–294, IAEA, Vienna.

Acknowledgements

The SCHLUCHSEEWERKE AG made this test site available to the Department of Applied Geology of the University Karlsruhe (AGK) for scientific research purposes. With its installations (reconnaissance galleries, horizontal and vertical wells) it offers a great opportunity to study the water circulation and transport in a fissured rock. We have to thank the SCHLUCHSEEWERKE AG for entrusting us this test site for detailed research programs and we appreciate their technical support in the ongoing research work.